TCR : 99-4317

577001

Copper Mines of Tasmania Pty Ltd

Exploration Licence 27/95 - Yolande River

Year 3 Annual Report

EL27/95PT1

See folio 64

Author P G Harbon
Contract Geologist

Distribution
MRT - Hobart
CMT - Queenstown
Paul Harbon

Authorised By D Garrard
Senior Mine Geologist
CMT Pty Ltd

Report No. T1999 - 001
Date 20 April 1999

577002

CONTENTS

EXECUTIVE SUMMARY

A regional stream sediment survey for gold was completed, with 31 drainage sites sampled over an 11 km^2 area underlain by Yolande River Sequence porphyries between Pearl Creek and Yolande River (total 67 sites). Visible gold shows cluster around Diamond Hill and the southern part of Madam Howards, with a maximum value of 930 ppb and four values in the range 29 to 52 ppb.

A BSc Honours project identified two porphyry types within the Yolande River Sequence based on petrography and geochemistry: rhyolitic Quartz-Feldspar-Biotite (QFB) and dacitic Quartz-Feldspar-Hornblende (QFH) porphyries.

Compilation of data from Ashley Griffiths' Honours project supports the concept that the Diamond Hill QFB porphyry has elevated background gold. It is thought that the brittle and strongly altered Diamond Hill porphyry is located on a structure which allowed fluid movement and hence localised quartz veining, with gold added during hydrothermal alteration.

The Diamond Hill grid was extended and a program of underground mapping, rock chip and soil geochemistry completed. Adit mapping and channel sampling results show consistent elevated background gold levels in the porphyry and the quartz veins, in contrast to barren host sediments.

Soil geochemistry was carried out on the Diamond Hill grid in an attempt to determine a pattern to gold distribution in the porphyry. Unfortunately neither A nor B/C horizon soil chemistry was sufficiently sensitive to gold, arsenic or base metals to be an effective exploration tool.

After trying various exploration methods in the Diamond Hill area, it is concluded that pan concentrate gold geochemistry combined with mapping and rock chip sampling is the most effective way of generating drill targets.

Copper Mines of Tasmania Pty Ltd (CMT) experienced financial difficulties in 1998, reflected in reduced funding for exploration. Following the appointment of an Administrator to CMT's parent company Mt Lyell Mining Ltd on 12 December 1998, a survival plan was initiated. The plan involved mining and milling of high grade ore and excluded funding for exploration, while a new owner was sought. All exploration staff were retrenched. The Sterlite Group, through its associate company Twin Star Holdings Pty Ltd, became the new mine owner on 7 April 1999, operated by subsidiary CMT. Consequently, there has been no exploration activity since November 1998 and a suspension of work on CMT exploration licences has been agreed between Sterlite and the State Government from 1 April 1999 to 31 March 2001.

Exploration will recommence following the two year exemption period. Plans proposed by CMT prior to change of ownership are to continue to explore the gold potential at Diamond Hill prospect and for regional scale prospect generative work based on aeromagnetics, mapping and structural geology.

TENEMENT INFORMATION

EL 27/95 is a 64 km^2 block centred 7 km northwest of Queenstown (Figure 1). The licence was awarded to Copper Mines of Tasmania in May 1996, as a successful bidder for the 66 km^2 Exploration Tender Area 389. CMT have 100% equity.

This report deals with exploration conducted in licence year 3, which runs from 24 May 1998 to 24 May 1999.

GEOLOGICAL SETTING AND PROSPECTIVITY

The southwest end of the Henty Fault system extends down the western side of EL 27/95 and intersects a major E-W structure with a series of major dextral and minor sinistral offsets (the Firewood Siding-Pearl Creek Fault system). These two structures subdivide the geology into three sectors (Figure 2):

1) In the NW corner, Cambrian Dundas Group marine sediments are in part overlain by Denison Group siliceous sediments and Gordon Group limestone.

2) Along the southern edge and in the southwest corner of the area, Eldon Group Bell Shale is faulted against Mount Read Volcanics.

3) 60% of the area is underlain by the Yolande River Sequence, a subdivision of the Mount Read Volcanics SE of the Henty Fault and considered to be synchronous with and possibly partly underlying the Central Volcanic Complex (Corbett, 1992). The Yolande River Sequence is thought to be a correlate of the Mt Charter Group (hosting Que River and Hellyer) north of the Henty Fault and the Dundas Group, the three sub-units of the Western Volcano-Sedimentary Sequence.

Five sites with minor abandoned diggings are known within the licence area. These are documented in the Year 2 Annual Report (Morrison and Griffiths, 1998):

1) Sisters Hills: Ironstone development in Dundas Group

2) Gold Creek: Alluvial gold diggings on a tributary of Langdon River

3) Diamond Hill: Quartz veins in a pipe-like porphyry body with gold workings

4) Raggedy Ann: Gold bearing quartz vein on a fault within Eldon Group

5) Madam Howards: Barite mine; possibly hydrothermally altered lenticular bodies

The vein type occurrences in the SE of the licence have been considered by previous explorers to be of Devonian origin as are other quartz vein gold shows within brittle host rocks elsewhere in the region. However, Madam Howards is an enigma, with substantial barite development and three holes drilled under the prospect (Department of Mines, 1962) which did not intersect significant vein widths.

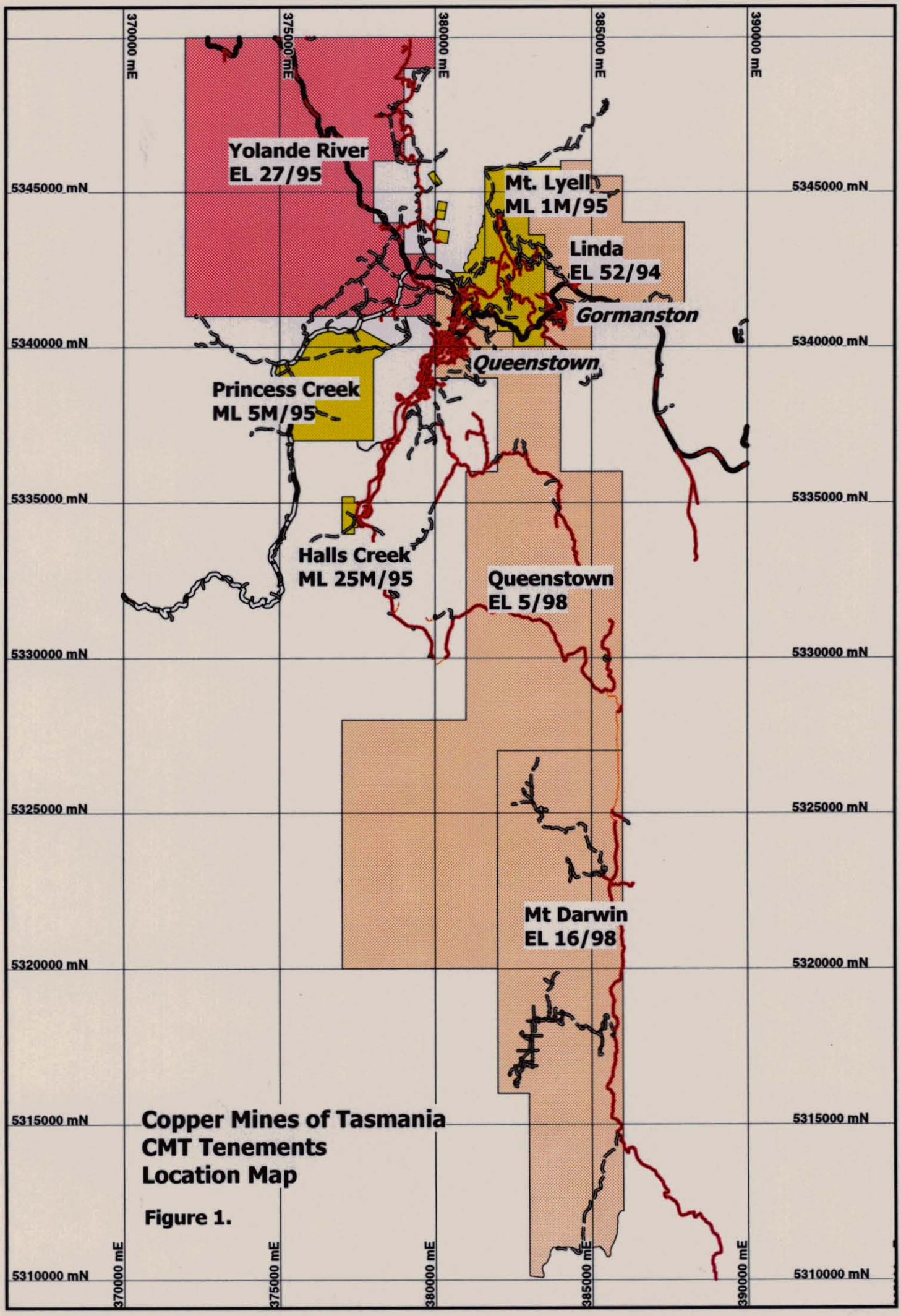

Copper Mines of Tasmania
CMT Tenements
Location Map

Figure 1.

577005

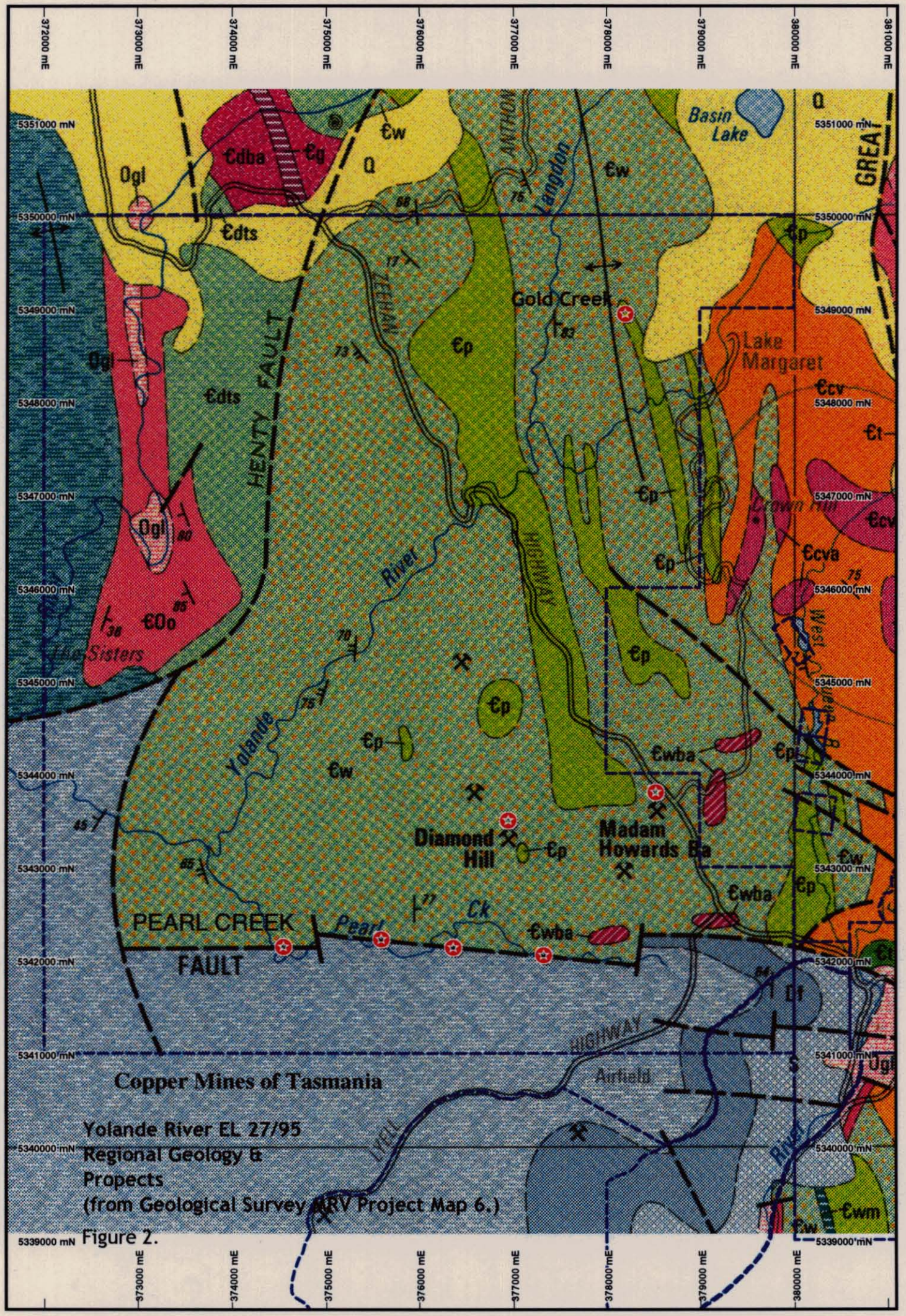

Copper Mines of Tasmania

Yolande River EL 27/95
Regional Geology &
Propects
(from Geological Survey MRV Project Map 6.)

Figure 2.

577006

SUMMARY OF PRE - EL 27/95 EXPLORATION

The three shallow cored drill holes at Madam Howards (Mines Department, 1962) are the only exploration holes in the licence area. Effective exploration has been conducted since 1971 by three groups: MLMRC/Goldfields, Cyprus and Pasminco (see Table 1). Regional coverage consists of a 1980 airborne EM survey, several generations of stream sediment surveys and a 1993 aeromagnetic/radiometrics survey.

The history of early prospecting and modern company exploration is compiled in detail in the Year 2 annual report (Morrison and Griffiths, 1998). The following table summarises the main activities relevant to current CMT exploration strategy.

Table 1: Pre EL 27/95 Exploration Summary

Period	Company	Tenement	Activity
1971-83	Mt Lyell Mining & Railway Co.	EL 47/71 & EL 9/66	Rock chip geochemistry (ironstone gossans) Stream sediment geochemistry (anomalous Zn, Gold Ck) Gridding & IP survey - Madam Howards; follow up soil geochemistry yielded one 200 ppm Pb anomaly Rock chip geochemistry - Diamond Hill (max 2 ppm Au) Dighem survey - numerous noncultural anomalies within survey noise level Regional stream sediment and rock chip geochemistry - Gold Ck (Zn, Au), Pearl Ck (Cu, Pb, Zn), Madam Howards (Au), Sister Hills (Zn), Truscott Ck (Cu, Zn)
1983	Gold Fields Exploration Ltd	EL 9/66	Supplementary stream sediment and rock chip geochem - Gold Ck (Zn, Au), Pearl Ck (Cu), Madam Howards (Au)
1985-89	Cyprus Minerals Australia Co.	EL 11/85	Rock chip sampling (Au,As,Sb) - Sisters Hills (not anomalous)
1990	Pasminco	EL 11/85	Joint Venture with Cyprus; Pasminco operators
1991-95	Pasminco & minor partners Hudspeth/ Norgold/Arimco	EL 25/91	Helimag/radiometrics survey - regional structural geology interpretation Collation of all previous stream sediment data

SUMMARY OF EL 27/95 YEAR 1 EXPLORATION

An 11 km access walking track along the southern side of the Yolande River was cut. The track connects Lyell Highway to Zeehan Highway and includes a re-established helipad near the Pearl Creek-Yolande River junction.

Reconnaissance prospecting was conducted along the Yolande River, where good outcrop exists in repeated cycles of Tyndall Group basal volcaniclastics/lithic conglomerates grading up stratigraphy to planar laminated ash fall tuffs.

At Madam Howards, barite, barite/quartz and quartz veins exposed in shallow abandoned workings and on access tracks were chip sampled and assayed for gold. All samples scored < 0.005 ppm and trace amounts of pyrite, galena and fluorite observed in some samples.

Core from the three diamond drill holes at Madam Howards was continuously sampled by sawn fillets. The 94 samples of quartz, carbonate, barite vein rocks and felsic volcanic host rocks were assayed for gold only (not previously assayed). The results were only marginally higher than surface samples with best results being hole MHD1: 225.6 - 230 feet, 0.12 ppm and hole MHD3: 137.6 - 145.8 feet, 0.11 ppm.

The above work is detailed in the Year 1 Annual Report (Morrison, 1997).

SUMMARY OF EL 27/95 YEAR 2 EXPLORATION

In conjunction with and complementing CMT's exploration program, an honours thesis began on a 20 km^2 area within EL 27/95 (A Griffiths, 1998), investigating the geology, geochemistry and magnetic character of Yolande porphyries. A secondary aim was to determine if a genetic relationship exists between the porphyries and quartz vein-style gold mineralisation known in the area (principally at Diamond Hill).

Regional Stream Sediment Survey

A pan concentrate drainage survey for gold, across the region underlain by Yolande River Sequence porphyries between Pearl Creek in the south and Yolande River in the north, commenced and was approximately half finished at the time of reporting.

Results showed frequent gold in streams draining the Diamond Hill and Madam Howards areas, with maximum values also occurring in those areas. Assay results correlated well with visual scores of gold particles counted during panning.

These results are in marked contrast to results from the comprehensive -80# stream sediment survey conducted over the region by Mt Lyell Mining and Railway Company Ltd in 1983, who generated only one gold anomaly - in a steam draining the southern side of the Madam Howards barite prospect. This contrast probably reflects gold particle size distribution, with most of the gold being coarser than 80#. Rock chip sampling from Diamond Hill detected a coarse gold problem during assaying.

Diamond Hill Prospect

a) Surface Rock Chips
Samples of outcrop, subcrop and float were taken from vein quartz and quartz-feldspar porphyry around Diamond Hill during reconnaissance prospecting. Ten of the 51 samples returned gold assays >1 ppm, with a maximum value of 18.3 ppm.

b) Gridding
Following the encouraging rock chip results and the re-location of old underground and alluvial workings around Diamond Hill, five grid lines (total 3 km) were cut and a program of mapping, soil geochemistry and ground magnetics commenced.

c) Soil Geochemistry
B/C horizon soil samples were taken by hand auger along the North Diamond Hill line and the Diamond Hill baseline. Attempts to sample the Diamond Hill cross lines were unsuccessful, due to the thin soil cover overlying coarse talus covered slopes.

The only reliable relationship between soil chemistry and bed rock type (determined from rock chips in the soil profiles) is a depression of lead, and to a lesser extent copper, over the porphyry. A strong lead high corresponds to the Adit-1 waste dump. Gold highs occur adjacent to small alluvial gold diggings.

One anomalous gold value appears in soil above the quartz-feldspar porphyry. A marked increase in lead, zinc and copper concentration defines the western contact of the feldspar-quartz-hornblende porphyry.

General conclusions from work to date are that there is no consistent gold elevation in soil overlying quartz-feldspar porphyry, but subtle depression of lead appears to discriminate the acid porphyries from the adjacent volcaniclastics.

d) Magnetics

Ground magnetic surveys were conducted along all grid lines in the Diamond Hill area, with surveyed responses varying only slightly from background magnetic response. A subtle local high may be inferred over areas of quartz-feldspar porphyry.

The quartz-feldspar porphyry bodies within EL 27/95 are not directly mappable from regional aeromagnetic data but the combination of ground magnetics, soil chemistry and mapping is being applied at Diamond Hill to determine the sub surface geometry.

e) Adit Channel Sampling

Continuous wall sampling of adits on Diamond Hill was carried out in order to locate rock units, veins or structures showing anomalous metal values.

Three different sets of quartz vein attitudes were identified, although no cross-cutting or relative age differentiation could be determined. Assay results show a general increase in gold values within quartz veins and quartz-feldspar porphyry. A section of quartz veins showing anomalous As values was identified within volcaniclastic breccia in Adit number 1. Cu and Pb values appear to show random local elevations.

Yolande River Sequence volcaniclastic rocks, which surround the porphyry body, are characterised by gold values less than detection level (0.01 ppm).

A direct correlation between the quartz-feldspar porphyry at Diamond Hill, quartz veining and increased gold levels was tentatively interpreted but detailed adit wall mapping of veins and structures is needed before conclusions are made.

The above work is detailed in the Year 2 Annual Report (Morrison and Griffiths, 1998).

EL 27/95 YEAR 3 EXPLORATION

Year 3 exploration focused on three tasks. At a regional scale, the stream sediment survey begun in Year 2 was completed and reconnaissance mapping undertaken. At a prospect scale, investigation continued at Diamond Hill to determine whether the porphyry has elevated gold, using exploration methods that may assist drill targeting.

In conjunction with CMT's exploration was a company sponsored Honours project on Yolande River Sequence porphyries in the licence area. This project began in licence Year 2, was completed in licence Year 3 and is included in full as the Attachment.

Regional

Reconnaissance Mapping
A north trending track (1.6 line km) was cut from Diamond Hill prospect towards Yolande River, to provide exploration access (see Figure 3). It was hoped that some small porphyry outcrops (gold hosting at Diamond Hill), shown on MRT maps corresponding to a low magnetic belt may be seen, however, reconnaissance mapping found only volcaniclastics. Further investigation is required to be confident whether possible gold bearing porphyries similar to Diamond Hill exist in this area or not.

Stream Sediment Survey
The regional stream sediment survey was completed and evaluated, with 67 drainage sites sampled over an 11 km^2 area underlain by Yolande River Sequence porphyries between Pearl Creek and the Yolande River. Thirty six of these samples were collected in Year 2 exploration. Sample data is shown on Maps 1 and 2.

Sampling in Year 3 (31 sites) was in the southeast and northwest areas, bounded by Pearl Creek Fault and Yolande River respectively. Visible gold shows cluster around Diamond Hill and the southern part of Madam Howards (barite veins) area, with a maximum value of 930 ppb and four values in the range 29 to 52 ppb. A broad area of elevated gold (panned) has been identified, with the source to be determined.

Four stream sediment samples were taken in the vicinity of the northern access track, with two panning gold. This was reflected in assay results: 14 and 18 ppb, in contrast to <5 ppb in the other two samples.

Diamond Hill Prospect

Compilation of data from Ashley Griffiths' Honours project on the Yolande River porphyries supports the concept that the quartz-feldspar-biotite porphyry has elevated background gold (and warrants drill targeting).

a) Surface Rock Chips
Whole rock analyses were made on 12 samples of varying lithologies in the licence area, including the Diamond Hill porphyry. Results are given in the Attachment. (P. 68, BSc Honours Thesis)

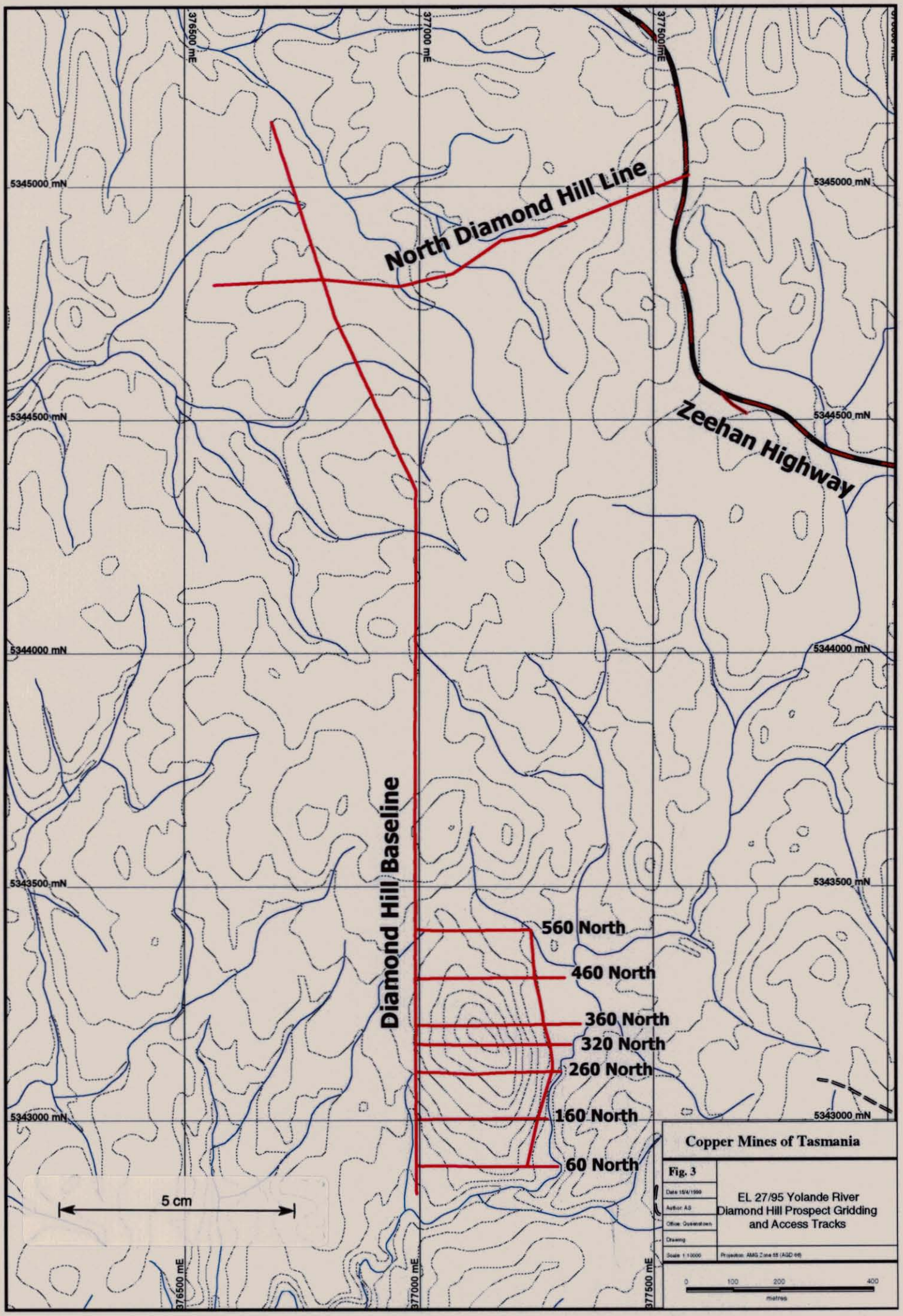
376500 mE
377000 mE
377500 mE
5345000 mN
5344500 mN
5344000 mN
5343500 mN
5343000 mN
North Diamond Hill Line
Zeehan Highway
Diamond Hill Baseline
560 North
460 North
360 North
320 North
260 North
160 North
60 North
5 cm
Copper Mines of Tasmania
Fig. 3
Date 15/4/1999
Author AS
Office: Queenstown
Drawing
Scale 1:10000
EL 27/95 Yolande River
Diamond Hill Prospect Gridding
and Access Tracks
Projection: AMG Zone 55 (AGD 66)
0 100 200 400
metres

577012

b) Gridding

The grid was extended (total 2.5 km), with four eastwest lines, two north and two south of previous lines, and a tie line cut alongside a creek on the eastern prospect margin. The grid lines, together with the northern access track, were picked up with a GPS survey (Leica-Wild GPS 200 system in kinematic mode). Grid line locations are shown on Figure 3.

c) Soil Geochemistry

As a possible technique for delineating gold mineralisation and to target drilling at Diamond Hill, it was felt that further soil sampling of the area would be useful. With sampling by hand auger in this area ineffective, some other means of penetration through the deep and widespread quartz layer was needed.

An alternative method of sampling A-horizon soil was tried, to be followed by Mobile Metal Ion analysis if results warranted (which they did not). Orientation A-horizon soil samples were taken over Diamond Hill line 360N to determine whether trace amounts of gold could be detected. If this proved to be, sampling would be extended over the entire grid in order to delineate any pattern to gold distribution in the porphyry which could be used to focus on a target zone.

Unfortunately neither A nor followup B/C horizon soil chemistry on the grid baseline and 360N was sufficiently sensitive to gold, arsenic or base metals to be an effective exploration tool (see Table 2) and soil sampling was discontinued. Gold results were below detection (0.01 ppb) in 111 of 114 samples taken. A horizon results were not reflected in B/C horizon, except for a single Pb anomaly (see Figure 4).

d) Magnetics

Ground magnetics were not read over the new grid lines due to equipment failure and lack of personnel. The magnetometer was sent interstate for repair and calibration, when it was found to be inoperable prior to field use, taking considerable time to be repaired. When it returned, field staff were redeployed on Mt Lyell drilling and retrenched in December 1998. While normally the new grid lines would have been surveyed by ground magnetics, it was not expected to show much character, given that the preceding work (Year 2 program) showed ground magnetic responses at Diamond Hill varied only slightly from background response.

e) Adit Channel Sampling

Adit mapping and channel sampling at Diamond Hill was completed. Results show consistent elevated gold levels in the porphyry ranging from 0.01 to 0.52 ppm, as well as in the quartz veins in contrast to barren host sediments (Map 3). These results reflect surface rock chip sampling results from Year 2.

The main conclusion after trying various exploration methods in the Diamond Hill area is that pan concentrate gold geochemistry combined with mapping and rock chip sampling is the most effective way of generating drill targets.

377950 mE
377000 mE
377050 mE
377100 mE
377150 mE
377200 mE
377250 mE
377300 mE

5343300 mN
5343250 mN
5343200 mN
5343150 mN
5343100 mN

Line 460N
Line 360N
Line 320N

Diamond Hill Baseline

H4698 14
H4697 6
H4696 7
H4695 9
H4694 9
H4693 5
H4692 74
H4691 4
H4690 3
H4689 6
H4688 6
H4687 <3
H4686 4

H1503 25 14
H1502 29 18
H1501 21 10
H1500 94 29
H1499 29 12
H1498 78 188
H1497 54 51
H1496 16 3
H1495 31 6
H1494 53 14
H1493 50 3
H1492 58 <3
H1491 16 10
H1490 25 6
H4717 18
H4718 22
H4719

H4721 <3
H4720 24

280
290
300
310
320
270

Legend

Sample ID

Pb ppm A horizon. Pb ppm B/C horizon.

5 cm

Copper Mines of Tasmania

Diamond Hill Prospect
Soil Sampling Data
Sample ID and Pb ppm
Figure 4.
Scale 1:1000

577014

YOLANDE RIVER EL 27/95

TABLE 2: SOIL SAMPLE DATA

Sample no.	amg E	amg N	Grid line	Element / Unit / Analabs method / Detection limit	Au ppm F630 1	Au(R) ppm F630 1	Cu ppm A102 2	Pb ppm A102 3	Zn ppm A102 2	As ppm A102 50	As(R) ppm H102 1	Soil horizon	Rock type
H4615	376563	5344789	N Diamond Hill		<0.01	<0.01	19	36	26	<50	11	B/C	Volc sst/slst
H4616	376588	5344790	N Diamond Hill		<0.01		3	8	18	<50	<1	B/C	Volc sst/slst
H4617	376613	5344792	N Diamond Hill		<0.01		3	5	18	<50	<1	B/C	Volc sst/slst
H4618	376637	5344793	N Diamond Hill		<0.01	<0.01	10	25	18	<50	<1	B/C	Volc sst/slst
H4619	376662	5344794	N Diamond Hill		<0.01		3	4	13	<50	2	B/C	Volc sst/slst
H4620	376687	5344796	N Diamond Hill		<0.01		3	5	14	<50	<1	B/C	Volc sst/slst
H4621	376712	5344797	N Diamond Hill		<0.01	<0.01	5	5	14	<50	1	B/C	QFB porphyry
H4622	376737	5344798	N Diamond Hill		<0.01		5	11	16	<50	1	B/C	QFB porphyry
H4623	376762	5344800	N Diamond Hill		<0.01	<0.01	4	7	18	<50	<1	B/C	QFB porphyry
H4624	376787	5344801	N Diamond Hill		<0.01		2	3	12	<50	1	B/C	QFB porphyry
H4625	376812	5344800	N Diamond Hill		<0.01		3	<3	8	<50	<1	B/C	QFB porphyry
H4626	376837	5344797	N Diamond Hill		<0.01	<0.01	3	8	10	<50	1	B/C	QFB porphyry
H4627	376862	5344795	N Diamond Hill		<0.01	<0.01	4	7	21	<50	1	B/C	QFB porphyry
H4628	376887	5344792	N Diamond Hill		<0.01		4	4	22	<50	<1	B/C	QFB porphyry
H4629	376912	5344790	N Diamond Hill		<0.01		3	<3	19	<50	1	B/C	QFB porphyry
H4630	376937	5344787	N Diamond Hill		<0.01		4	4	19	<50	<1	B/C	QFB porphyry
H4631	376961	5344787	N Diamond Hill		0.04		4	3	17	<50	<1	B/C	QFB porphyry
H4632	376986	5344792	N Diamond Hill		<0.01		3	3	16	<50	<1	B/C	QFB porphyry
H4633	377007	5344798	N Diamond Hill		<0.01	<0.01	4	6	16	<50	1	B/C	QFB porphyry
H4634	377032	5344803	N Diamond Hill		<0.01		3	4	15	<50	<1	B/C	QFB porphyry
H4635	377056	5344809	N Diamond Hill		<0.01	<0.01	4	3	16	<50	<1	B/C	QFB porphyry
H4636	377079	5344818	N Diamond Hill		<0.01		<2	4	15	<50	<1	B/C	QFB porphyry
H4637	377099	5344832	N Diamond Hill		<0.01		6	6	17	<50	1	B/C	QFB porphyry
H4638	377120	5344847	N Diamond Hill		<0.01		2	4	18	<50	<1	B/C	QFB porphyry
H4639	377141	5344861	N Diamond Hill		<0.01		6	8	31	<50	1	B/C	QFB porphyry
H4640	377161	5344875	N Diamond Hill		<0.01	<0.01	4	5	19	<50	<1	B/C	QFB porphyry
H4641	377183	5344884	N Diamond Hill		<0.01		3	4	10	<50	<1	B/C	QFB porphyry
H4642	377198	5344887	N Diamond Hill		<0.01		2	<3	11	<50	<1	B/C	QFB porphyry
H4643	377208	5344889	N Diamond Hill		<0.01		2	4	11	<50	1	B/C	QFB porphyry
H4644	377232	5344894	N Diamond Hill		<0.01		2	3	13	<50	1	B/C	QFB porphyry
H4645	377256	5344901	N Diamond Hill		<0.01		4	8	16	<50	<1	B/C	Volc sst/slst
H4646	377279	5344910	N Diamond Hill		<0.01	<0.01	4	5	15	<50	<1	B/C	Volc sst/slst
H4647	377303	5344919	N Diamond Hill		<0.01		2	4	12	<50	2	B/C	Volc sst/slst
H4648	377326	5344928	N Diamond Hill		<0.01	<0.01	2	<3	21	<50	<1	B/C	QFH porphyry
H4649	377349	5344937	N Diamond Hill		<0.01		21	69	72	<50	<1	B/C	QFH porphyry
H4650	377372	5344946	N Diamond Hill		<0.01	<0.01	4	8	24	<50	<1	B/C	QFH porphyry
H4651	377396	5344955	N Diamond Hill		<0.01		9	15	26	<50	3	B/C	QFH porphyry
H4652	377419	5344964	N Diamond Hill		<0.01		9	21	35	<50	6	B/C	QFH porphyry
H4653	377442	5344973	N Diamond Hill		<0.01		75	261	64	<50	2	B/C	QFH porphyry
H4654	377466	5344982	N Diamond Hill		<0.01		21	7	32	<50	1	B/C	QFH porphyry

577015

16/04/99

TABLE 2: SOIL SAMPLE DATA

				Element	Au	Au(R)	Cu	Pb	Zn	As	As(R)		
				Unit	ppm	ppm	ppm	ppm	ppm	ppm	ppm		
				Analabs method	F630	F630	A102	A102	A102	A102	H102		
Sample no.	amg E	amg N	Grid line	Detection limit	1	1	2	3	2	50	1	Soil horizon	Rock type
H4655	377489	5344992	N Diamond Hill		<0.01		5	9	40	<50	1	B/C	QFH porphyry
H4674	376994	5342840	D Hill baseline		<0.01		6	5	18	<50	1	B/C	Volc sst/slst
H4675	376994	5342860	D Hill baseline		<0.01	<0.01	4	4	12	<50	<1	B/C	Volc sst/slst
H4676	376994	5342880	D Hill baseline		<0.01		4	8	12	<50	1	B/C	Volc sst/slst
H4677	376994	5342900	D Hill baseline		<0.01		3	<3	7	<50	3	B/C	Volc sst/slst
H4678	376994	5342920	D Hill baseline		<0.01		2	16	12	<50	2	B/C	Volc sst/slst
H4679	376994	5342940	D Hill baseline		<0.01		2	<3	7	<50	2	B/C	Volc sst/slst
H4680	376995	5342960	D Hill baseline		<0.01	<0.01	3	7	7	<50	1	B/C	Volc sst/slst
H4681	376995	5342980	D Hill baseline		<0.01		10	25	13	<50	3	B/C	Volc sst/slst
H4682	376995	5343000	D Hill baseline		<0.01		4	17	13	<50	2	B/C	Volc sst/slst
H4683	376995	5343020	D Hill baseline		<0.01		5	12	16	<50	3	B/C	Volc sst/slst
H4684	376995	5343040	D Hill baseline		<0.01		4	<3	11	<50	2	B/C	Volc sst/slst
H4685	376994	5343060	D Hill baseline		<0.01	0.02	2	3	10	<50	2	B/C	Volc sst/slst
H4686	376994	5343080	D Hill baseline		<0.01	<0.01	<2	4	8	<50	1	B/C	Volc sst/slst
H4687	376994	5343100	D Hill baseline		<0.01		6	<3	7	<50	3	B/C	Volc sst/slst
H4688	376994	5343120	D Hill baseline		<0.01		4	6	10	<50	1	B/C	Volc sst/slst
H4689	376993	5343140	D Hill baseline		<0.01	<0.01	4	6	9	<50	1	B/C	Volc sst/slst
H4690	376993	5343160	D Hill baseline		<0.01	0.03	<2	3	<2	<50	1	B/C	Volc sst/slst
H4691	376993	5343180	D Hill baseline		<0.01	<0.01	3	4	4	<50	2	B/C	Volc sst/slst
H4692	376993	5343200	D Hill baseline		<0.01		6	74	17	<50	8	B/C	Volc sst/slst
H4693	376993	5343220	D Hill baseline		<0.01		5	5	10	<50	<1	B/C	Volc sst/slst
H4694	376992	5343240	D Hill baseline		<0.01		5	9	14	<50	3	B/C	Volc sst/slst
H4695	376992	5343260	D Hill baseline		<0.01		5	9	12	<50	8	B/C	Volc sst/slst
H4696	376991	5343280	D Hill baseline		<0.01		7	7	11	<50	3	B/C	Volc sst/slst
H4697	376991	5343300	D Hill baseline		<0.01		4	6	11	<50	<1	B/C	Volc sst/slst
H4698	376991	5343320	D Hill baseline		<0.01		10	14	16	<50	2	B/C	Volc sst/slst
H4699	376991	5343340	D Hill baseline		<0.01	<0.01	7	3	13	<50	1	B/C	QFB porphyry
H4700	376991	5343360	D Hill baseline		<0.01	<0.01	3	<3	11	<50	1	B/C	QFB porphyry
H4701	376993	5343380	D Hill baseline		<0.01		4	39	22	<50	1	B/C	QFB porphyry
H4702	376993	5343400	D Hill baseline		<0.01		2	7	10	<50	2	B/C	QFB porphyry
H4703	376993	5343420	D Hill baseline		<0.01		3	11	16	<50	1	B/C	QFB porphyry
H4704	376993	5343440	D Hill baseline		<0.01		2	3	7	<50	1	B/C	QFB porphyry
H4706	376993	5343480	D Hill baseline		<0.01		4	<3	12	<50	2	B/C	QFB porphyry
H4708	376993	5343520	D Hill baseline		<0.01		3	<3	13	<50	5	B/C	QFB porphyry
H4709	376993	5343540	D Hill baseline		<0.01		2	<3	11	<50	3	B/C	QFB porphyry
H4710	376993	5343560	D Hill baseline		<0.01	<0.01	3	<3	9	<50	1	B/C	QFB porphyry
H4711	376993	5343580	D Hill baseline		<0.01		4	<3	11	<50	2	B/C	QFB porphyry
H4712	376993	5343600	D Hill baseline		<0.01		3	<3	11	<50	3	B/C	QFB porphyry
H4713	376993	5343620	D Hill baseline		<0.01		3	3	9	<50	2	B/C	QFB porphyry
H4714	376993	5343640	D Hill baseline		<0.01	<0.01	3	3	10	<50	5	B/C	QFB porphyry

TABLE 2: SOIL SAMPLE DATA

Sample no.	amg E	amg N	Grid line	Element / Unit / Analabs method / Detection limit	Au ppm F630 1	Au(R) ppm F630 1	Cu ppm A102 2	Pb ppm A102 3	Zn ppm A102 2	As ppm A102 50	As(R) ppm H102 1	Soil horizon	Rock type
H4717	377293	5343204	360N		<0.01	<0.01	7	18	25	<50	2	B/C	Volc sst/slst
H4718	377313	5343204	360N		<0.01	<0.01	6	18	30	<50	2	B/C	Volc sst/slst
H4719	377333	5343204	360N		<0.01	<0.01	10	22	22	<50	3	B/C	Volc sst/slst
H4720	377175	5343100	260N		<0.01	<0.01	8	24	22	<50	17	B/C	Clay
H4721	377035	5343100	260N		<0.01		3	<3	19	<50	<1	B/C	Volc sst/slst
H1603	377013	5343204	360N		<0.01	<0.01	28	25	18	<50	<1	A	
H1477	377033	5343204	360N		<0.01		21	29	58	<50	<1	A	
H1478	377053	5343204	360N		<0.01		15	21	27	<50	4	A	
H1479	377073	5343204	360N		<0.01		99	94	33	<50	12	A	
H1480	377093	5343204	360N		<0.01		40	29	33	<50	1	A	
H1481	377113	5343204	360N		<0.01		21	78	42	<50	6	A	
H1482	377133	5343204	360N		<0.01		31	54	33	<50	6	A	
H1483	377153	5343204	360N		0.04	0.03	38	16	37	<50	<1	A	
H1484	377173	5343204	360N		<0.01		83	31	63	<50	4	A	
H1485	377193	5343204	360N		<0.01		92	53	47	<50	10	A	
H1486	377213	5343204	360N		0.18	0.21	94	50	77	<50	7	A	
H1487	377233	5343204	360N		<0.01		181	58	65	<50	2	A	
H1488	377253	5343204	360N		<0.01	0.01	18	16	30	<50	7	A	
H1490	377273	5343204	360N		<0.01	<0.01	25	25	34	<50	3	A	
H1489	377273	5343204	360N		<0.01	<0.01	12	6	22		<1	B/C	
H1491	377253	5343204	360N		<0.01		13	10	17		<1	B/C	
H1492	377233	5343204	360N		<0.01		6	<3	4		2	B/C	
H1493	377213	5343204	360N		<0.01		7	3	6		<1	B/C	
H1494	377193	5343204	360N		<0.01		30	14	28		25	B/C	
H1495	377173	5343204	360N		<0.01		15	6	15		<1	B/C	
H1496	377153	5343204	360N		<0.01		10	3	7		<1	B/C	
H1497	377133	5343204	360N		<0.01	<0.01	21	51	24		<1	B/C	
H1498	377113	5343204	360N		<0.01		9	188	15		14	B/C	
H1499	377093	5343204	360N		<0.01		18	12	23		<1	B/C	
H1500	377073	5343204	360N		<0.01		31	29	26		<1	B/C	
H1601	377053	5343204	360N		<0.01		10	10	19		<1	B/C	
H1602	377033	5343204	360N		<0.01		17	18	19		4	B/C	
H1604	377013	5343204	360N		<0.01		14	14	9		<1	B/C	

527011

16/04/99

General

In addition to the being involved in the regional and prospect work discussed above, Ashley Griffiths undertook other exploration studies on the licence as part of his Honours thesis. This work is summarised below.

All exploration data and methods collected as part of this project (whole rock, stream sediment, soil, ground magnetics, surface rock chip, adit channel sampling, magnetic susceptibility and rock density) are given in Appendices II to X of the thesis.

A literature review on forms, contact relationships and modes of emplacement of porphyry bodies was undertaken to recognise porphyry characteristics and apply this to the identification of Yolande River Sequence porphyries (thesis Appendix I).

Geology (A Griffiths, 1998)

Porphyritic units within the Yolande River Sequence are of two compositions:

1) Rhyolitic, Quartz-Feldspar-Biotite (QFB) and
2) Dacitic, Quartz-Feldspar-Hornblende (QFH)

Regular northsouth porphyry orientation concurs with the dominant volcaniclastic and sedimentary host rock bedding direction (Map 2), together with pepperitic contacts infer porphyry intrusion into unconsolidated sediment as sill-like structures. QFH porphyry units weather preferentially, with contacts difficult to locate.

Both porphyry types show partial to complete sericitisation of feldspar crystals. Rhyolitic porphyries underwent extensive pseudomorphing of feldspars to muscovite. Dacitic porphyries have undergone selective alteration of hornblende to chlorite, while retaining primary textures.

Porphyry units crop out at seven locations (see Map 3). These were studied and classified geochemically using whole rock and immobile element determinations. Four porphyries were mapped and sampled (P1 to P4), with data obtained on four others (P5 to P8) from J Everard (MRT). Analyses are consistent with petrographical and field observations of the two porphyry types. Rhyolitic and dacitic divisions group within previously characterised suite I and suite II classifications for the Mount Read Volcanics respectively, based on TiO_2 *vs* SiO_2 and Ti/Zr *vs* SiO_2 ratios.

Analysis of thin sections from rock chip samples collected in 1998 were completed for primary mineralogy determination. This enabled petrological descriptions to be made of the host sequence (volcaniclastic pumiceous sandstone and siltstone and ash tuff), QFB and QFH porphyries and basalt units (see Attachment Chapter 5). Embayed quartz crystals observed in both porphyry units indicates extensive periods within melt and subsequent resorption.

Alteration indices calculated on rock chip samples as a measure of hydrothermal alteration, showed feldspar/muscovite/sericite/chlorite alteration matching the two porphyry types and correlated with thin section petrology. Indices for rhyolitic porphyries show varying degrees of alteration in contrast to less altered dacitic units.

The most altered QFB porphyry is Diamond Hill, which is gold enriched compared to barren host rocks. Extensive quartz veining throughout this porphyry also shows anomalous gold assay values. The porphyry is thought to be significantly altered due to its brittle nature (competency contrast with surrounding host rocks). This has allowed post magmatic localisation of quartz veining in the porphyry, related to similar Tabberabberan gold-rich quartz veining south of the Pearl Creek Fault. The intense quartz veining within the Diamond Hill porphyry has facilitated alteration.

The Diamond Hill porphyry is thought to be located on a structure which allowed fluid movement and localised quartz veining, with gold added during hydrothermal alteration. Previously mapped as a pipe-like body, recent mapping shows the porphyry extends to the northwest and is more sill-like in shape. Strike direction is anomalous to other porphyries in the region (dominant North strike), suggesting a different structure controlling emplacement.

Gold enriched quartz veining is interpreted to relate to local structures which allowed fluid movement, rather than to porphyry bodies. Postulated age of veining is Devonian (strike subparallel to Pearl Creek Fault), sourcing gold from Cambrian porphyries and fluid enrichment during the Tabberabberan. Consequently, exploration for quartz vein-type gold mineralisation should focus on areas with localised structures and favourable host rocks such as occur at Diamond Hill.

Magnetics

Dacitic porphyries show a high magnetic response due to primary fine grained magnetite. In contrast, rhyolitic porphyries (Diamond Hill) exhibit a weak magnetic response, slightly elevated from surrounding sediments in ground magnetics.

Magnetic susceptibility readings were taken on Diamond Hill adit sample pulps (87), with results shown in Map 3. Using rock type of density samples (see below), there is weak magnetic character in the porphyry from adits 2 and 3 compared to negligible response from the sediments.

Rock Density

Density determinations (specific gravity) were made of the dominant rock types in the Diamond Hill adits (12 samples). Summary results show no obvious density contrast:

Sandstone	2.43 - 2.69 g cm^3
Siltstone	2.28 - 2.51 g cm^3
QFB Porphyry	2.48 - 2.55 g cm^3

Consequently, a gravity survey over the Diamond Hill grid to delineate geometry of the porphyry would require close spacing and tight survey control in order to detect subtle density contrasts.

EXPENDITURE

Expenditure on EL 27/95 for the 12 month period ending 31 March 1999 was $37,624, compared to $40,587 for the year to 31 March 1998. Total expenditure since licence granting in May 1996 is $130,616, with no work since December 1998.

YEAR 4 WORK PROGRAM PROPOSAL

The new owners of CMT Pty Ltd, Twin Star Holdings (a member of the Sterlite group of companies), have been granted exemption from work commitments on all four CMT exploration licences in Tasmania until 31 March 2001, while the company focuses on making Mt Lyell mine profitable.

Consequently, exploration on Yolande EL 27/95 is postponed, however a Year 4 work program had been proposed by CMT prior to change of ownership:

Regional Exploration

Yolande is a relatively unexplored licence, with only limited vehicle and pedestrian access. From work to date, interpretation of and possibly additional regional airborne surveys are recommended to identify likely areas of possible gold hosting porphyries to be followed up by detailed evaluation.

A structural geology study based on both existing aeromagnetics and radiometrics (1993 Pasminco survey) and field mapping, similar to that carried out over Linda EL 52/94 (by Steve King of Solid Geology Pty Ltd) was proposed for the Year 3 program but not undertaken due to lack of funds. This study would be of benefit in delineating possible porphyries in the northern part of the licence and structural lineaments which may have been pathways for mineralisation.

In conjunction with regional exploration, work is proposed on Diamond Hill and Madam Howards prospects. Methods may include mapping, track cutting, rock chip and soil geochemistry, ground magnetic and gravity surveys and diamond drilling.

Prospect Exploration

Diamond Hill
A close spaced gravity survey with tight survey control has been proposed to resolve subsurface shape of the porphyry and optimise a drill target (one or two shallow cored holes). Detailed mapping has been proposed over the Pearl Creek-Diamond Hill area in the southern part of the licence, Gold Creek and Truscott Creek.

Madam Howards
The 1998 regional stream sediment survey found anomalous gold results sourced from Madam Howards, in contrast to core resampling and rock chip results. Vein sampling and mapping has been proposed, together with an orientation A horizon soil geochemistry survey, to determine the source.

REFERENCES

Corbett, K.D., 1992. Stratigraphic-volcanic Setting of Massive Sulphide Deposits in the Cambrian Mount Read Volcanics, Tasmania. Economic Geology, volume 87, 1992, pp 564 - 586.

Griffiths, A.G., 1998. The Geology, Geochemistry and Magnetics of Yolande River Sequence Porphyries, Northwest of Queenstown. Honours research thesis with CODES SRC/ School of Earth Sciences, The University of Tasmania.

Morrison, K.C., 1997. CMT Pty Ltd Exploration Licence 27/95 - Yolande River, Year 1 Annual Report.

Morrison, K.C., and Griffiths, A.G., 1998. CMT Pty Ltd Exploration Licence 27/95 - Yolande River, Year 2 Annual Report.

To Zeehan

375000 mE

377500 mE

Lake Margaret

5347500 mN

5345000 mN

5342500 mN

Yolande River

Murchison Highway

North Diamond Hill Line

Diamond Hill

Diamond Creek

Pearl Creek Fault

To Queenstown

To Strahan

Magnetic North

0 500m

SCALE

Lithological Boundaries

Interpreted Boundaries

Main Roads

4WD Access Tracks

Rivers

Creeks

*Z#### Location of thin sections provided by J. Everard

*H#### Research Sample Locations

*#### Sites of assayed samples

*H#### #### Stream sediment sample sites + Au assay levels (ppb)

Cut Grid Lines

Major Fault

Minor Fault

Bedding strike and dip direction

Cleavage direction

Quartz - Feldspar - Biotite Porphyry

Quartz - Feldspar - Hornblende Porphyry

Ash Tuff

Volcaniclastic Siltstone

Pumiceous Volcaniclastic Sandstone

Bell Shale

Basalt

Map 1 - Outcrop Geology Map of study area, within EL 27/95.

5 cm

577022

99-4317

ANNUAL REPORT(YR 3) EL 27/95
COPPER MINES TAS. P HARBON
YOLANDE RIVER

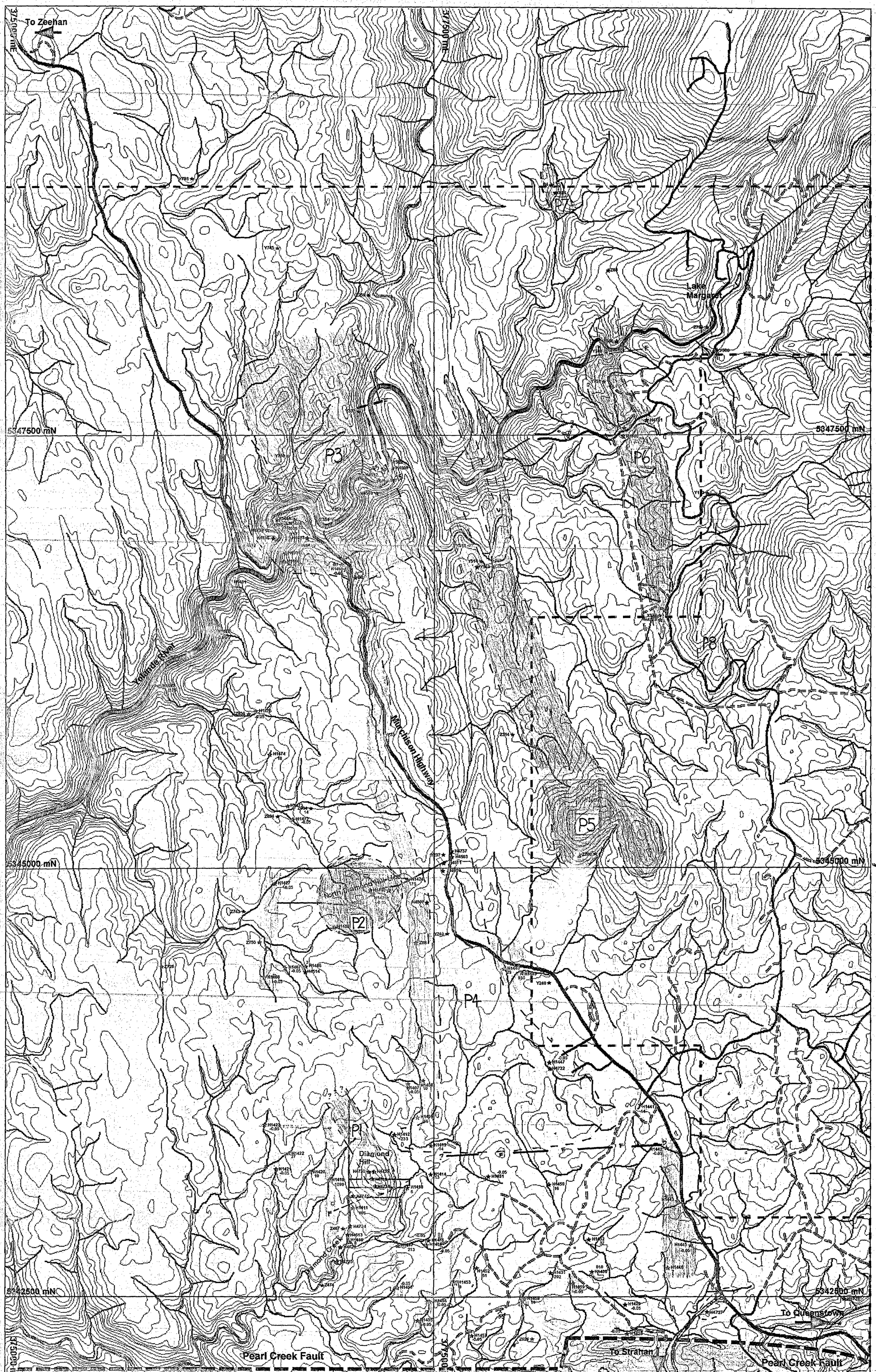

577023

99-4317

ANNUAL REPORT(YR 3) EL 27/95
COPPER MINES TAS. P HARBON
YOLANDE RIVER

Map 2 - Exploration License 27/95 Yolande River : Interpreted regional geology within study area, combined with regional data from Geol. Surv. Tas. Queenstown map

5 cm

YOLANDE EL 27/95

MAP 3 : DIAMOND HILL ADITS

MAPPING OF QUARTZ VEINS AND LITHOLOGIES

Author: A Griffiths

99-4317

ANNUAL REPORT(YR 3) EL 27/95
COPPER MINES TAS. P HARBON
YOLANDE RIVER

577024

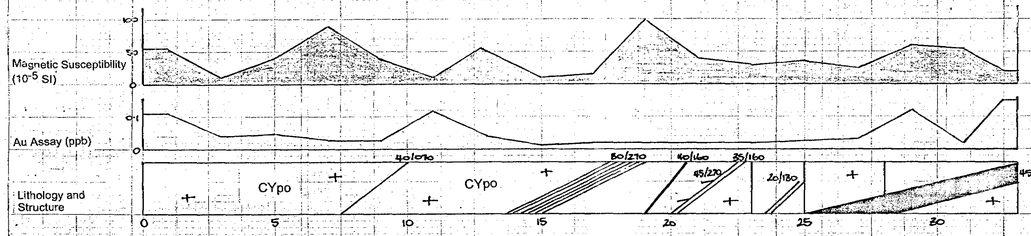

ADIT #3

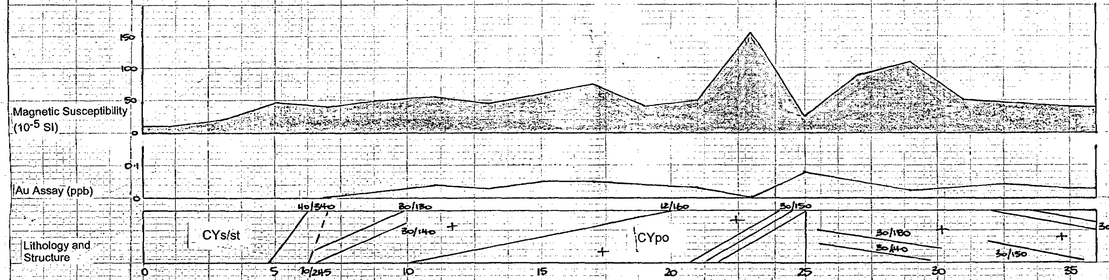

ADIT #2

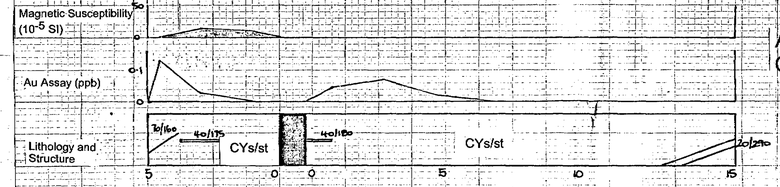

ADIT #1
CROSS-CUT

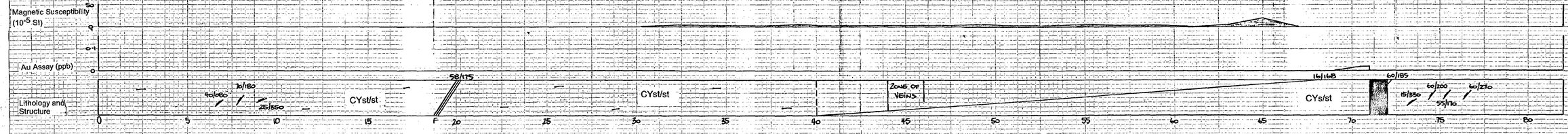

ADIT #1
MAIN DRIVE

0 1 2 5
SCALE IN METRES

5 cm

LEGEND

- CYpo — Yolande River Sequence Quartz-feldspar-biotite porphyry
- CYs/st — Yolande River Sequene Volcaniclastic sandstone
- CYst/st — Yolande River Sequence siltstone
- Quartz Veins + Dip/Dip direction
- Fault
- Joints + joint direction
- Lithological contact

ATTACHMENT

THE GEOLOGY, GEOCHEMISTRY AND MAGNETIC CHARACTER OF YOLANDE RIVER SEQUENCE PORPHYRIES

ASHLEY GRIFFITHS

BSc HONOURS THESIS

The geology, geochemistry and magnetic character of Yolande River Sequence porphyries, northwest of Queenstown.

Ashley Griffiths (B.Sc.)

University of Tasmania

A research Thesis submitted in partial fulfilment of the requirements of the Degree of Bachelor of Science with Honours.

Centre for Ore Deposit Research (CODES SRC)

School of Earth Sciences

University of Tasmania

November 1998

ABSTRACT

Porphyritic units sampled, crop out at seven locations within the study area. The units lay within a defined area north of the Pearl Creek Fault and south of the township of Lake Margaret, northwest of Queenstown. Rhyolitic, quartz-feldspar-biotite and dacitic, quartz-feldspar-hornblende mineralogies characterize the two porphyry types. Regular north-south porphyry orientation concurs with dominant volcaniclastic and sedimentary host rock bedding direction, implying sill-like intrusive structures. Peperitic basal and upper contacts infer intrusion into wet, unconsolidated sediment, as burrowing lavas or sill-like intrusives.

Regional mineralogies are affected by pervasive-sericite and selective chlorite alteration. Both porphyry types show complete to partial sericitisation of feldspar crystals. A crude cleavage is developed by alteration of primary feldspar matrix by muscovite. Dacitic porphyries have undergone selective chlorite alteration of hornblende, but retain primary textures. Embayed quartz crystals in both porphyry units indicates extended periods within melt and subsequent resorption.

Whole rock and trace element analyses show consistencies with petrographical and field observations of the two porphyry compositions. Rhyolitic and dacitic divisions, group within previously characterized Suite I and Suite II classifications for the Mount Read Volcanics respectively.

Dacitic porphyries show high magnetic response in contrast with rhyolitic porphyry units. Magnetic responses of dacitic porphyries, occur due to primary composition, fine-grained magnetite, absent in rhyolitic porphyries.

Quartz vein-type gold mineralisation is recognised within the most altered porphyritic unit, at Diamond Hill. Gold is also present within the porphyry unit itself, and is inferred to have been added during hydrothermal alteration. Anomalous strike direction of this unit suggests structural control during emplacement. The subsequent quartz vein concentration at this site, is inferred to have also been localized due to this structure, and occurred post magmatism.

DEDICATION

This thesis is dedicated to my family and relatives who have offered me invaluable support and encouragement throughout not only my honours career, but my entire education.

In particular to my parents, Marie and Arthur, and my sister Sondra. I would like to extend my love for their continual support in my chosen career, and belief in my ability. Without the affection and assistance of these special people, this thesis would never have been completed.

AKNOWLEDGEMENTS

Firstly, I would like to extend my thanks to Walter Herrmann, my honours year supervisor. Wally has not only given me his time, but his knowledge and patience, throughout my field work and the development of this thesis. Assistance in petrography and geochemistry, along with interpretation of all facets of my thesis have been invaluable and in excess of that expected of a supervisor.

Thank you to the Exploration Department and all staff of Copper Mines of Tasmania Pty. Ltd. This honours project has extended my knowledge and hopefully been of benefit to the company overall.
The few years that I have frequented Queenstown have been both enjoyable and educational, in the work and social sense. Friends that I have made during this time will always be valued and remembered. Special thanks to Peter, Paul, Wil, Al, Mark, Troy, Ted, Dutchy, Dan, Jason and Eddie who have shared their skills and resultantly helped build my own.

To my friends and fellow students best of luck and thank you for the great undergraduate years and the honours experience. Thanks to my mates in the geology department and my Nelson Road flatmates for keeping me sane and still socially active during the most tedious times.

Thankyou to John Everard, Mineral Resources of Tasmania (MRT), for geochemical data and thin sections made available from the study area.

Love and thanks to Kellie for her help in getting the final thesis together, her support during hard times, and most of all for her wonderful company during a stressful but enjoyable year.

Last and importantly, I would like to especially thank Ken Morrison for his time, patience, generosity, and more importantly friendship. From my initial contact with Copper Mines of Tasmania and throughout my honours year, you have kept me inspired and confident. For the skills and knowledge I have acquired from your tutorage I am grateful.

TABLE OF CONTENTS

APPENDICES

LIST OF FIGURES

LIST OF PLATES

PAGE

LIST OF TABLES

PAGE

LIST OF MAPS

CHAPTER 1 : INTRODUCTION

1.1 AIMS

The primary aim of this project was to investigate the geology, geochemistry and magnetic character of several bodies of porphyritic volcanic rocks within the Mount Read Volcanics, northwest of Queenstown (Figure 1.1).

A secondary aim was to determine if a genetic relationship exists between the porphyries and quartz vein-type gold mineralisation known in the area.

1.2 THE STUDY AREA

The 20 km^2 study area lies within a 64km^2 exploration license, EL 27/95 Yolande River (Figure 1.2), held by Copper Mines of Tasmania Pty. Ltd. The study area is bounded by the Murchison Highway to the east, the Yolande River to the north, a major fault (Firewood Siding Fault) to the south and the extent of known porphyries to the west.

The area is relatively flat, with Diamond Hill standing out as the major topographical high landmark. The Yolande River is defined by substantial hill slopes and scattered cliff faces.
Vegetation is dominated by thick regrowth scrub, developed as a consequence of fire denudation. Belts of rain forest are preserved within some creeks and along the Yolande River.

Access to the area was obtained by several 4WD vehicle tracks connected to the Murchison and Lyell Highways. Most of the field work was centered around Diamond Hill (Figure 1.3) where some exploration grid lines and walking tracks were utilized. A grid line to the north of Diamond Hill was also utilized during exploration and research.

577043

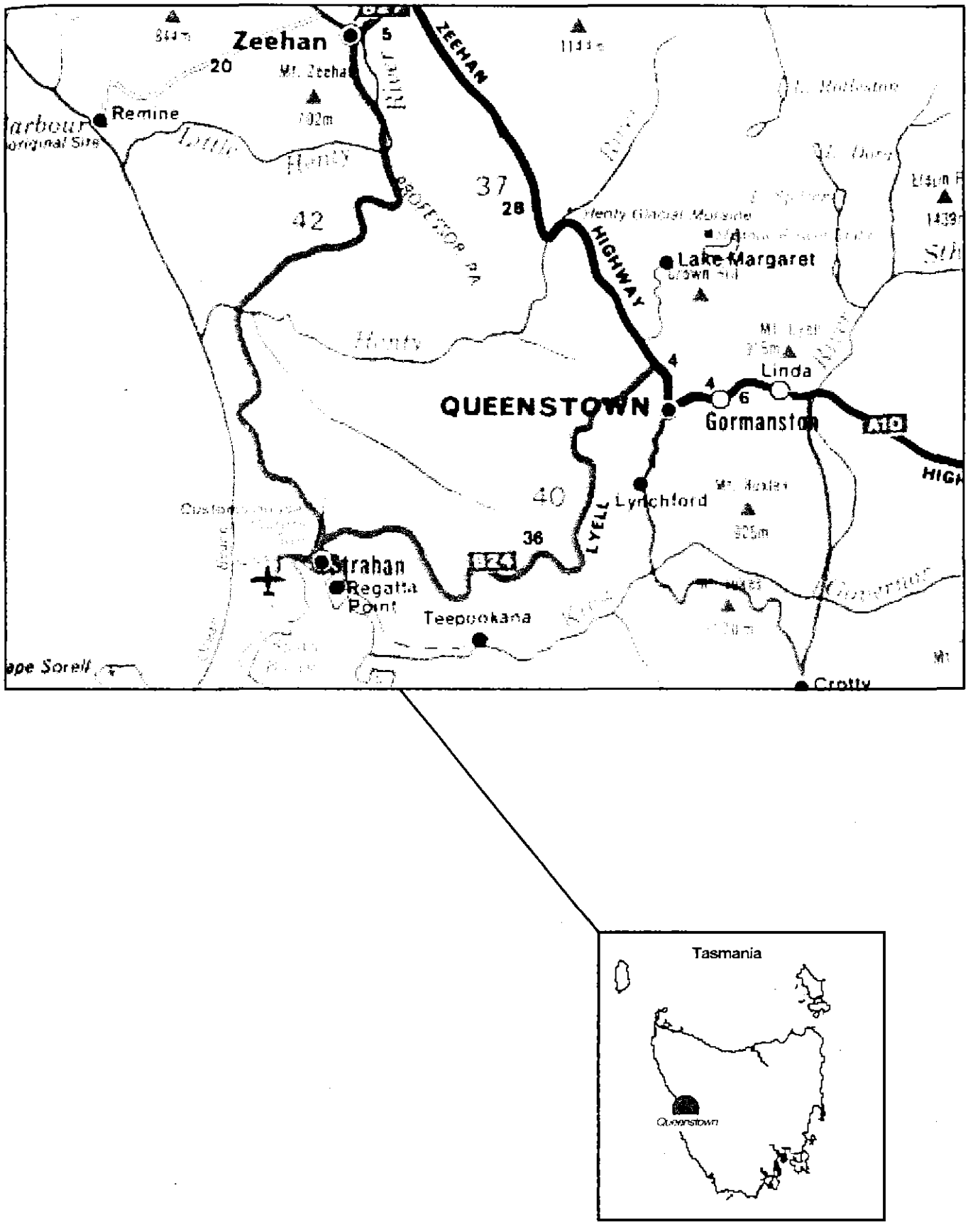

Figure 1.1 - Locality Map of Queenstown, nothwest coast Tasmania.

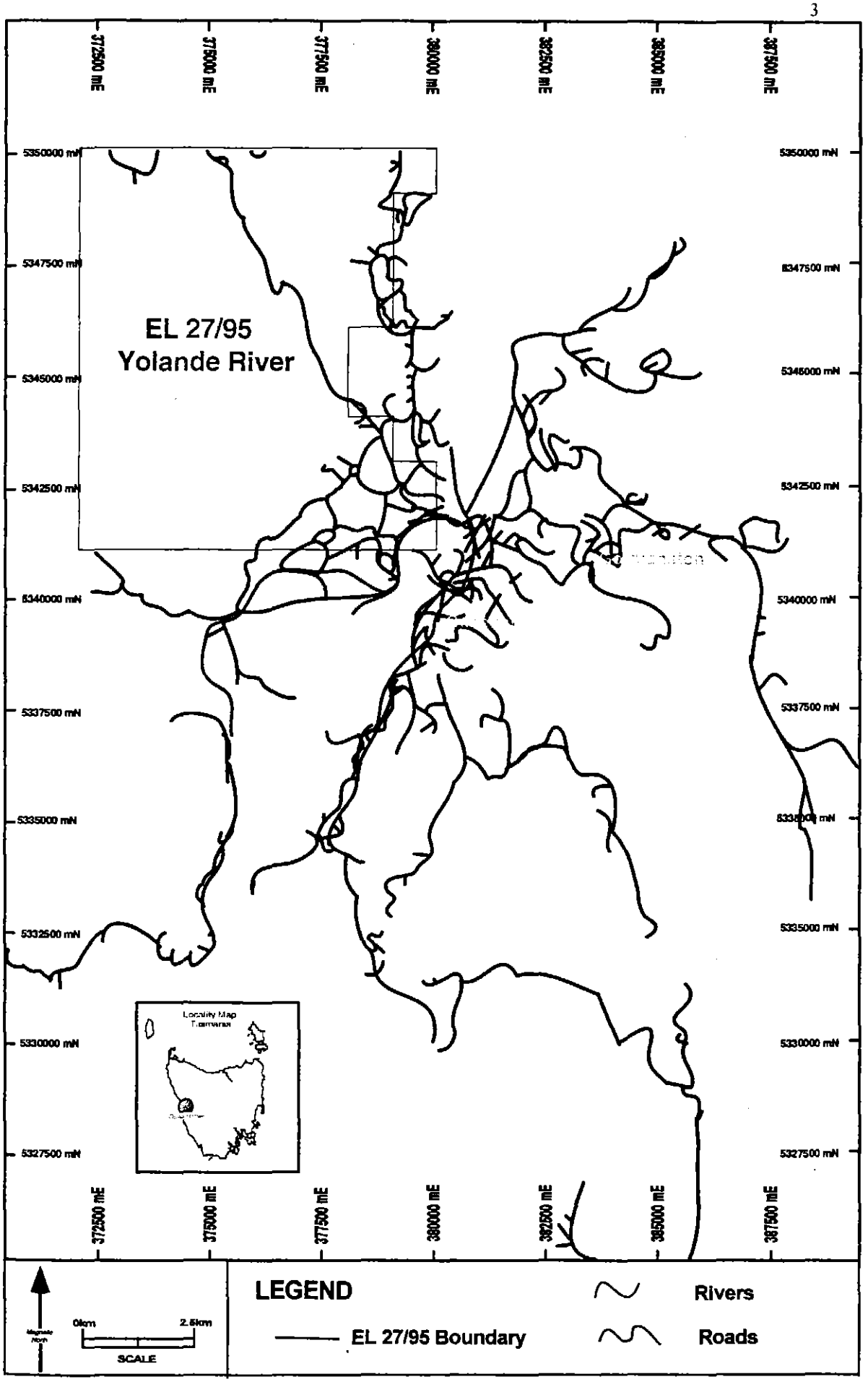

Figure 1.2 - Location of EL 27/95 Yolande River with respect to Queenstown. (After Geol. Surv. Tas. Q'town 1:25000 and Mt Read Volc. Proj. Map 6, 1:1000).

5 cm

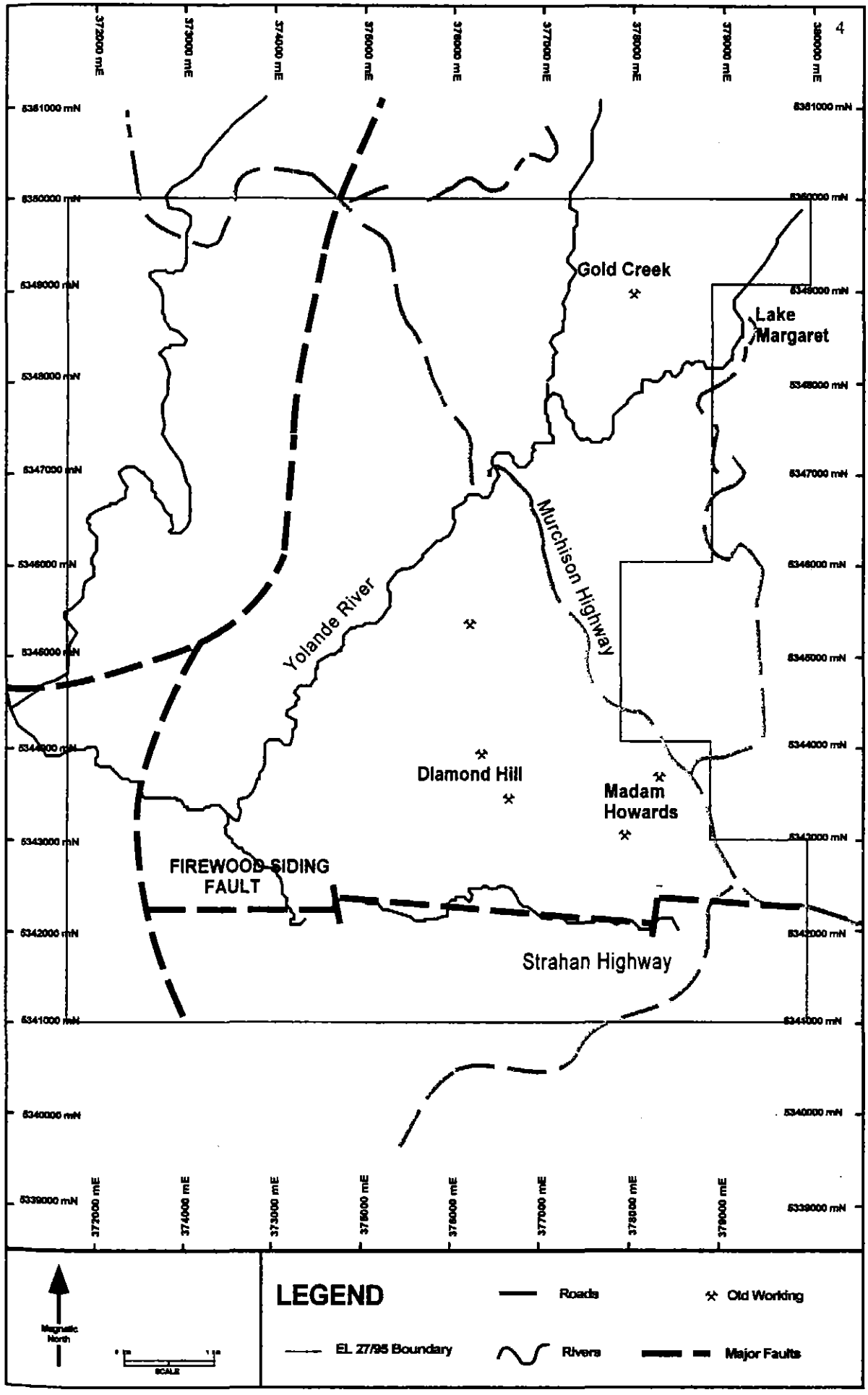

Figure 1.3 - Geographical features and locations within EL 27/95 Yolande River. (After Geol. Surv. Tas. Q'town 1:25000 & Mt Read Volc. Proj. Map 6, 1:100000)

5 cm

1.3 METHODOLOGY

The study was conducted in three phases. An initial phase of field work consisted of mapping, outcrop and adit rock chip sampling and soil and magnetometer surveys.

Samples collected in the field were analyzed by a combination of trace and major element assays and thin section petrography. Magnetic data were plotted as line profiles.

The final phase involved interpreting the geological, geochemical and magnetic data acquired in this study, together with existing data and literature made available to the writer.

CHAPTER 2 : REGIONAL GEOLOGY

2.1 INTRODUCTION

The study area lies in the Queenstown region, among the Mount Read Volcanics (MRV). The MRV are dominated by rhyolite, dacite and andesite volcanics, (Corbett and Solomon, 1989). The MRV host many economic deposits of the West Coast of Tasmania, and form part of an area known as the Dundas Trough (Corbett & Turner, 1989). The Dundas Trough is bounded to the east by the Tyennan Region, and to the west by the Rocky Cape Region (Corbett and Turner 1989). The relationships of major units of the Dundas trough are shown below in Figure 2.1.

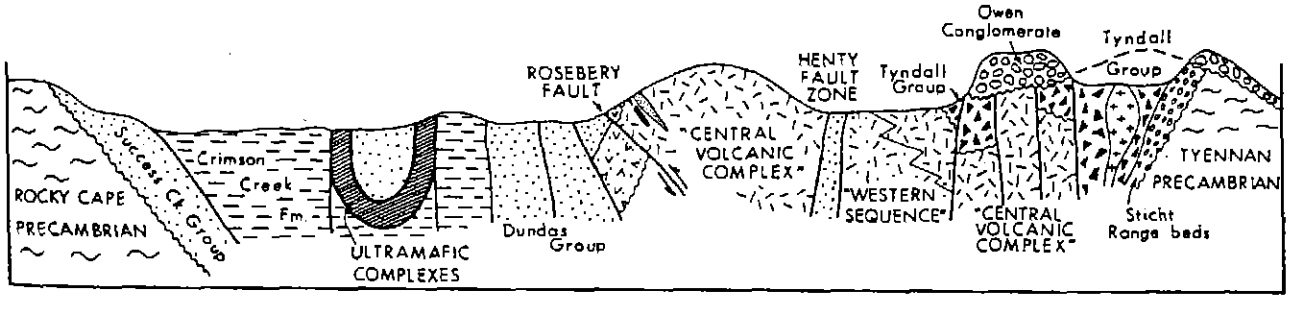

Figure 2.1 - Cross-section showing elements of the Dundas Trough, between the Pieman River and Mt Read. Not to scale. (Corbett and Turner IN Burrett & Martin, 1992).

2.2 MOUNT READ VOLCANICS

The Mount Read volcanic belt is around 200 kilometres long and 20 kilometres wide (Crawford et al., 1992) The belt lies along the western and northern margin of a Precambrian basement known as the Tyennan region. The MRV interfinger westward with Cambrian volcano-sedimentary sequences of the Dundas trough. The MRV can be thought of in terms of four lithologic associations; The Eastern Quartz-Phyric Sequence; The Central Volcanic Complex; The Western Volcano-Sedimentary Sequences; and The Tyndall Group (McPhie & Allen, 1992; Corbett, 1992). The Western Volcano-Sedimentary Sequence encompasses the area of interest in this report and will be further described within subsequent chapters.

2.2.1 Eastern Quartz-Phyric Sequence

Units of the Eastern Quartz-Phyric Sequence (EQPS) are mainly composed of quartz-feldspar phyric lavas, volcaniclastics and porphyritic intrusives (Crawford et al., 1992; Corbett, 1992). Other units of sandstone, siltstone and mudstone exist within the sequence and indicate subaqueous conditions (Corbett, 1992). The sequence is known to have an interfingering and erosional relationship with the Central Volcanic Complex (Corbett, 1992; Corbett et al., 1993).

2.2.2 Central Volcanic Complex

The Central Volcanic Complex (CVC) is made up of predominantly feldspar-porphyritic volcanics, with sparse lavas and volcaniclastics (Corbett, 1992). Extrusive and intrusive porphyritic andesites exist near the Tyndall Range and also Queenstown (Corbett and Less, 1987). Potassic rhyolites, weathered pink, exist as prominent ridges and carry some chalcopyrite-pyrite mineralisation (Corbett and Less, 1987). Units of the CVC interfinger with the Western Volcano-Sedimentary Sequence to the west, and the EQPS to the east (White, 1975; Corbett, 1992; Crawford et al., 1992).

2.2.3 Western Volcano-Sedimentary Sequence

The Western Volcano-Sedimentary Sequence (WVSS) consists of mass-flow deposits, turbiditic sandstones, tuffaceous mudstones, micaceous siltstones, and graphitic shales (Corbett, 1992). Felsic and andesitic lavas, breccias, and large intrusive porphyries exist within some areas (Corbett, 1992). The WVSS has been divided into sub-units according to location. The Dundas Group; Mount Charter Group; and Yolande River Sequence, make up the three classified by Corbett (1992). Pyroxene-phyric basaltic andesites exist in three areas, south of Queenstown near the base of the Tyndall Group (Corbett and Lees, 1987). The WVSS underlies the CVC south of Queenstown, but appears to interfinger with the CVC to the north (Corbett and Lees, 1987).

2.2.4 Tyndall Group

The Tyndall Group (TG) consists of crystal-rich sandstones and breccias, with abundant volcanolithic conglomerates in the upper section (Corbett, 1992). The TG has been interpreted as the final stage of volcanism in the MRV (McPhie and Gemmell, 1992; Pemberton and Corbett, 1992). Middle Cambrian trilobite fauna in a basal limestone unit (Jago et al., 1972), justify a shallow-marine environment on the perimeter of a subaerial volcanic chain, as the likely area of deposition. Volcaniclastic units in the EQPS and the TG are indistinguishable (Pemberton and Corbett, 1992), which suggests a relationship between these units. The TG overlies the CVC (White, 1975, Corbett, 1992).

2.3 REGIONAL STRUCTURE

Deformation throughout the Mid Cambrian-Early Ordovician developed a Mid Cambrian and the Jukesian Unconformity, which separate MRV from the Tyndall Group, and MRV from overlying Owen Conglomerate respectively (Banks & Baillie, 1989; Corbett & Solomon, 1989; Corbett & Turner, 1989).

Two stages of Devonian deformation are recognized in the Queenstown area (Berry, 1990). The D2 phase, changes from upright tight folding in Siluro-Devonian sediments, to steep faults in the CVC (Berry, 1990). D1 is related to thrusting and folding around the Mt. Lyell area (Berry, 1990).

The north-northeast trending Henty Fault, is the major fault which divides the MRV (Corbett & Lees, 1987). At Henty, the North and South Henty Faults meet, and the Great Lyell Fault is also intersected (Corbett & Lees, 1987). A single broad fault zone is evident at the joining of these faults (Corbett & Lees, 1987), and may be important with relevance to mineralisation in the area. All faults are recognized as Cambrian structures which have been subsequently reactivated during later orogenic events (Berry, 1989).

2.4 REGIONAL MAGNETICS

2.4.1 Data Acquisition

A regional helimag/radiometrics survey was flown by Pasminco Pty. Ltd. during 1993. The data was recorded at 80 metre nominal sensor height and 200 metre line spacing, on an E-W orientation.

The total magnetic intensity image in Figure 2.2 shows areas of low magnetic response in purple, with colour scale ranging through blue, green, orange to red for areas of highest magnetic intensity.

2.4.2 Magnetic Intensity Patterns

The main study area containing quartz-feldspar-biotite (Qfb) porphyries stretches along a low magnetic corridor, between two intense magnetic highs. All rhyolitic, quartz-feldspar-biotite, porphyry bodies within the main sample area lie within this corridor.

The magnetic high to the western side of the section corresponds with TG rock units. These units are dominantly sedimentary with minor volcaniclastics included in interbedded sections.

The eastern magnetic high is also within the YRS, over an area containing rhyo-dacitic porphyries and volcaniclastic units. The quartz-feldspar-hornblende (Qfh) porphyries show magnetic properties which are well indicated in regional magnetic images. Some boundaries to this unit have been mapped within the field, during ground magnetic surveys and during soil sampling exercises. Results of these analyses are indicated within Chapter 6.

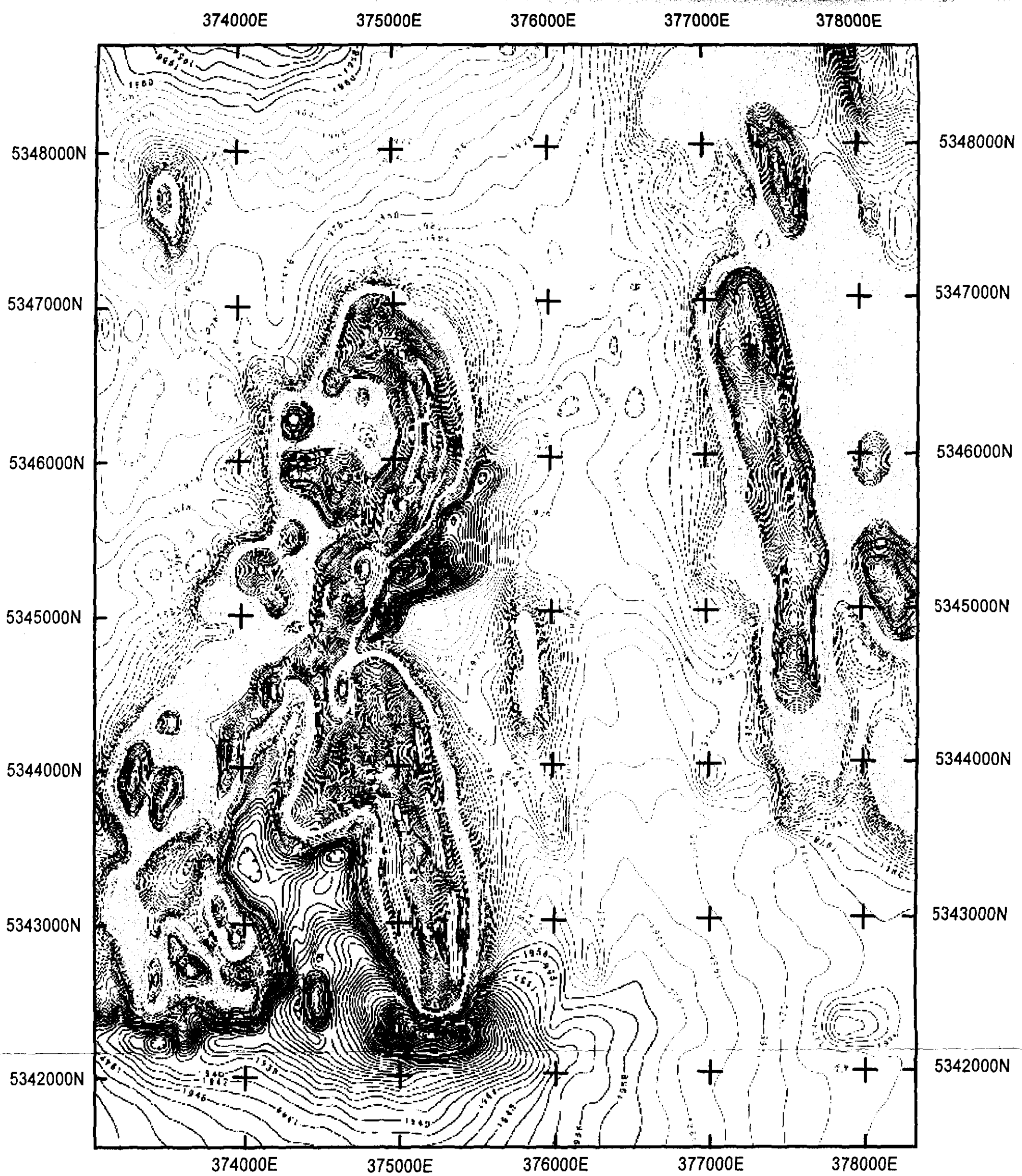

Contour Interval = 2 nT

Blue represents lowest magnetic response

Red represents largest magnetic response

Figure 2.3 - Regional total magnetic intensity (TMI) image of central region of EL 27/95 Yolande River.

2.4.3 Structural Interpretation

The majority of the regional magnetic image shows north-south trending magnetic responses. Variation in the magnetic intensity of responses is between 1882 and 2102 nT.

Interpreted cross-cutting major structures are scattered through the regional magnetic image (Figure 2.3). Magnetic features to the south of the map are terminated by the east-west Pearl Creek Fault. Similarly, the direction of the Yolande River appears to be controlled by a major north-east, south-west trending inferred structure. Anomalous low magnetic responses occur along both of these structures.

The major north-east, south-west structure terminates east of the Murchison Highway-Yolande River junction, where dominant north-south magnetic responses are evident. This structure marks the boundary of change from Qfb porphyry in the north, to Qfb porphyry in the south (Figure 2.3).

Movement along this major structure may be interpreted due to folding in the TG magnetic response. To the north of this structure the units would be interpreted to have moved in a north-easterly direction.

2.4.4 Summary And Conclusions

It appears unlikely that Qfb porphyritic units can be identified from regional magnetic images, due to their low magnetic response.

High magnetic responses arise from Tyndall Group rocks which lie to the west of the central corridor of low response.

High magnetic responses to the east of the low central corridor can be related to Qfh porphyry units, which are recognizable from aeromagnetic images. These bodies may not however be discriminated from other magnetically responsive units without adequate mapping of geology in the field.

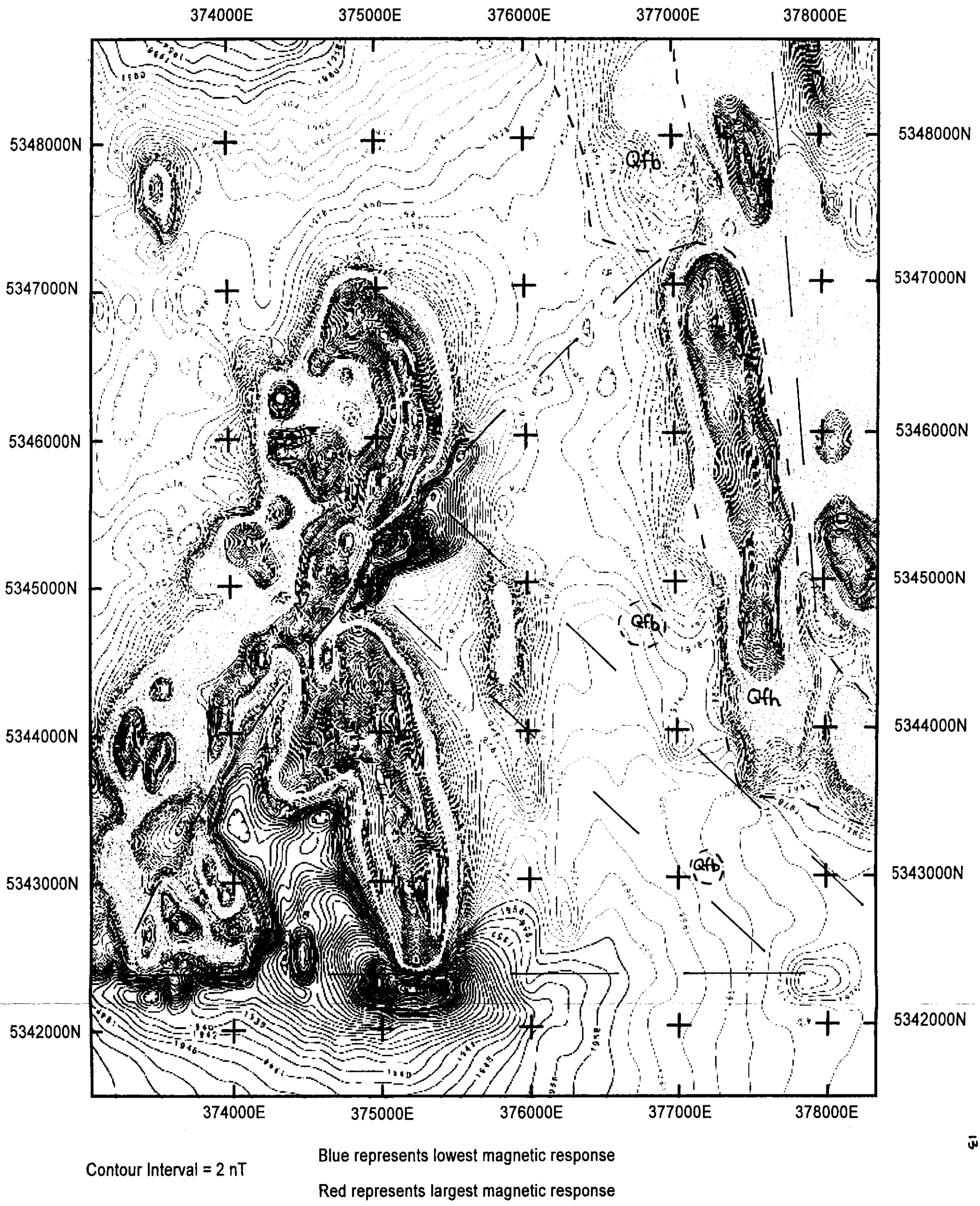

Figure 2.3 - Regional total magnetic intensity (TMI) image of central region of EL 27/95 Yolande River, with interpreted faults and porphyry units. Qfb=Quartz-feldspar-biotite porphyry; Qfh=Quartz-feldspar-hornblende porphyry.

Structural controls over porphyry units are evident in some areas, such as the intersection of the Yolande River and the Murchison Highway. In other cases, such as the Qfb porphyries cropping out in the low magnetic corridor, there may be fault controlled orientations imposed during emplacement.

It is likely that some structural control has affected the positioning of most of the YRS porphyry units during emplacement, however evidence for this is restricted to a minority of the units.

CHAPTER 3 : HISTORY OF EXPLORATION

3.1 HISTORICAL OVERVIEW

This overview has been compiled from records within the Copper Mines of Tasmania library and from references at MRT.

~1900

Prospecting on auriferous quartz veins occurred at both Diamond Hill and Gold Creek prospects, around the turn of the century. Production amounts are unknown but probably minor (Groves 1964).

Adits have been dug in to the Diamond Hill prospect following major quartz veining. Four adits are present, ranging from 10 to 82 metres in length. Several other smaller scale prospects are visible in the region, such as Sisters Hills, Raggedy Ann, and Madam Howards.

Effective exploration since 1971 has been conducted by four companies - Mt. Lyell Mining and Railway Company Ltd./Gold Fields Exploration Pty Ltd., Cyprus Minerals Australia, Pasminco Exploration, and Copper Mines of Tasmania Pty. Ltd. on five exploration licenses EL's 9/66, 47/71, 11/85, 25/91, and 27/95.

1971

The area was held by Mt. Lyell Mining and Railway Company between the years of 1971 and 1983, as EL 47/71 until 1976 and later as part of EL 9/66. They discovered gossan like outcrops near the junction of the Lyell and Murchison Highways (Brophy & Stephens-Hoare, 1976).

Between 1973 and 1975 around 80 stream sediment samples were taken within the EL. These were assayed for copper (Cu), lead (Pb), zinc (Zn), cobalt (Co)

and nickel (Ni). One Zn anomaly of 115 parts per million (ppm) was found in Gold Creek (Brophy & Stephens-Hoare, 1976).

A 7 line (6.4 km) grid was cut over the Madam Howards prospect. Induced potential (IP) and magnetics surveys were conducted, and discovered one moderate and seven weak IP anomalies. No correlation between resistivity and rock type was noted (Howland-Rose, 1974).

Follow up soil sampling surveys were conducted across six of the IP anomalies. One anomalous Pb value of 200 ppm was recorded.

Rock chip sampling was conducted at the Diamond Hill and Sisters Hills workings. These recorded one quartz-vein gold anomaly at Diamond Hill and several base metal kicks at both localities (Sheppard, 1974 and 1975).

A helicopter Dighem survey was flown over the area in March 1980. Total coverage encompassing 344 line km at 150 metre interval line spacing. A total of 55 weak anomalous responses were recorded. These were divided into 4 definite and 8 possible geological anomalies, 19 responses due to surface effects and 24 due to cultural effects. The data was re-interpreted by John Bishop, (1981) (Mitre Geophysics), who inferred another 201 non-cultural anomalies and downgraded 3 of the supposed geological anomalies.

Between 1981 and 1983, 379 stream sediment and 72 rock chip samples were assayed for base metals, with some tested for gold (Au) as well. Five anomalous sites were recognized (Purvis *et al.*, 1983).

- Gold Creek showed anomalous Zn in stream sediments (maximum 330 ppm) and 1.2 ppm Au in rock chips. Alluvial gold workings were found in the anomalous area.
- In Pearl Creek, anomalous Cu, Pb and Zn (up to 1050 ppm Cu) values were found in stream sediment samples.
- A creek south of Madam Howards barite prospect yielded one anomalous value of 1.2 ppm Au.
- From creeks draining the Sisters Hills workings, a single 270 ppm Zn value was recorded from stream sediment samples.
- Two sites in Truscott Creek yielded high Zn values in stream sediments. With one site also recording high Cu levels also.

1983

Gold Fields Exploration were operating EL 9/66 by 1983. Further drainage and rock chip sampling around anomalies and known workings were undertaken. This work concluded that only the Zn anomaly in Gold Creek and the Cu anomaly in Pearl Creek deserved follow exploration. The Au anomalies were considered real and unexplained (Purvis, Fitzgerald *et al.*, 1983; Purvis, Jones *et al.*, 1983; Meares *et al.*, 1982).

1985

The area was operated by Cyprus Minerals Australia Company, a subsidiary of Amoco, during 1985 as part of EL 11/85. The company targeted the Sisters Hills prospect between 1987 and 1989, conducting rock chip sampling. Assays for Au, As, Sb failed to yield any results above minimum level of detection (Calver, 1995).

1990

A Joint Venture on EL 11/85 resulted in Pasminco Exploration operating between 1990 and 1995.

A helimag/radiometrics survey by Geoterrex Pty Ltd. was conducted during 1993. A nominal sensor height of 80 metres and 200 metre line spacing were used on an E-W orientation. Results were interpreted by David Leaman (Leaman Geophysics), who produced three main conclusions.

-Sedimentary units have low magnetic background and are interbanded with high magnetic tuffs. A major synform, shaped by NE, NW and subordinate E-W structures, has been defined from magnetic contrasts.

- Dominant N-S trends are found in volcanic units to the east. These units are distinct both structurally and magnetically from others in the region.

- Between the volcanics and the sedimentary tuffs porphyry units can be recognized.

Pasminco relinquished EL 21/95 in mid 1995 after collating all prior stream sediment survey sites (Quayle, 1985; Fitzgerald and Poltock, 1991).

1995

Since acquiring EL 27/95, Copper Mines of Tasmania Pty. Ltd. have conducted further stream sediment sampling, surface rockchip and quartz vein sampling, soil sampling and performed ground magnetic surveys in promising areas (Morrison & Griffiths, 1998). The aim of exploration being to find gold mineralisation thought to be related to porphyry units in the Yolande River Sequence. Gold mineralisation with porphyry units is evident at old workings; Diamond Hill and Gold Creek, forming some of the philosophy behind exploration for such units.

Adits on Diamond Hill have been channel sampled and mapped. Diamond Hill surface mapping and regional mapping has also been conducted. The author has been involved in most of these operations, therefore further analysis of exploration and results will be discussed within subsequent chapters.

CHAPTER 4 : MAPPING

4.1 REGIONAL MAPPING

Mapping of geology, has mainly been derived from outcrop and subcrop sighted during expeditions in to the field area, Map 1. Grouping this information together with data collected during soil and rockchip sampling, gives an accurate indication of dominant rock types and aided in the development of the regional interpretation, Map 2.

4.2 LITHOSTRATIGRAPHY AND VOLCANIC FACIES

4.2.1 Host Sequence

The host sequence is a series of interbedded volcaniclastics and sedimentary units. The prevalence of these two units fluctuates throughout the study area, being prominantly sedimentary in the west, and volcaniclastic in the east. Major strike direction of beds is of north-south orientation, throughout the study area. Younging direction is generally west, although is easterly in several places where tight folding is evident.

4.2.1.1 Volcaniclastic Pumiceous Sandstone

Volcaniclastic pumiceous sandstone is cream and yellow coloured in hand specimen. Colouration is due to dominant clasts of feldspar and chlorite-altered pumice fragments.

Major clasts range in size between 0.5 and 1 centimetre, and are dominantly rhyolitic in composition.

4.2.1.2 Volcanic Ash Tuff

Ash tuff is highly consolidated with layering evident in outcrop. Typical layers range between 2 and 30 centimetres. The tuff is gray to black and highly siliceous, as evident in assay value (Appendix II). Felsic composition and relict glassy fabrics identify the unit as being derived from volcanic origin. Layering evident in thin section suggests marine derivation, consistent with settings proposed for the MRV.

4.2.1.3 Volcaniclastic siltstone

Siltstone is one of the major outcropping units within the study area. Dominant north-south strike direction is recognized extensively, with near vertical westerly dipping beds.

The unit ranges in colour from pale gray to a pastel green. Weathering of outcrop is extensive, but most units maintain recognizable bedding.

4.2.1.4 Eldon Group Bell Shale

The Bell Shale outcrops at the southern extent of EL 27/95, below the Pearl Creek Fault, Figure 1.3. Dark brown to black in colour, this shale is rich in fossiliferous material. Brachiopod fossils are found throughout this unit and range in size between 0.5 and 3 centimetres. Predominance of brachiopod fossil shells indicates marine deposition.

4.2.2 Porphyritic Units

4.2.2.1 Quartz-Feldspar-Biotite Porphyry

Quartz-feldspar-biotite (Qfb) porphyries within the YRS contain visible quartz phenocrysts which are generally well dispersed. Phenocryst sizes range between 1 to 5mm, with anomalous quartz phenocrysts up to 1 centimetre. Porphyries with similar mineralogy within the area, vary in colour from a dull pink, through white and into a

pale lime green. Colouration is due to alteration from primary composition and reflects dominant mineralogy.

4.2.2.2 Quartz-Feldspar-Hornblende Porphyry

Quartz-feldspar-hornblende (Qfh) porphyries show a distinct colour difference from Qfb porphyries. This unit is a dark yellow to orange-brown rock with specs of green hornblende throughout. Most hornblende has been altered to chlorite, although relict hornblende texture is preserved, allowing identification.

The Qfh porphyry weathers to a rich clay soil, present on all identifiable boundaries. Although this creates problems for determining relationships with the host sequence, the weathered clay boundaries form readily identifiable positions for litholigical change.

4.2.3 Emplacement Style

The Qfb porphyry which crops out at the Yolande River Bridge - Murchison Highway intersection has traceable boundaries marked with peperitic textures. The unit is coherent and uniform, without brecciation, suggesting volcanic derivation. Peperitic contacts on upper and lower surfaces of the unit indicate that it has been emplaced into unconsolidated sediments, as a sill or burrowing lava (Appendix 1 - Literature Review).

Absence of quench fragmented tops and lateral breccias of equivalent composition, suggest that the magmas were not erupted and only intruded at high levels, therefore indicating the likelihood of the unit being a sill.

The dimensions of the Qfh porphyry, located south of the Yolande River Bridge are equivalent to those of the Qfb porphyry cropping out at the river-bridge intersection. Increased weathering of this porphyry and surrounding host rocks at contacts, have erased exposure of any contact relationships. The similarity in size, locality and dominant strike direction of this unit with regards to the Qfb porphyry sill to the north, suggest that the likely style of emplacement of this porphyry unit is as a sill also.

Other outcrops of less extensive Qfb porphyries are exposed within the study area. Outcropping Qfb porphyries of this size are indicative of sill-like or pipe-like intrusions. The Qfb porphyry located at Diamond Hill has an undisturbed contact, visible within an old adit. Surrounding volcaniclastic pumiceous volcaniclastic rocks show no signs of alteration or disturbance along the contact. Faulting along the major identified boundary of this porphyry may have accounted for any alteration of surrounding host rock.

The contact here is visible over a distance of two metres, remains near vertical and north-south striking. This conforms with dominant bed dip and dip direction in the vicinity, although no bedding readings can be made within the pumiceous unit.

4.2.4 Basalt Units

Three basalt bodies are located along the Firewood Siding Fault. Non-vesicular in hand specimen, the basalts display large crystals of pyroxene and plagioclase.

4.3 CONCLUSIONS TO REGIONAL MAPPING

Major developments from the regional mapping of EL 27/95 include:

- The extension of the Qfh porphyry (P4, Map 2) which outcrops along the Murchison Highway between the Yolande River Bridge and the Strahan turnoff. Extension of this unit is based on data gathered during field exploration and sampling surveys.

- The extension of the Diamond Hill porphyry (P1, Map 2) to the north of previously interpreted boundaries for this unit. Previously mapped as a pipe-like intrusive, and subsequently mapping as a circular unit, it is apparent that the porphyry body extends to the north-west (Map 2) and is more sill-like in shape.

- The re-evaluation of porphyry unit P5 (Map 2), from a Qfh unit to a characteristic Qfb porphyry. Evidence for the re-evaluation of this unit is founded by petrographical and geochemical analysis.

4.3 LOCAL MAPPING

Local surface mapping of the Diamond Hill region has been interpreted with subsurface adit mapping so as to project a basement geology for the immediate area, Figure 4.1. Outcrop geology which aided in the derivation of a local map is shown in Figure 4.2.

4.3.1 Adit Mapping

The 4 adits located on Diamond Hill (Figure 4.3) expose three different rock types and two lithological contacts, Map 3.

Rock types studied during adit mapping were a volcaniclastic siltstone, volcaniclastic pumiceous sandstone and a Qfb porphyry unit. The contacts between siltstone-sandstone and breccia-porphyry are undisturbed and appear conformable. No evidence of bedding or cleavage are contained within any units contained within adits on Diamond Hill.

Adit number 1 contains the first lithological boundary, between siltstone and sandstone volcaniclastics. The boundary occurs 40 metres in from the adit entrance. Volcaniclastic sandstone makes up the remaining 42 metres of Adit number 1 main drive. Jointing within this sandstone units is less dominant than within the volcaniclastic siltstone unit.
One cross-cutting drive is located within this adit at 72 metres. To the left this drive continues for 5 metres, and to the right 15. The cross-cutting drive has been extended along the surface of a steep, westerly dipping, quartz vein .

Adit number 2 contains the recognized boundaries between volcaniclastic sandstone and Qfb porphyry. This contact dips 70 degrees south-west and strikes at 245 degrees.

Adit number 3 consists of Qfb porphyry. This adit changes direction and chases a quartz vein at 23 metres, similar to the cross-cutting drive in Adit number 1.

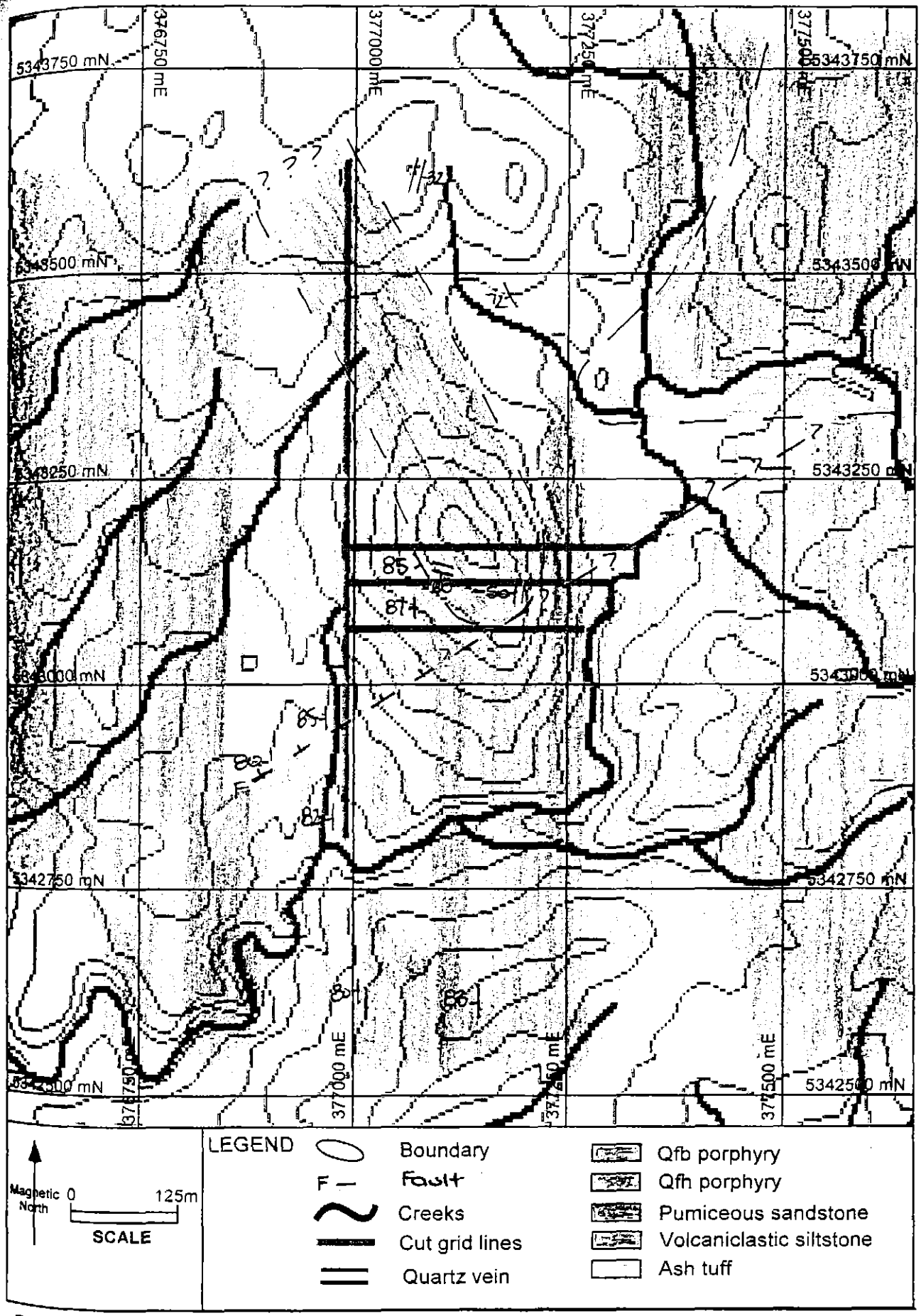

Figure 4.1 - Interpreted local geology of the Diamond Hill area.

5 cm

577066

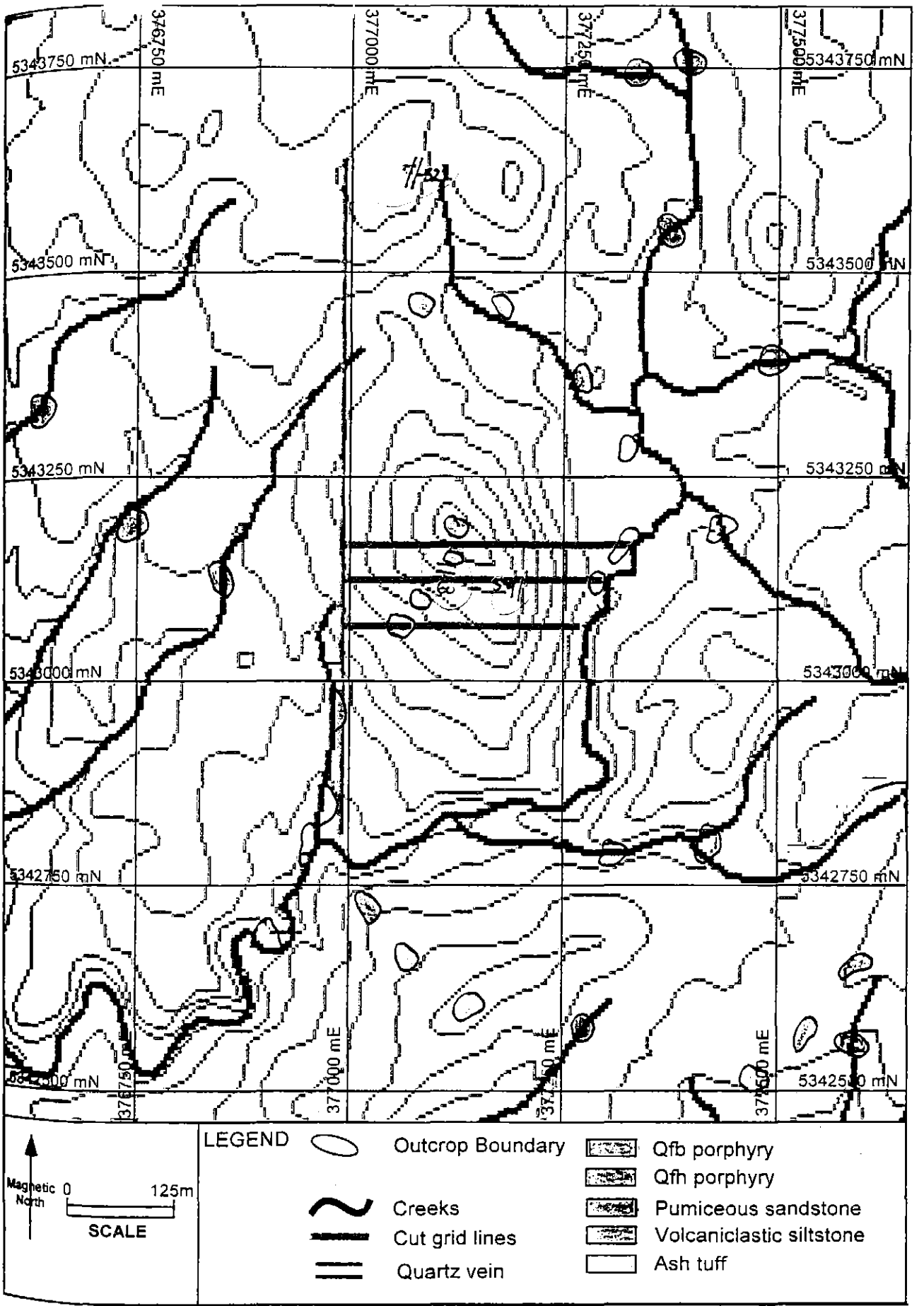

Figure 4.2 - Outcrop local geology of the Diamond Hill area.

5 cm

577067

577068

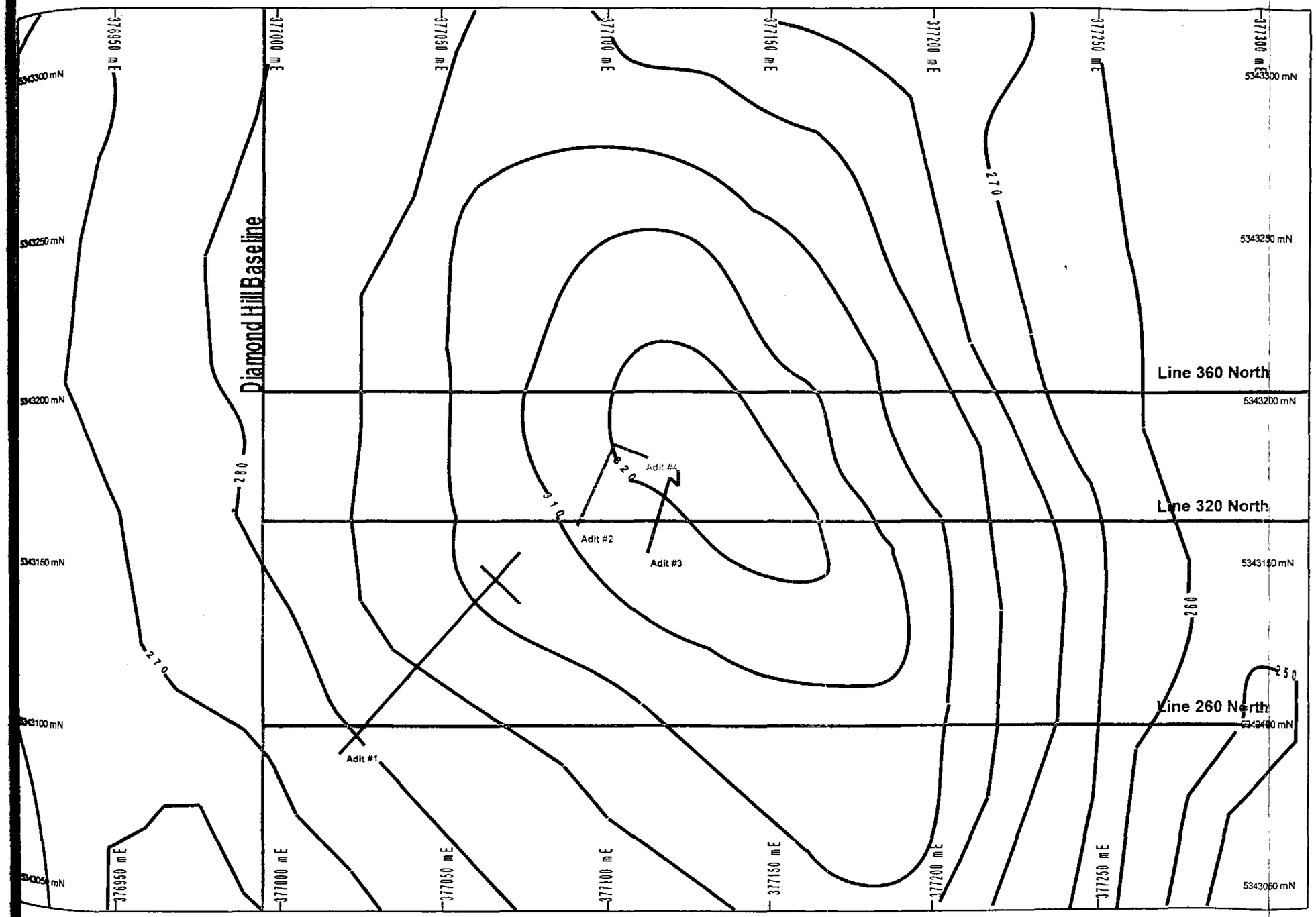

Figure 4.3 - Location of Diamond Hill adits with respect to grid lines (After Morrison and Griffiths, 1998).

The porphyry unit is highly weathered/altered and contains no visible structures. Quartz veining which is dominant around the Diamond Hill area is increased within the Qfb porphyry in comparison to the two other lithologies.

Adit number 4 is fully contained within the porphyritic unit and contains quartz veining of similar strike and dip to that contained within adit number 1.

Three different sized quartz vein types have been mapped within the four adits on Diamond Hill. No cross-cutting relationships within these groups could be identified.

4.4.2 Surface Mapping

A substantial soil covering and scattered outcrop in the Diamond Hill area make ground mapping difficult. Creeks containing outcrop and subcrop indicate the best picture of geology, (Figure 4.2). Quartz rich talus deposits cover a majority of Diamond Hill itself and blanket any geology underneath.

Bedding and facing of tuff in the western tributary of Diamond Creek is available. Rocks are facing west, dipping close to vertical and striking in a north-south direction.

Large quartz veins outcrop on surface section of the Diamond Hill prospect with strike and dip directions varying from

The dominance of Qfb porphyry is indicated by the topographic high of Diamond Hill. Surrounding this porphyritic unit are randomly scattered outcrops of volcaniclastic siltstone and pumiceous sandstone, most evident within tributaries of Diamond Creek on either side of Diamond Hill.

CHAPTER 5 : PETROLOGY

5.1 PETROGRAPHY

Analysis of thin sections were completed for primary mineralogy determination. Tabulated sample numbers and locations are found in Appendix III.

5.1.1 Host Sequence

5.1.1.1 Volcaniclastic Pumiceous Sandstone

Volcaniclastic sandstone (H4503, H4725 and H4741, Appendix II) is a distinct cream colour and contains pumiceous and feldspathic clasts as major components of the rock. Degrees of dominance of these two clast types vary with different outcrops. The sandstone contains 40-50% phenocrysts composed of quartz (10-15%), pumice pieces (20-30%) and feldspar (20-30%). Groundmass is dominantly sericitised and composed of minor quartz and feldspar crystals. Quartz veins and micaceous alteration zones crosscut major clasts.

5.1.1.2 Volcanic Ash Tuff

The volcanic ash tuff (H4724) contains ash sized particles, glassy shards and occasional lithic clasts. Particle sizes are less than 4mm and show orientation. Layering is present within hand specimen and thin section, alternating through dark and light bands, no greater than 10 mm in thickness.

5.1.1.3 Volcaniclastic Siltstone

Volcaniclastic siltstone (H4513 and H4726) contains glassy fragments, mudstone and quartz clasts. Euhedral to subhedral quartz crystals are up to 2mm in diameter.

Rock unit appears as pale grey to green in thin section and exhibits occassional relict primary bedding textures.

5.1.2 Porphyritic Units

5.1.2.1 Quartz-Feldspar-Biotite Porhyry

The Quartz-feldspar-biotite (Qfb) porphyry (H4613, H4614, H4733, H4735, H4736, H4738 and H4739) contains large quartz phenocrysts in thin section, with feldspar crystals either present or altered to sericite. Dominant feldspar and quartz phenocrysts in the matrix are surrounded, and pervasively altered, by muscovite. Scattered biotite is characteristic of this unit and separates it from the Quartz-feldspar-hornblende porphyry .

Quartz phenocrysts (up to 30%) are often embayed with muscovite altered matrix, or contain sections of muscovite altered melt inclusions, suggesting extended periods within the melt and consequent minor resorption.

5.1.2.2 Quartz-Feldspar-Hornblende Porphyry

Feldspar crystals dominate the mineralogy of this unit, with quartz always present but often scarce (H4610, H4732, H4737 and H4740, Plates 5.1 and 5.2). Hornblende is most commonly fully altered by chlorite, but retains relict crystal textures allowing identification. The presence of hornblende and magnetite, with an absence of biotite, is a diagnostic feature of this unit (Plates 5.1 and 5.2).

The matrix of this unit is identical in mineralogy to the Qfb porphyry, with a mosaic of feldspar and quartz crystals. Crystals are subhedral to euhedral, with boundaries often altered by pervasive muscovite. Muscovite lies between crystals in the matrix and forms a crude cleavage. The fine grained, hypocrystalline fabric suggests a fairly slow cooling intrusive.

Plate 5.1 – Plate of thin section H4610, (PPL). Large central quartz crystals shows sericite alteration around all edges. This implies extended periods in the melt, and subsequent partial resorbtion. Feldspar crystal in the bottom right corner has undergone total muscovite alteration. Hornblende crystal in the bottom left corner is partially chloritised and partially sericitised. Black flecks in the groundmass are magnetic and chlorite grains.

Plate 5.2 – Plate of thin section H4610, (XPL). Hornblende in the bottom left corner shows dark patches of chlorite alteration. The groundmass is a mosaic of primary feldspar and quartz crystals, with muscovite pervasive alteration in between. The muscovite forms a crude cleavage in some samples.

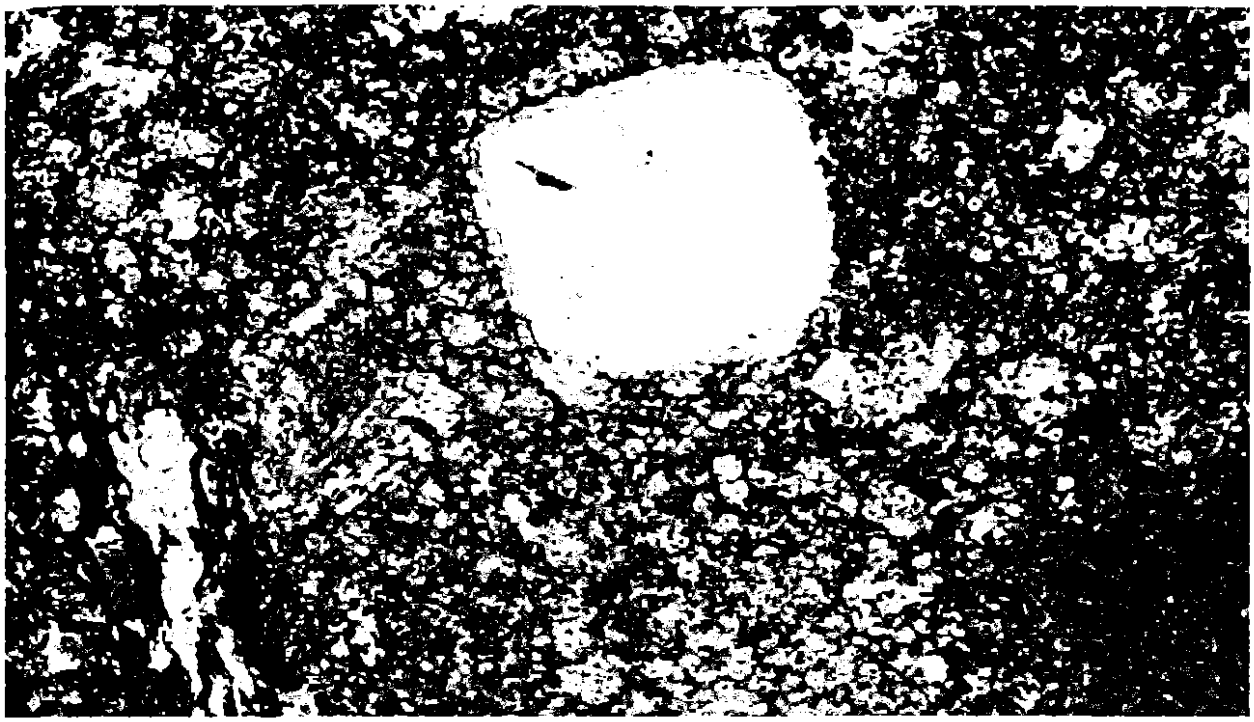

Plate 5.1

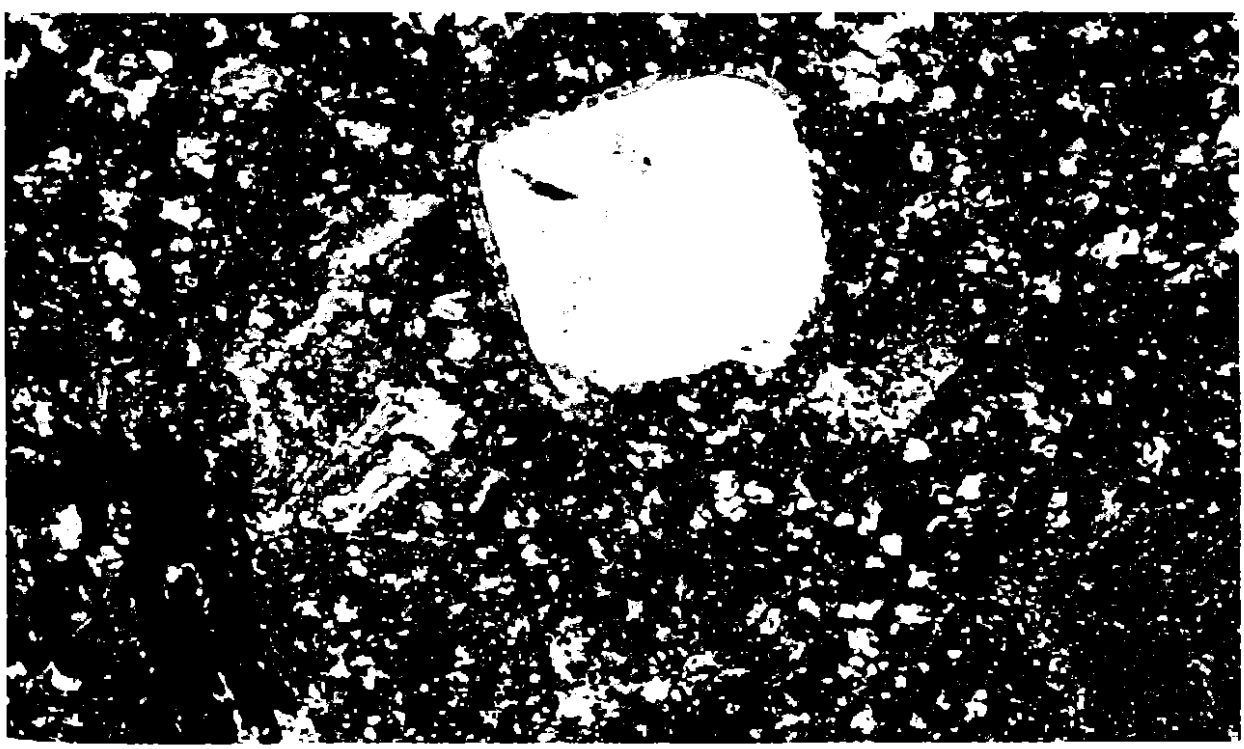

Plate 5.2

5.1.3 Basalt Units

Two basalt units cropping out along the Pearl Creek Fault contain dominant pyroxene crystals and minor plagioclase phenocrysts within a chlorite altered matrix (H4743 and H4744).

The two units are compositionally different, with respect to percentage of minerals. The basalt sampled from the Zeehan/Murchison Highway intersection (H4743) contains much less pyroxene (40-50%) and increased percentage of plagioclase (20-30%), than that which outcrops along the Pearl Creek Fault, pyroxene (70-80%); plagioclase (1-5%). Size of crystals also decrease within the basalt located at the highway intersection.

5.2 GEOCHEMISTRY

5.2.1 Introduction

Major and trace element geochemistry offers a means of comparing intrusive and extrusive rocks and their volcano-sedimentary associates. This can be used to characterize different suites, determine a fingerprint for the primary magma types, and assist in interpreting relationships between intrusive, extrusive and volcaniclastic units. Genesis and alteration history can be derived from plots comparing different element ratios.

When comparing graphs plotted with SiO_2 content along the x-axis, we may determine trends during fractional crystallization, provided that major element concentrations have not been substantially modified by hydrothermal alteration.
In hydrothermally altered rocks, some relatively immobile trace elements such as Ti, Zr and the REE which are likely to retain primary ratios, are more reliable indicators of magmatic affinity than the major components of the rock (Crawford et al., 1992).

The analysis of rock types in comparison with the work done by Crawford *et al.*, (1992), can help to identify different porphyries bodies and units of the YRS.

5.2.2 Whole Rock X-Ray Fluorescence

5.2.2.1 Sample Collection, Preparation And Analysis

Samples from four different porphyritic units, P1 to P4 (Map 2 - Interpreted Regional Geology), along with dominant host rocks, were collected during field work and analyzed at Analabs, Welshpool. All whole rock samples were first thin sectioned, so as the mineralogy of samples could be compared to dominant chemical signature after analysis. Wide distributions throughout the study area were favoured, so as to incorporate as many porphyritic units and lithologies as possible. Assay results for all sample units are shown in Table 5.1 and Appendix II.

Samples were prepared for analysis for elements SiO_2, TiO_2, Al_2O_3, Fe_2O_3, MnO, MgO, CaO, Na_2O, K_2O, P_2O_5 and Zr. Major elements were determined by glass fusion, XRF, and silicate rock analysis. Trace elements by pressed powder, XRF, and Trace determination.

Table 5.1 - Assay results for samples collected in study area.

Oxide	SiO_2	Al_2O_3	Fe_2O_3	MnO	MgO	CaO	Na_2O	K_2O	P_2O_5	TiO_2	Zr
Sample Number	%	%	%	%	%	%	%	%	%	%	ppm
H4503	65.31	17.34	4.76	0.03	1.07	0.18	5.19	2.54	0.09	0.35	314
H4513	73.90	12.05	3.25	0.02	0.81	0.00	0.16	5.43	0.02	0.30	190
H4514	71.96	15.35	0.69	0.00	0.25	0.06	1.69	3.62	0.01	0.26	289
H4610	63.85	14.86	6.49	0.10	2.78	0.10	2.10	4.29	0.11	0.39	245
H4612	75.34	14.81	1.49	0.00	0.45	0.01	1.38	3.41	0.03	0.23	268
H4613	75.41	14.04	0.98	0.00	0.36	0.02	1.53	5.19	0.03	0.17	186
H4614	76.65	13.14	1.84	0.04	0.34	0.02	1.07	5.05	0.04	0.17	181
H4724	78.73	10.41	2.69	0.04	0.76	0.52	0.00	3.69	0.04	0.18	181
H4725	69.70	14.27	3.72	0.12	0.85	1.48	1.32	4.29	0.08	0.26	248
H4726	72.56	11.57	3.36	0.10	1.11	1.89	1.29	3.70	0.07	0.27	216
H4732	65.48	14.73	5.31	0.05	2.78	0.08	2.41	4.19	0.07	0.42	252
H4733	73.99	15.9	1.33	0.00	0.46	0.00	0.06	5.06	0.04	0.19	198
H4735	73.28	16.74	1.18	0.00	0.47	0.00	0.00	5.36	0.03	0.22	201
H4736	75.64	13.13	2.07	0.02	0.96	0.26	1.57	4.02	0.05	0.18	192
H4737	63.31	16.15	6.41	0.14	1.93	0.08	1.8	3.66	0.07	0.43	247
H4740	76.88	12.33	1.24	0.00	0.39	0.05	2.15	5.56	0.02	0.17	181

Data from four additional porphyry units, P5 to P8 (Map 2 - Interpreted Regional Geology), assayed in the region were obtained from J Everard, Mineral Resources of Tasmania. This data is supplemented with additional assay data from the four porphyritic units sampled as part of this thesis. Assay values for those rock types are shown below in Table 5.2.

Table 5.2 - Assay results for rock units in the Yolande River region.

Oxide	SiO_2	TiO_2	Al_2O_3	Fe_2O_3	MnO	MgO	CaO	Na_2O	K_2O	P_2O_5	Zr
Sample Number	%	%	%	%	%	%	%	%	%	%	ppm
B4	71.10	0.45	13.00	2.56	0.05	1.30	0.28	3.50	4.20	0.07	302
Y586	72.03	0.46	13.41	2.78	0.06	1.77	0.31	3.50	3.44	0.08	250
B5	65.00	0.60	12.30	5.93	0.20	4.05	3.72	3.05	3.59	0.65	250
B7	65.50	0.58	13.10	3.89	0.20	3.00	2.00	3.00	4.10	0.11	257
B8	66.12	0.71	14.19	6.52	0.30	3.36	1.74	2.84	4.17	0.41	260
Y344A	76.11	0.29	13.28	1.34	0.02	0.85	0.06	1.02	3.60	0.03	175
Z488	65.56	0.60	13.91	3.90	0.20	3.03	1.87	2.46	4.40	0.11	230
Z208	71.02	0.38	14.18	2.59	0.06	0.72	0.58	3.78	3.92	0.09	230
Y549	69.77	0.33	14.14	2.78	0.09	0.72	1.08	3.86	4.32	0.11	230

5.2.2.2 Whole Rock Chemistry

Plotting values of $K_2O + Na_2O$ versus SiO_2 (wt%) allows for the description of rock composition to be inferred, (Rollinson, 1993). Porphyry samples from the project area, plotted in Figure 5.1, orient in quadrants which infer rhyolitic to dacitic composition. Only two of the seven sampled units correspond with the plot as dacitic, porphyry IV and VII. Values of $Na_2O + K_2O$ range between 4.62 and 8.18 percent, with SiO_2 values varying between 63.85 and 76.65 percent. Dacitic porphyry units have at least 3 percent less SiO_2 content than those of rhyolitic composition.

A similar plot of K_2O versus SiO_2 (wt%), shown in Figure 5.2 , defines all units within high K, calc-alkaline series, (Rollinson, 1993). Description of rocks falling in this category are high in K levels with the dominant feldspar being Ca-rich. Calc-alkaline rocks will tend to contain calcium-bearing ferromagnesian minerals, hornblende, augite, etc (Rollinson, 1993).

5.2.2.3 Analysis of Suites

Suites of the MRV have been divided and categorized by Crawford *et. al.*, 1992.
The five recognised suites have been divided into three calc-alkaline and two tholeiitic groups.
Suite I rocks contains units from the EQPS, CVC, TG, intrusive porphyries and granitoids, and andesitic lavas of the Que-Hellyer footwall sequence (Crawford *et. al.*, 1992).
Suite II is made up of intrusive and extrusive andesites and dacites from the CVC, which are often hornblende porphyritic.
The Suite III division contains basalts from Lynch Creek and the Howards Plains area, with basaltic and andesitic lavas from the Que-Hellyer sequence.
Pillow basalts contained within the Henty fault wedge and dykes of the Henty dike swarm make up Suite IV rocks.
Suite V contains the Miners Ridge basalts, which correlate with rift sequences from the Crimson Creek Formation, and are considered part of the pre-MRV basement.

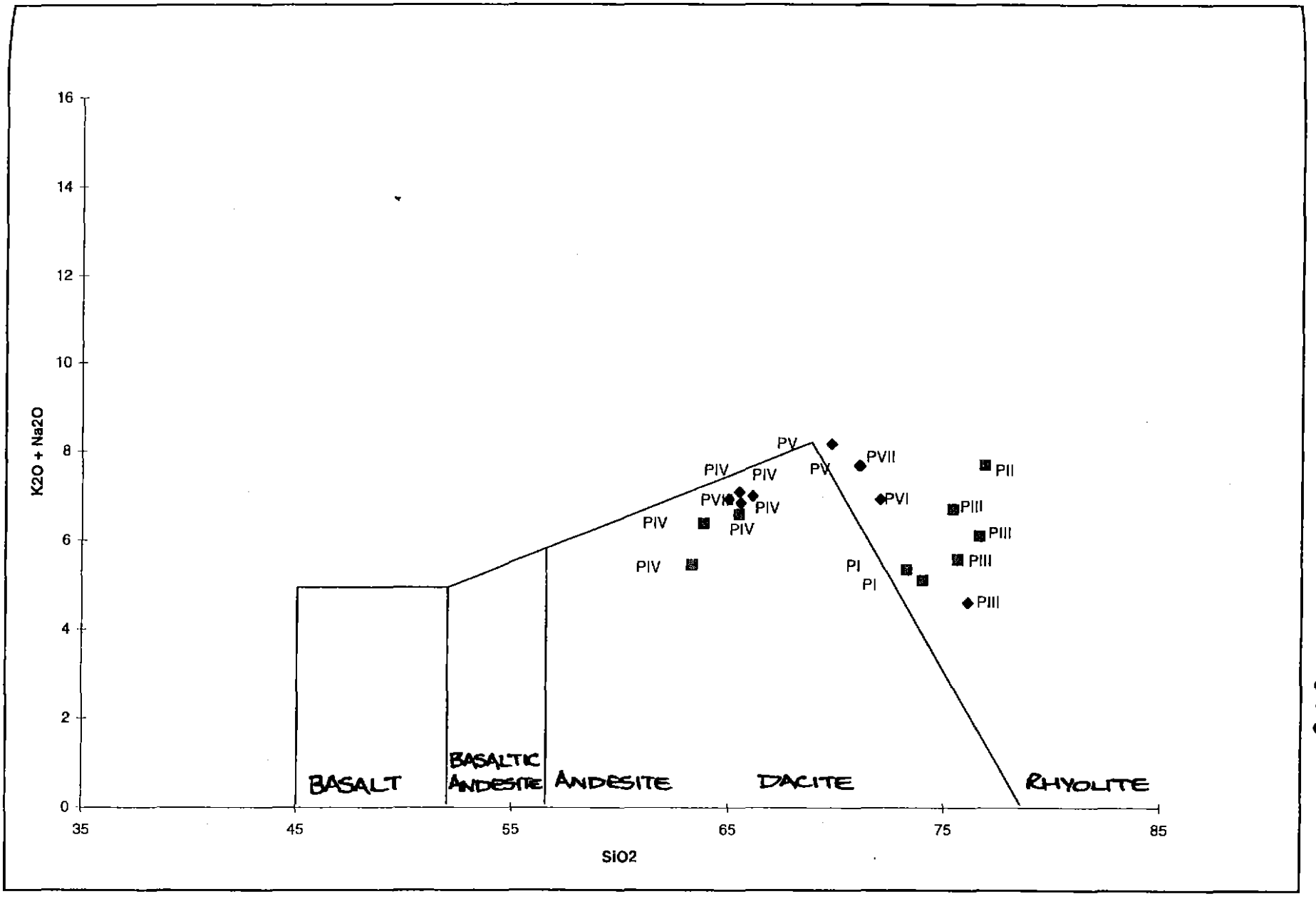

5770178

36

Figure 5.1 - Plot of K_2O versus SiO_2 for porphyritic samples from the study area. Plot discriminates samples into rhyolitic and dacitic compositional fields (Rollinson, 1993).

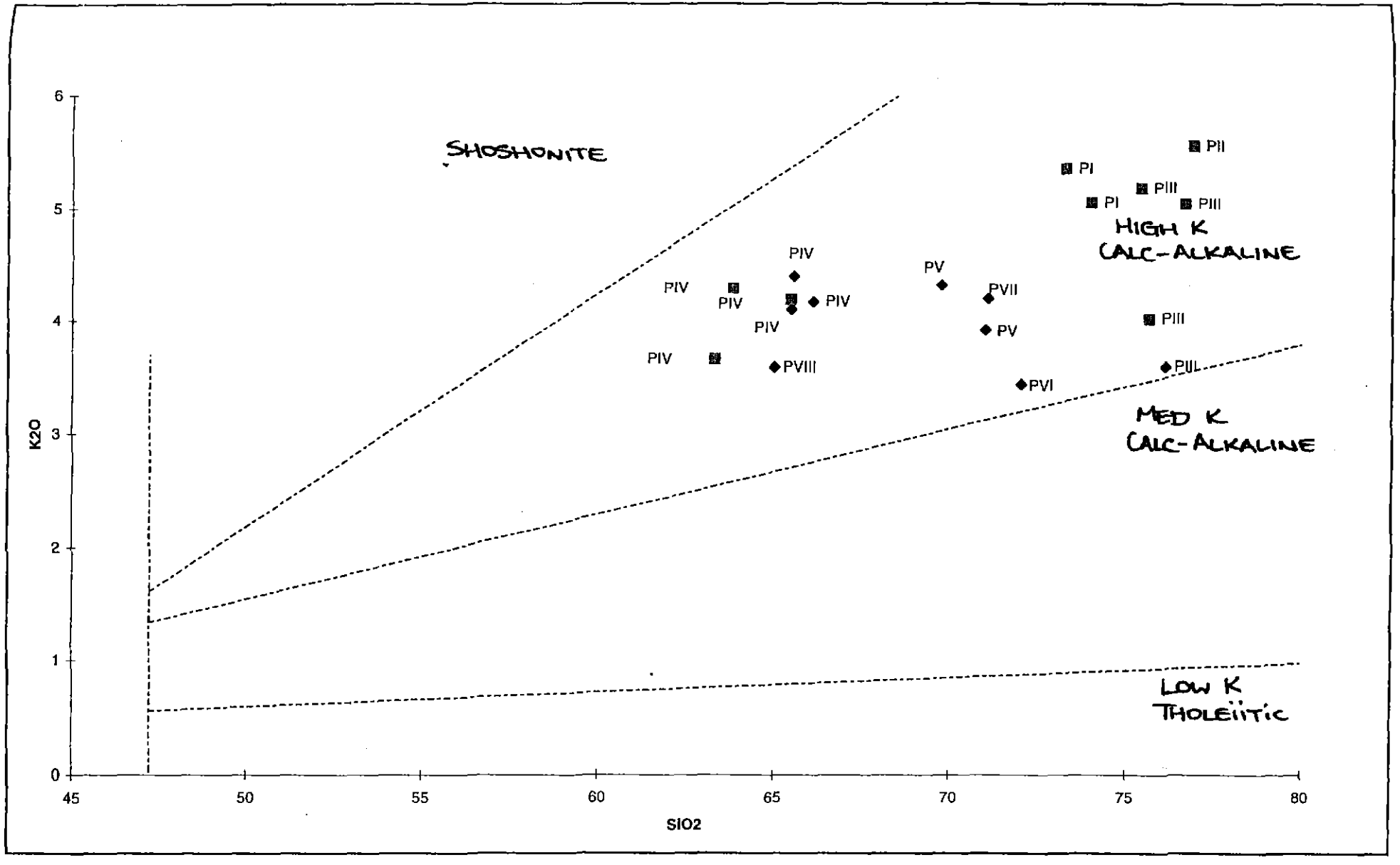

Figure 5.2 - Plot of K_2O versus SiO_2 (mass %) for porphyritic samples. All samples plot within the High K, calc-alkaline field (Rollinson, 1993).

Favourable elements used within this study are TiO_2, SiO_2, FeO and P_2O_5. Subsequent plotting of samples described within this paper, on these plots has discriminated the Yolande River porphyries into Suite I and Suite II divisions of the MRV.

Plotting of FeO values, calculated from determined Fe_2O_3, versus SiO_2 (Crawford et al., 1992) divides the porphyry samples into two groups which appear to correspond with Crawford's divisions of Suite I and Suite II. The datum is however removed from the original group boundaries, and must be depleted in iron (Figure 5.3).

A plot of TiO_2 versus SiO_2 (Figure 5.4) shows all samples bar two (Y549 and Z208) corresponding to Crawford's interpretation of Suite I and Suite II units. Samples which do not plot within the confines of these borders are depleted in TiO_2 content.

The P_2O_5/TiO_2 versus SiO_2 plot (Figure 5.5) is another of the useful discriminators used by Crawford et al., (1992). Porphyries interpreted with this data show different results from previous plots. One of the recognised Suite II rocks plots within the normal boundaries inferred for this rock type (B8); one plots extremely high in P_2O_5/TiO_2 (B5), which is not indicative of any Suite type; and five others plot within Suite I boundaries (B7, Z488, H4737, H4610, H4732).

Plotting Ti/Zr versus SiO_2 (Figure 5.6) is the final plot used for discrimination of Suites and by far the most successful. All porphyries which were inferred to be of dacitic composition, using plots from Rollinson, 1993, plot within the field for Suite II composition. Likewise, those porphyries indicated to be of rhyolitic composition, plot within the Suite I field.

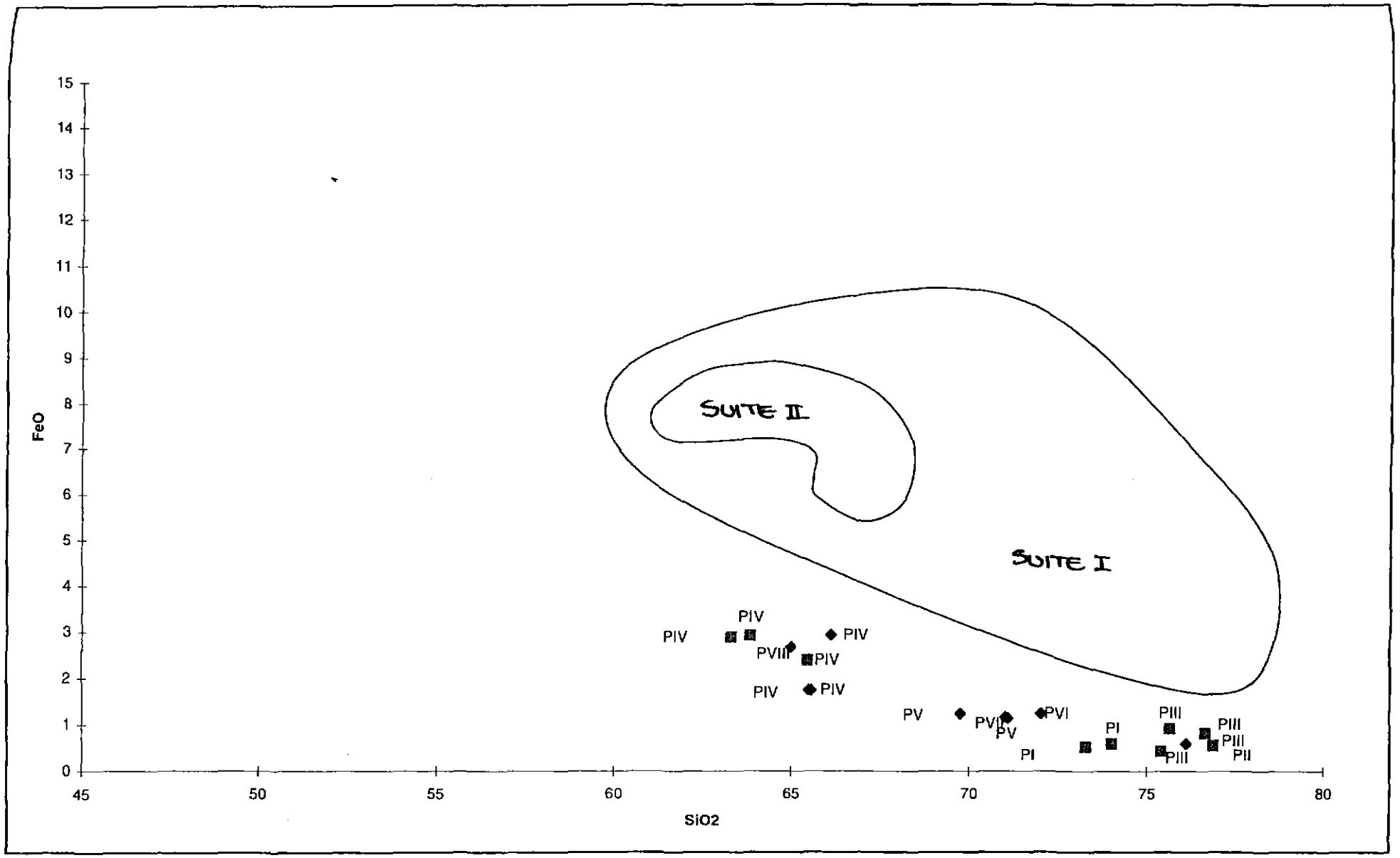

Figure 5.3 - FeO versus SiO_2 (mass %) plot for porphyritic units. Samples all plot out of recognised Suite boundaries (Crawford *et. al*., 1992).

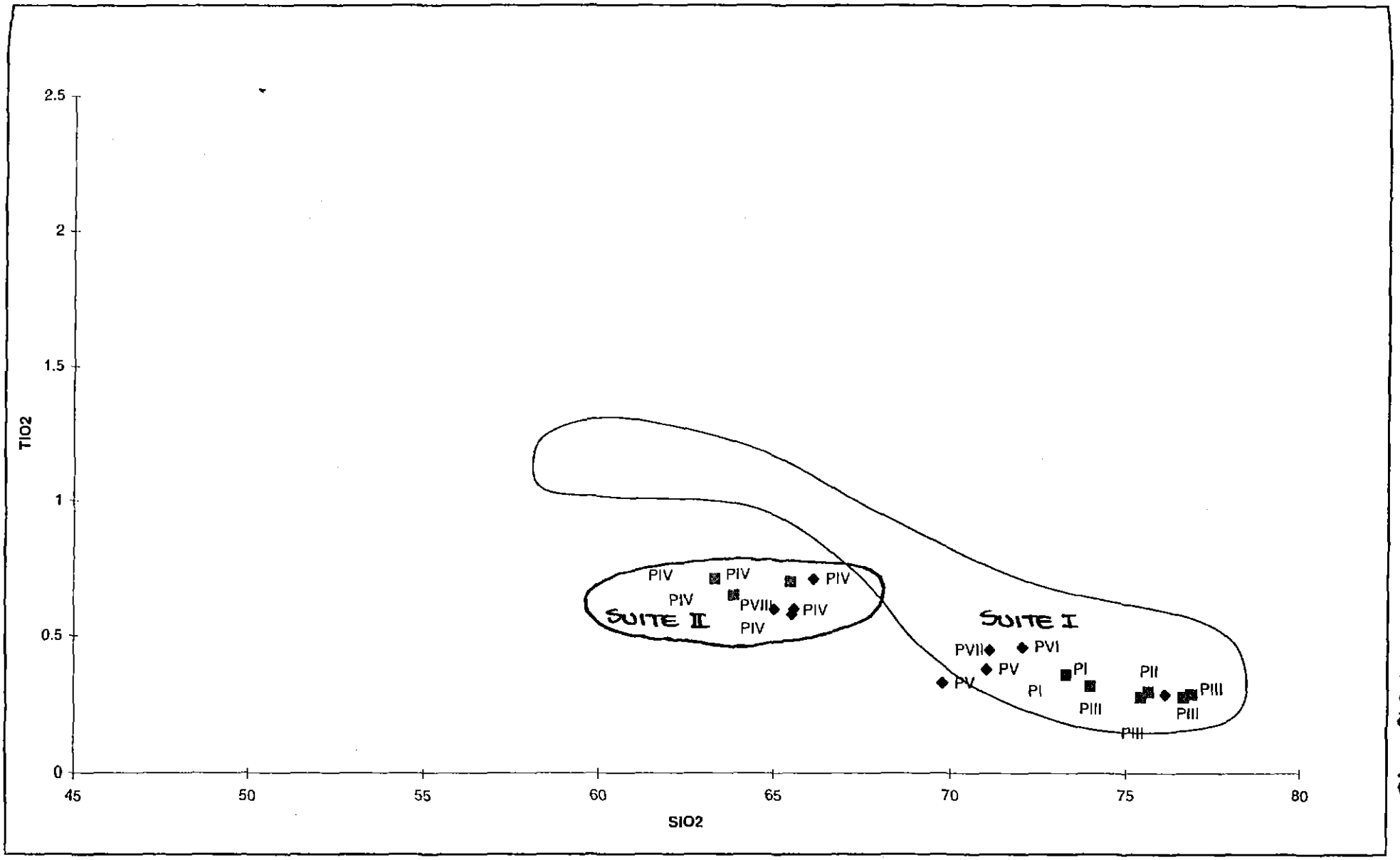

Figure 5.4 - TiO2 versus SiO2 (mass %) plot. Samples plot within Suite I and Suite II boundaries (Crawford *et. al*., 1992).

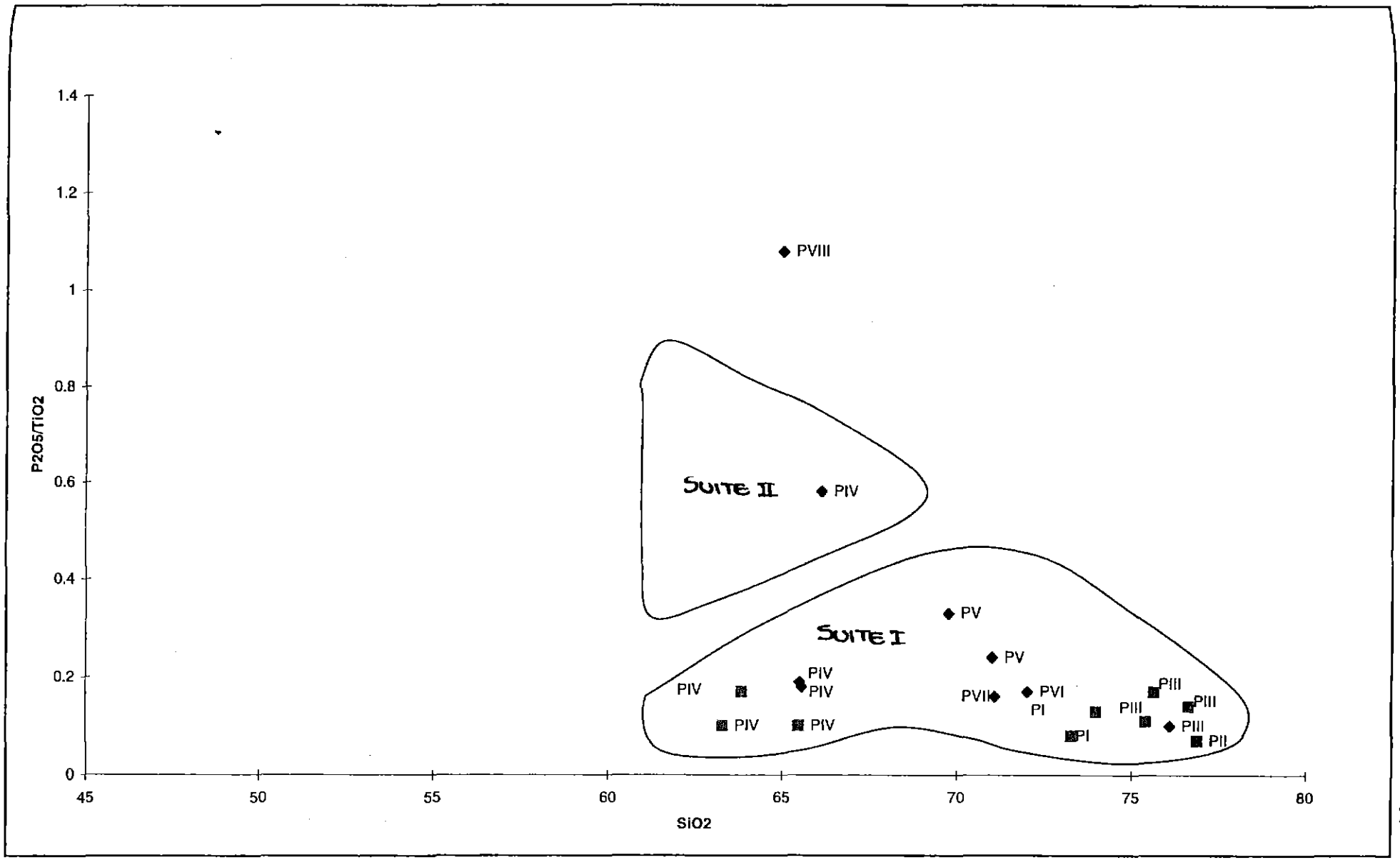

5770833

41

Figure 5.5 - Plot of P_2O_5/TiO_2 versus SiO_2 (mass %). Most porphyry units plot within Suite I boundaries (Crawford *et. al.*, 1992). Sample B8 plots within Suite II boundaries.

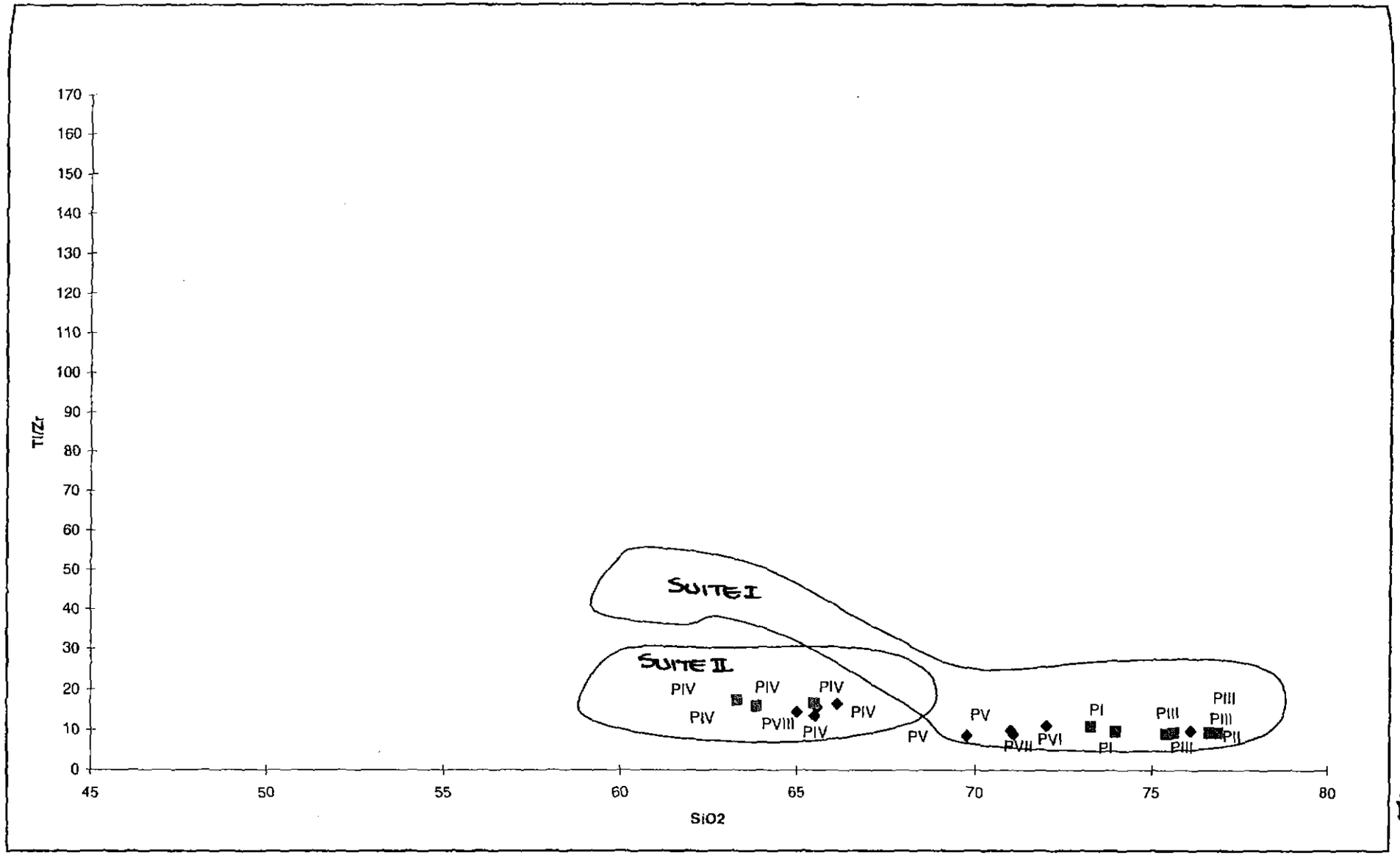

Figure 5.6 - Ti/Zr versus SiO_2 (mass %) plot. All samples lie with boundaries of Suite I or Suite II (Crawford et. al., 1992).

5.2.2.3.1 Suite I rocks

By classification (Crawford *et al.*, 1992) Suite I rocks have SiO_2 contents in excess of 58% and show calc-alkaline trend of decreasing FeO(total) and TiO_2 contents with increasing differentiation; Ti/Zr contents of YRS porphyries decrease with increasing fractionation; and at any SiO_2 content, P_2O_5/TiO_2 values are less than 0.4.
All of these factors are correct for the interpreted Suite I porphyries within this paper.

5.2.2.2.2 Suite II rocks

Classification of Suite II rocks (Crawford et al., 1992) states that these rocks are clearly more P_2O_5 rich and TiO_2 poor, and effectively discriminated on the P_2O_5/TiO_2 versus SiO_2 plot.
This is incorrect for most interpreted Suite II porphyries within this thesis. Possible solutions to this problem are; analytical errors within P_2O_5 and TiO_2 determination; or the presence of intermediate Suites within the classified range, that represent mixtures of Suite I and Suite II magmas. A porphyritic rock which falls between the two Suite boundaries may be developed from a magma which represents intermediate conditions of fractionation between the tow major magna types.

5.2.3 Immobile Element Geochemistry

The study of geochemistry has been concentrated on some elements considered to be essentially immobile (Crawford *et al.*, 1992). The most useful of the elements considered are Ti and Zr. These two elements are useful for discriminating volcanic categories i.e. rhyolite, dacite, andesite, etc. and for calculating mobile component mass changes due to alteration.
Other useful elements are FeO and MgO and their relative abundances, although these are mobile in alteration. SiO_2 is a useful discriminate and fractionation indicator when combined with Immobile Elements (IE) (Crawford *et. al.*, 1992).

5.2.3.1 Ti And Zr Immobility And Behaviour

High field strength elements Ti and Zr are conserved within alteration zones whereas other mobile elements may become redistributed away from the original area. These properties are useful for determining unrecognizably altered rocks, mapping similar emplacement units and for implying petrogenetic relationships, (Herrmann, 1998).
Pairs of immobile elements should define linear trends within plots. The trend should regress to the origin of the plot, (Herrmann, 1998).

5.2.3.2 Ti And Zr Patterns

Porphyry units plotted on a TiO_2 versus Zr graph, appear to group within two linear assemblages, Figure 5.7. These are grouped by line slope values of and , and as with whole rock interpretation plot within rhyolitic to dacitic fields.
The pattern suggested by this immobile element determination suggest that the porphyritic rocks in this study should be designated within two distinct groups, Suite I and Suite II.

It appears that a relationship can be inferred between rhyolitic Suite I porphyries 1, 2, 3, 5, 6 and 7; and likewise between dacitic Suite II porphyries 4 and 8. Porphyries within a single group would be derived from the same magma source, and although showing different whole rock element ratios due to fractional crystallization, can be identified through IE studies.

5.3 ALTERATION

5.3.1 Ishikawa Alteration Index

The Ishikawa Alteration Index (AI) helps in determining the intensity of hydrothermal alteration which has affected a rock. This is calculated as a measure of the amount of plagioclase and glass destruction (Large, 1998).
The higher the AI towards 100, the more altered the rock specimen. Alteration distinctly affects feldspars, hence in the equation, the AI value is dependent on the

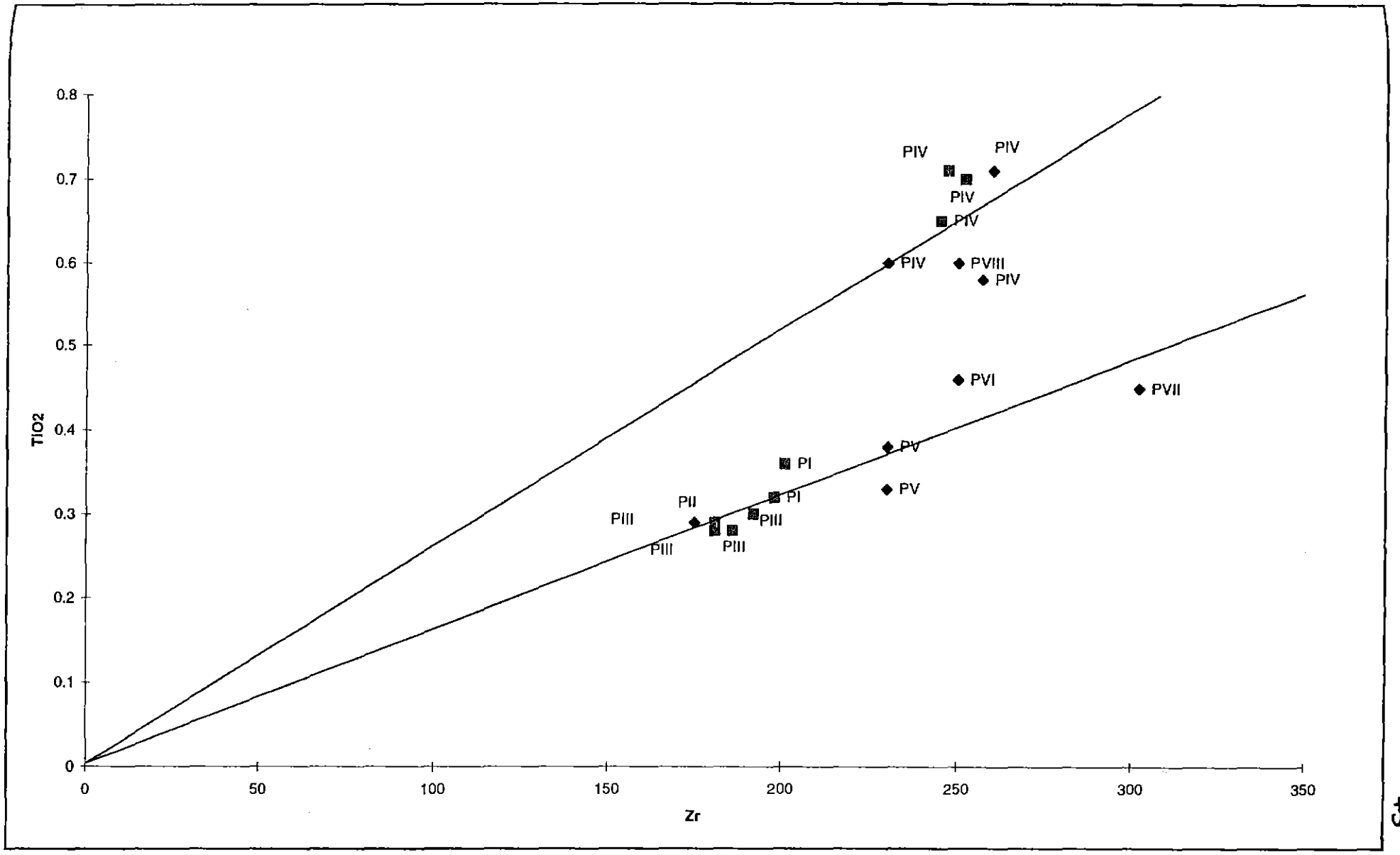

Figure 5.7 - TiO_2 versus Zr plot for porphyritic units, defines two linear trends which correspond with Suite I and Suite II groupings (Crawford *et al*., 1992).

amount of MgO and K_2O. AI is strongly driven by the amount of Na_2O and CaO depletion associated with some sericite or K-feldspar alteration zones; K_2O tends not to change significantly and MgO may or may not be added to form chlorite.

$$IAI = 100 * (MgO + K_2O) / (MgO + K_2O + Na_2O + CaO) \qquad \text{(Equation 1)}$$

Porphyry bodies of Suite I classification have AI values of between 50 and 100, Table 5.3. Suite II classified porphyries have AI values ranging from 46 to 76. These segregations suggest that Suite I porphyry bodies have undergone varied amounts of alteration, whereas Suite II rocks have remained relatively unaltered throughout the study area.

Table 5.3 - Alteration calculations for all samples.

Sample Number	Porphyry Number	Equation 1AI	Equation 2 FMA	Equation 3 FCA	Equation 4 CCPI
H4503		40.20	32.86	85.60	29.35
H4513		97.50	97.14	100.00	28.90
H4514		68.86	68.17	80.65	9.55
H4610	IV	76.27	67.14	96.53	47.15
H4612		73.52	71.19	97.83	18.96
H4613	III	78.17	77.23	94.74	10.65
H4614	III	83.18	82.52	94.44	16.02
H4724		89.54	100.00	59.38	34.81
H4725		64.74	76.47	36.48	31.03
H4726		60.20	74.15	37.00	34.44
H4732	IV	73.68	63.48	97.20	43.92
H4733	I	98.92	98.83	100.00	17.13
H4735	I	100.00	100.00	100.00	15.74
H4736	III	78.69	73.13	71.91	25.28
H4737	IV	96.02	74.83	67.03	46.86
H4740	II	88.64	73.01	72.11	10.95
B4	VII	59.27	54.55	82.28	24.14
Y586	VI	57.76	49.57	85.10	30.32
B5	VIII	53.02	54.07	52.12	50.30
B7	IV	58.68	57.75	60.00	40.09
B8	IV	62.18	59.49	65.88	47.31
Y344A	III	80.47	77.92	93.41	23.92
Z488	IV	63.18	64.14	61.84	41.09
Z208	V	51.56	50.91	55.38	19.67
Y549	V	50.50	52.81	40.00	19.41

The division of Suite I rocks into separate porphyry units shows different amounts of alteration intensity are inherent within different porphyry units, Table 5.4.

Table 5.4 - AI maximum and minimum levels within Suite I porphyry rocks.

Porphyry No.	1	2	3	5	6	7
AI minimum	98.92	88.64	25.28	50.50	57.76	59.27
AI maximum	100.00	88.64	83.18	51.56	57.76	59.27

Porphyry number 1 (H4735 and H4733, Appendix II) has undergone extensive alteration (AI values>98). This is evident in thin section with extensive and complete alteration of feldspars to muscovite.

Porphyries 5, 6 and 7 appear to have undergone the least alteration, with values between 50 and 59. Porphyry 3 shows varied amounts of alteration, ranging from 25 (unaltered) to 83.

Maximum and minimum levels within Suite II rocks are described within Table 5.5, below.

Table 5.5 - AI maximum and minimum levels for Suite II porphyry units.

Porphyry No.	4	8
AI minimum	46.86	53.02
AI maximum	76.27	53.02

Porphyry 4 of Suite II exhibits the highest level of alteration between the two units. Porphyry 8 appears to be unaltered. Thin section analysis suggests some alteration of feldspars, with pervasive muscovite common, and complete alteration of hornblende to chlorite within porphyry 4.

5.3.2 Feldspar-Muscovite Alteration

The degree of feldspar-muscovite alteration (FMA) can be estimated from the following equation

$$100*K_2O / (Na_2O + K_2O) \quad \text{(Equation 2)}$$

Suite II porphyries range in FMA between 54 and 74, whereas Suite I range between 49 and 100.

Table 5.6 - FMA maximum and minimum levels within porphyry units of the YRS.

Porphyry No.	1	2	3	4	5	6	7	8
FMA min.	98.83	73.01	73.13	57..75	50.91	49.57	54.55	54.07
FMA max	100.00	73.01	82.52	74.83	52.81	49.57	54.55	54.07

Table 5.6 reveals that porphyry 1 again is calculated to reveal high levels of alteration. Feldspar muscovite alteration within this unit is, as mentioned before, extensive and reflected with this data. Other high K/Na ratios could be due to primary shoshonitic compositions which can not be calculated from the equation.

5.3.3 Feldspar-Chlorite Alteration

The extent of feldspar-chlorite alteration (FCA) may be measured by the following equation:

$$100*MgO / MgO + CaO \quad \text{(Equation 3)}$$

Suite II porphyries show FCA values between 52.12 and 97.20. Suite I rocks range in FCA value between 40.00 and 100.00.

The rise in overall alteration limits within Suite II porphyries, is indicative of the extensive chlorite alteration of hornblende noticeable within thin section of these rock types. Suite I alteration is again wide ranging and reflective of the differing levels of alteration between different porphyry units within this Suite.

5.3.4 Chlorite/Carbonate/Pyrite Index

By plotting the chlorite/carbonate/pyrite index (CCPI), Equation 4, against AI (Equation 1) we can see if samples fall within the central least altered box, or plot out of the box towards the various alteration assemblages.

$$CCPI = 100 * (MgO + FeO) / (MgO + FeO + Na_2O + K_2O) \qquad \text{(Equation 4)}$$

Tabulated results showing the CCPI value for samples used in this study are found in Table 5.3.

Figure 5.8 shows a plot of CCPI versus IAI for geochemical samples used in this study. Some porphyry units appear within the box on the graph, suggesting low alteration. Whether sericite or K-feldspar alteration has occurred will determine movement along alteration lines shown on the right hand side of the plot. There is however a tendency for high primary K-feldspar rocks to plot along the K-feldspar alteration trend line, as the plot does not discriminate primary rock compositions from secondary alteration types.

Rock samples from porphyries 1,2 and 3 appear to have undergone K-feldspar alteration, whereas porphyry 4 shows signs of sericite alteration. These assumptions are shown to be correct upon analysis of thin sections from these units.

5.3.5 Mass Change Reactions

Quartz-feldspar porphyritic rocks from two sites, Yolande River Bridge (H4614) and Diamond Hill (H4733), exhibit similar characteristics implying a relationship during formation. These two samples lie on the same line in the TiO_2 versus Zr plot (Figure5.7), but in hand specimen appear quite different. The Diamond Hill sample appears more altered and weathered, in outcrop also. Analyses of these two porphyries shown below, can be used to determine mass change effects that have affected the more altered porphyry.

Mass change may be positive or negative depending on the amount each species moved. Calculation of mass change is done using the following equation from MacLean & Barrett, 1993:

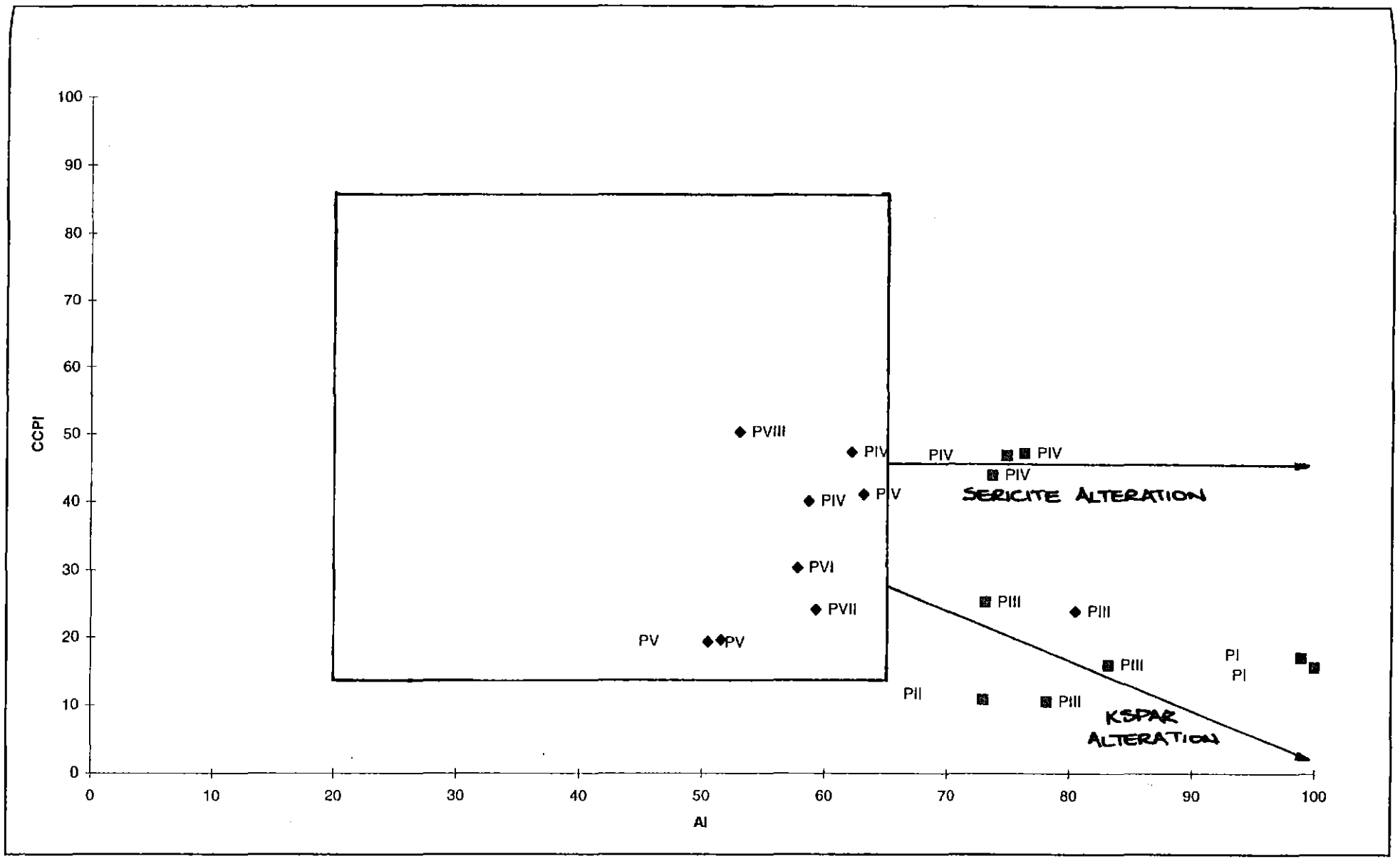

Figure 5.8 - Plot of Alteration Index versus Carbonate/Chalcopyrite/Pyrite Index (Large, 1998). Units plotting within the central box are relaively unaltered. Alteration types of other samples indicated by arrows.

$$[Zr_f/Zr_a * C\%_a] - C\%_f \qquad \text{(Equation 5)}$$

Where f = fresh outcrop

a = altered outcrop

C% = major oxide concentration in percent

Zr = assayed Zr concentration

Table 5.7 - Mass change calculated from porphyry assays H4614 and H4733.

	SiO_2	TiO_2	Al_2O_3	Fe_2O_3	MnO	MgO	CaO	Na_2O	K_2O	P_2O_5	Total
H4614	76.65	0.28	14.04	0.98	0.00	0.36	0.02	1.53	5.19	0.03	
H4733	73.99	0.32	15.9	1.33	0.00	0.46	0.00	0.06	5.06	0.04	
Mass change	-9.01	0.01	0.49	0.24	0.00	0.06	-0.02	-1.48	-0.56	0.01	-10.27

A mass change value of -10.27 indicates a mass loss in sample H4614, implying that it has been substantially altered. This specimen was sampled from porphyry 1, which has shown substantial AI, FMA and FCA alteration (Table 5.3). The most prominent value changes appear in SiO_2, Na_2O, K_2O, Al_2O_3 and Fe_2O_3.

SiO_2 levels will fluctuate through bodies that have been altered, because it is normally very mobile. Other components must be included within new forming minerals. The large net loss of Na_2O indicates sericitisation of Na bearing minerals such as plagioclase feldspar.

CHAPTER 6 : EXPLORATION METHODS

6.1 STREAM SEDIMENT SURVEY

6.1.1 Sediment Collection

Pan concentrate stream sediment samples were taken from tributaries between the Yolande River and the Pearl Creek Fault (Map 1). Samples of 50 gram were taken from sites with similar trapping characteristics. Fire assay for gold concentrations were performed by Analabs, results are tabulated in Appendix IV.

6.1.2 Results and Patterns

Anomalous gold concentration patterns (>100 ppb.) were recognized in four zones throughout the survey area, Figure 6.1. Background levels of concentration within host rocks vary between <0.05 ppb and 66 ppb.

A specific gold boundary of >100 ppb, highest reading 1090 ppb, occurs around Diamond Hill in a 50 to 100 metre radius. Visible flecks are noticeable in this area during collection of pan concentrates. It appears that weathering and movement of gold flecks has occurred in a radial pattern around the Diamond Hill area, indicating a likely source from the Qfb porphyry or from extensive quartz veins.

Another area which shows >100 ppb gold concentration is along the North Diamond Hill Line. The highest reading at this location is 175 ppb. This site is within close proximity to a Qfb porphyry, petrographically similar to the one located at Diamond Hill.

Two other areas with gold levels >100 ppb occur at, a point along the Murchison Highway, and along a 4WD track leading to Diamond Hill. Highest readings at these locations are 930 and 810 ppb, respectively.

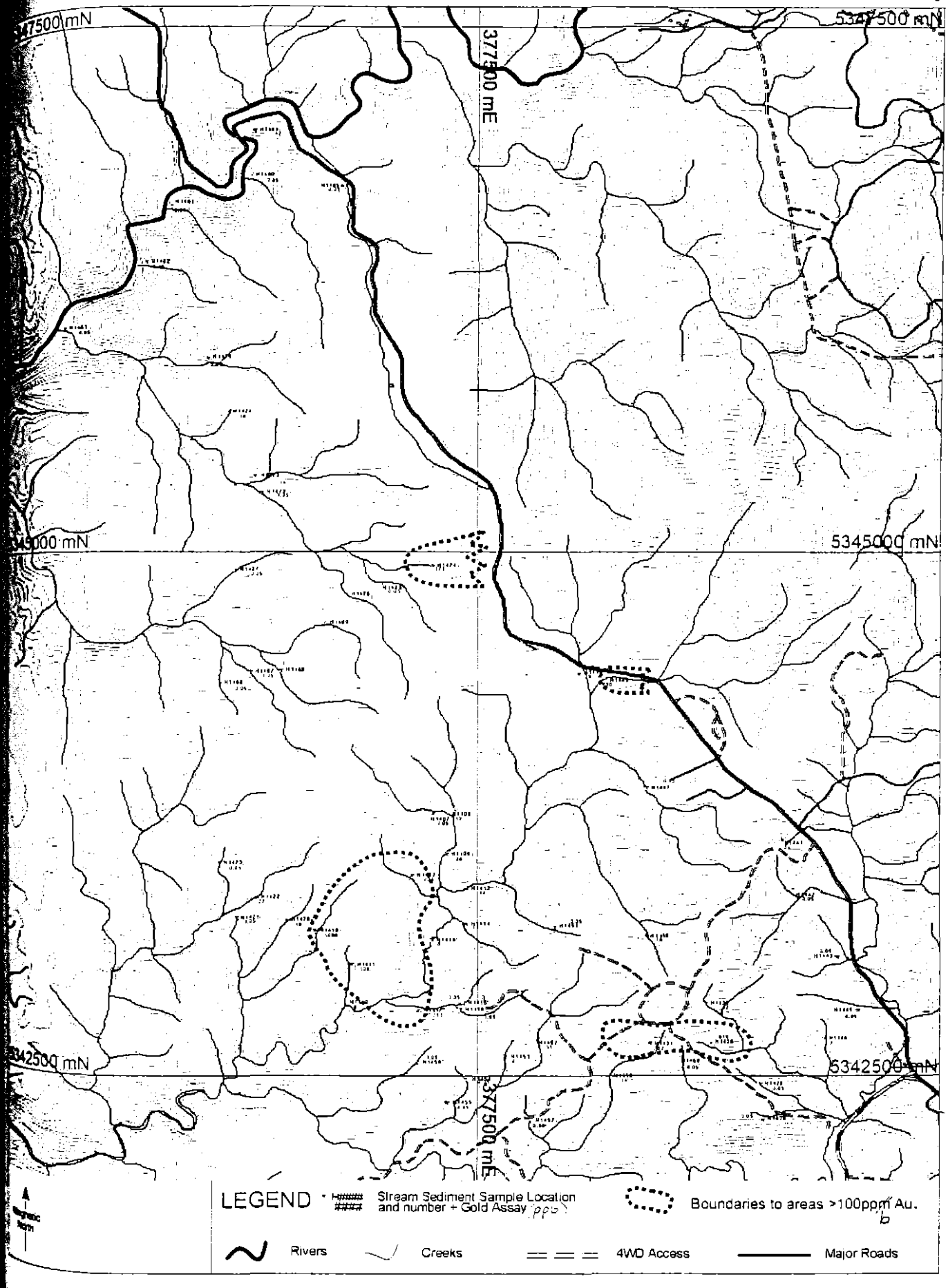

Figure 6.1 - Stream sediment sample locations and Au assay results. Dashed boundaries mark areas where Au concentration exceeds 100 ppm.

5 cm

6.2 SOIL GEOCHEMISTRY

6.2.1 Sample Collection, Preparation and Analysis

Samples were taken of B/C horizon soil, with a hand auger, at 25 metre intervals along the North Diamond Hill Line and at 20 metre intervals along the Diamond Hill Baseline (Figure 6.2). Attempts to sample three crosslines over Diamond Hill were virtually unsuccessful, due to a thick layer of quartz talus, which lay at or just below the surface.

Further soil sampling of A and B/C horizons has subsequently been completed by Ken Morrison, CMT, providing samples across Diamond Hill Grid Line 360 North.

Samples were analyzed at Analabs for Cu, Pb, Zn, Au, As. (Figures 6.3, 6.4, 6.5(a) and 6.5(b), tabulated in Appendix V).

6.2.2 Results

The North Diamond Hill soil profile shows decreased levels of lead and copper over the quartz-feldspar-biotite porphyry, Figure 6.3. This porphyry has boundaries at the 350 and 750 metre mark. Elevated levels of gold are found in the soil of this unit at the metre mark, and do not appear elsewhere on the plot.
The quartz-feldspar-hornblende porphyry, which lies between the 000 and 175 metre mark, is a distinct feature of the plot. Elevated levels of zinc, lead and copper define the soil created by the weathering of this porphyry.

The Diamond Hill baseline traverses YRS volcaniclastics between 000 metres to approximately the 560 metre mark. Quartz feldspar porphyry is the underlying rock type from 560 metres to the 800 metre mark, evident from horizons sampled during survey. It is likely that the porphyritic unit continues further north from the termination of the Diamond Hill Baseline.

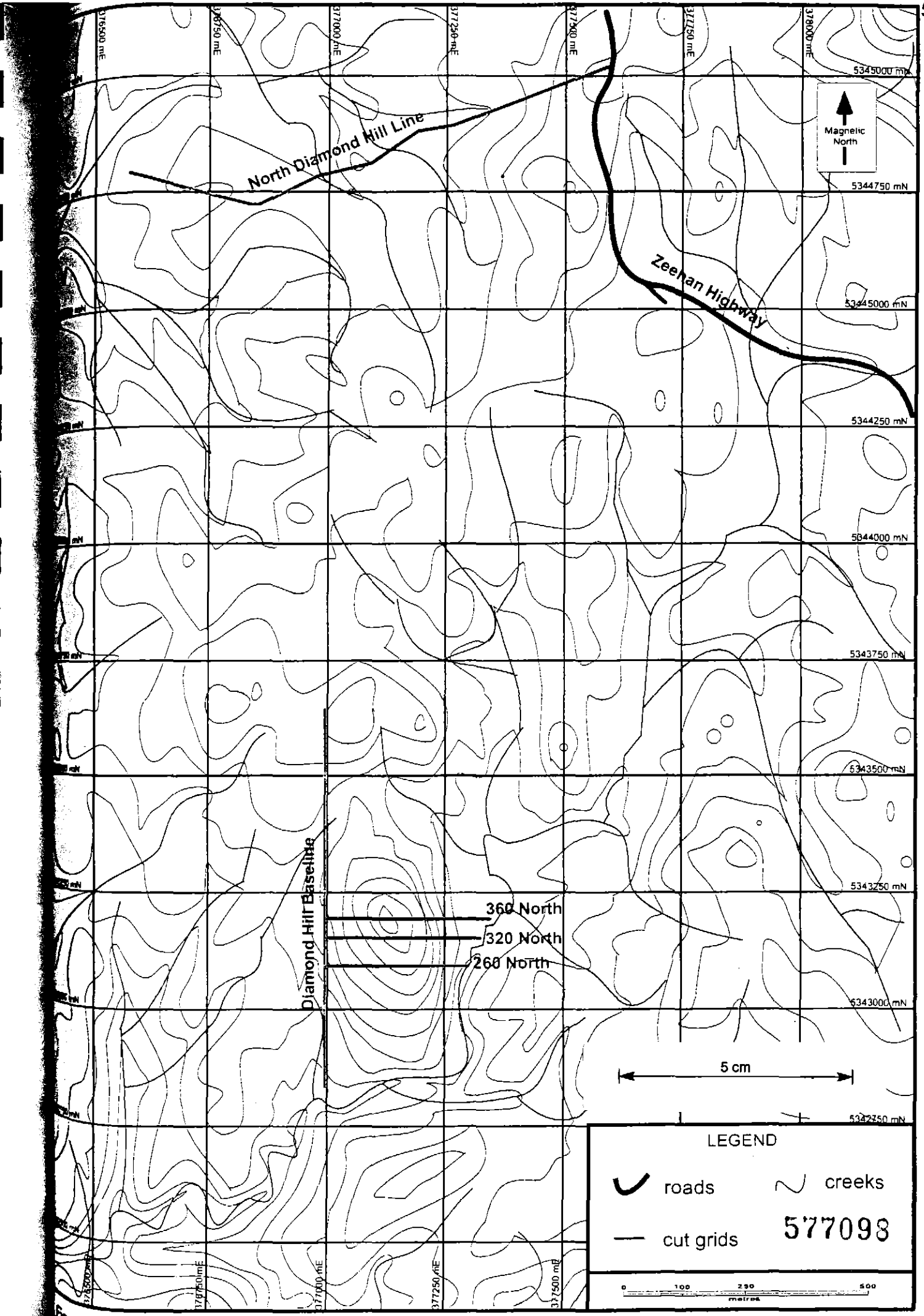

Figure 6.2 - Location of grid lines within EL 27/95 Yolande River. (After Morrison & Griffiths, 1998).

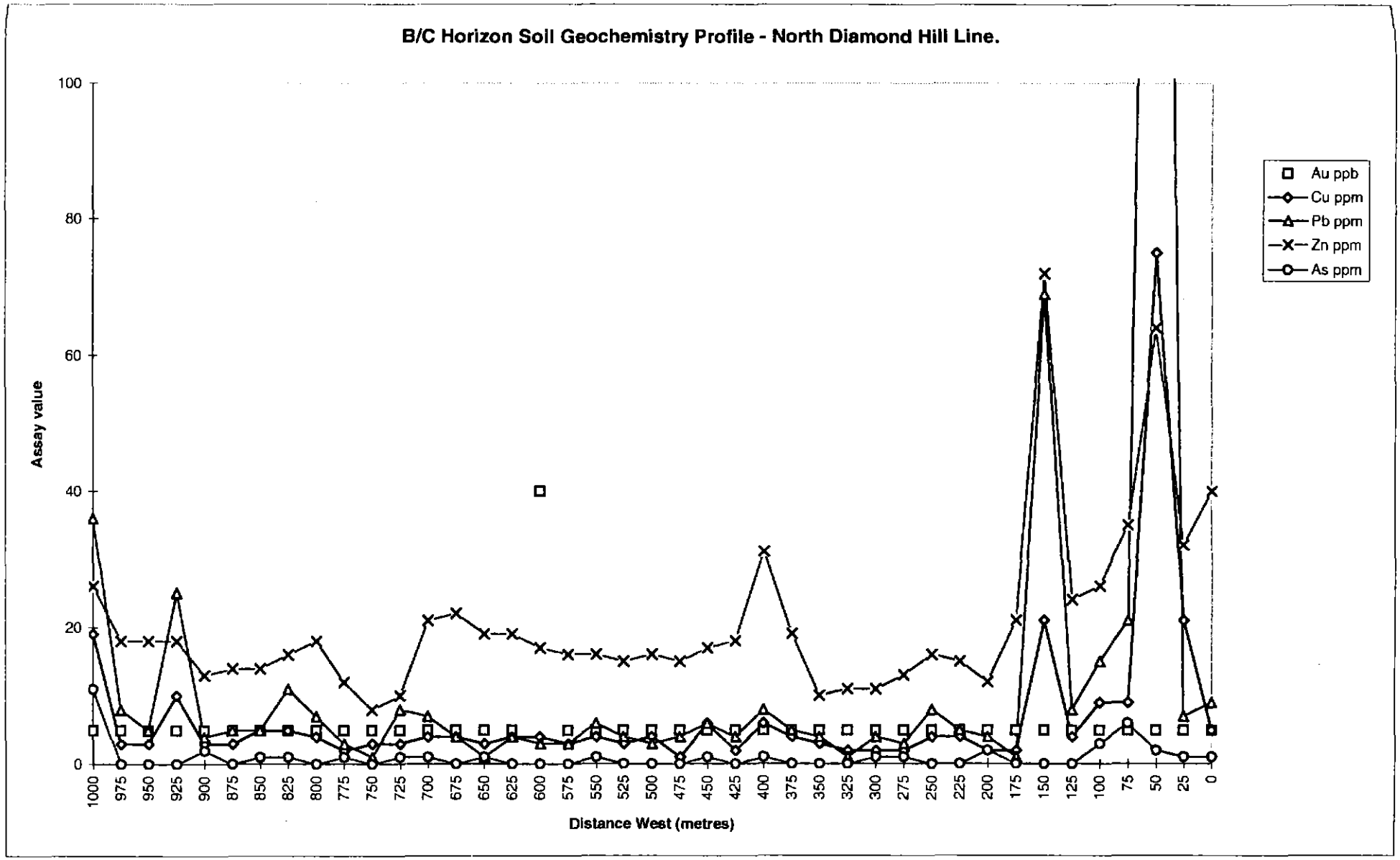

Figure 6.3 - Geochemistry profile for B/C horizon soil sampling survey conducted along the North Diamond Hill Line. Note: Gold assays as ppb, all other elements represented as ppm.

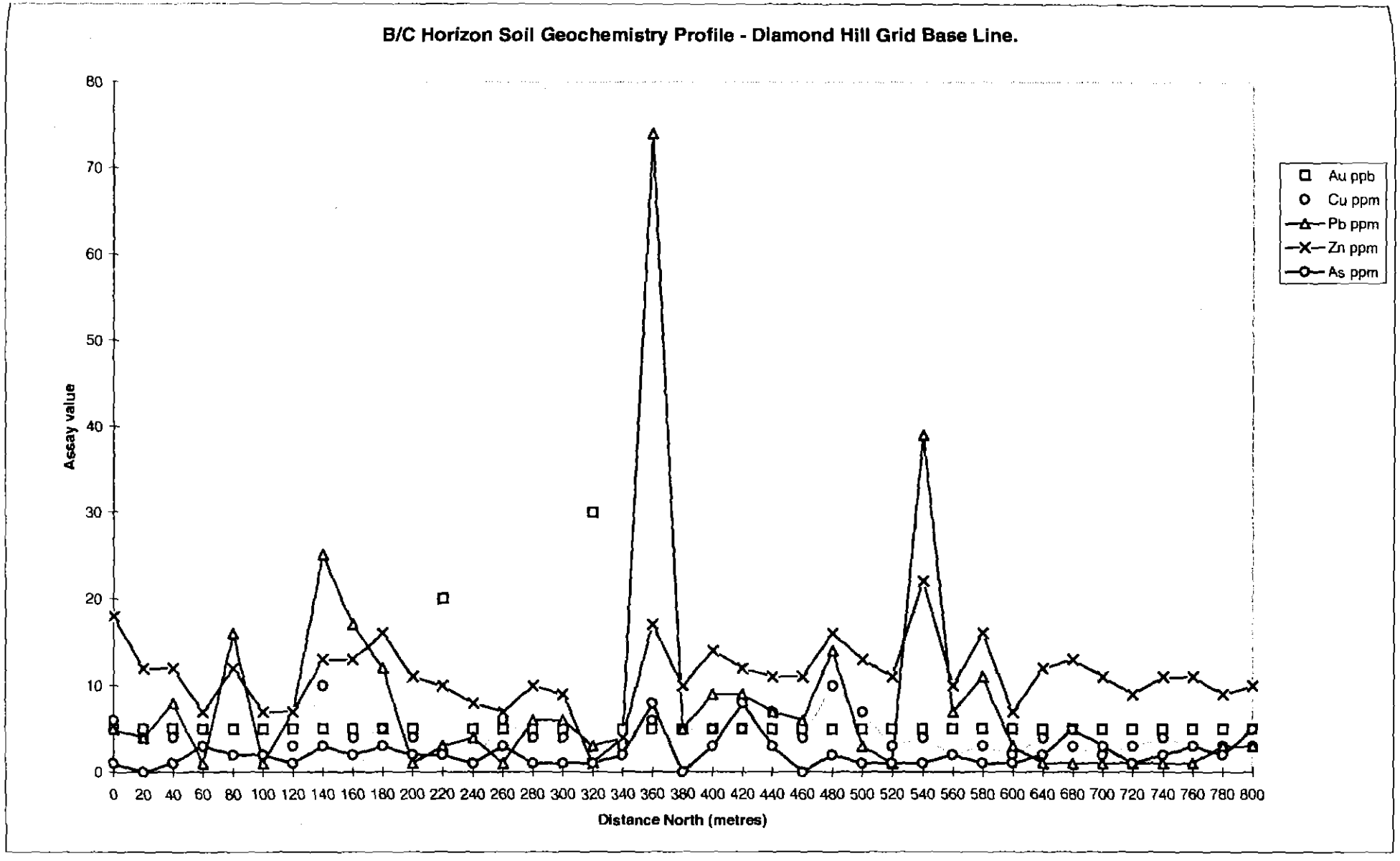

577100 as

Figure 6.4 - Geochemistry profile for B/C horizon soil sampling survey along the Diamond Hill Baseline. Note: Gold assay values as ppb, all other elements represented as ppm.

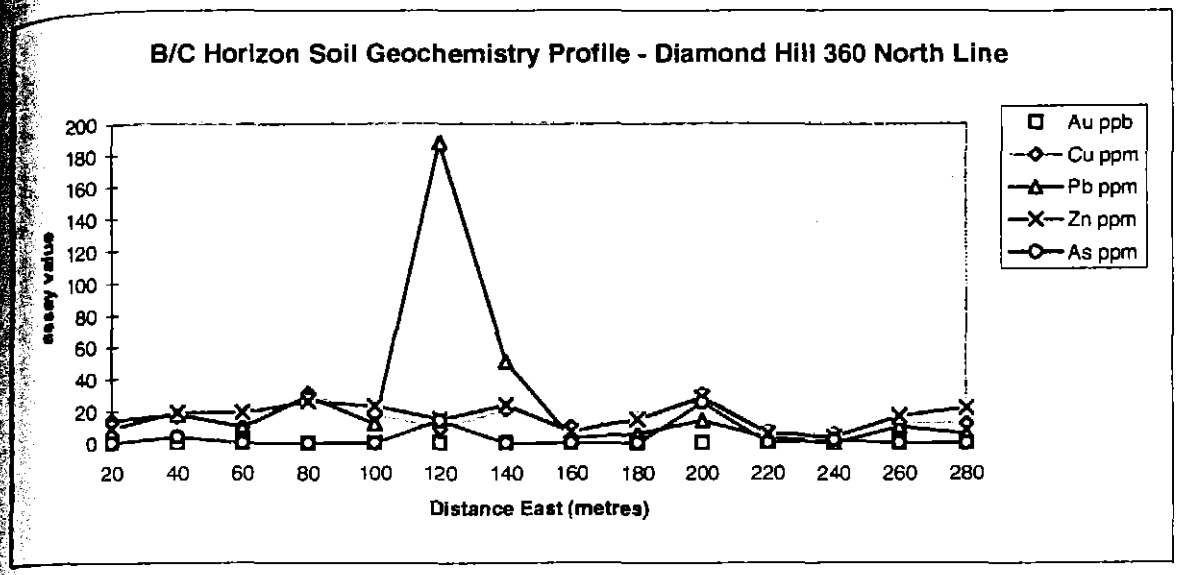

Figure 6.5(a) - Geochemistry profile for B/C horizon soil sampling survey over the Diamond Hill Grid Line 360 North. Note: Gold assay as ppb, all other elements represented as ppm.

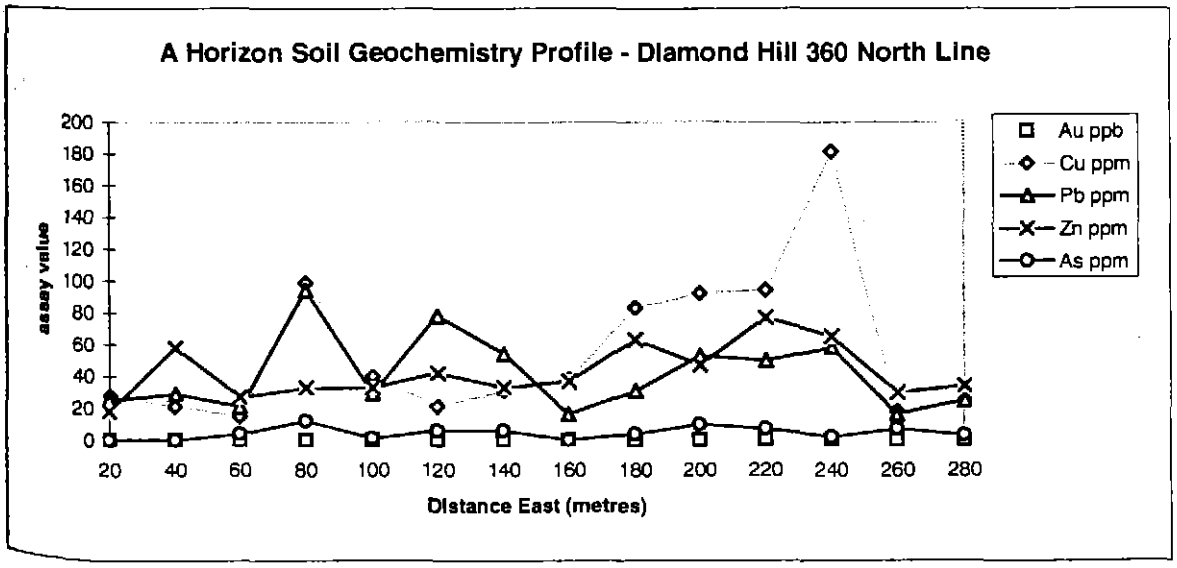

Figure 6.5(b) - Geochemistry profile for A horizon soil sampling survey over the Diamond Hill Line 360 North. Note: Gold assay as ppb, all other elements represented as ppm.

The only clear geochemical difference between the porphyry unit and volcaniclastics appears to be a decrease in lead and copper in soils lying over the porphyry unit (Figure 6.4).

The comparison between B/C and A horizon soil geochemistry can be viewed in Figure 6.5(a) and 6.5(b) respectively. The only observable relationship between the two can be seen with a lead anomaly at the 120 metre mark. The value recorded in B/C horizon assay is over twice as high as that recorded within A horizon assays. Other elements appear relatively undescriptive. The copper, lead and zinc variation in the A horizon graph, between 160 and 260 metres, is not reflected within B/C horizon samples.

6.3 LOCAL MAGNETICS

6.3.1 Introduction

A local ground-magnetic survey was conducted in order to recognize boundaries of porphyry units within the study area. Determination of different magnetic signatures for all units would be useful to identify changes in lithology. Raw data results of the Diamond Hill Grid magnetics and the North Diamond Hill Line magnetics surveys are found in Appendix VI.

6.3.2 Data Acquisition

Traverses with a proton precession magnetometer were performed along a baseline and 3 grid lines at Diamond Hill, and along the North Diamond Hill Line (Figure 6.2). The base line measured 800 metres in length, with crosslines of 350, 329 and 310 metres in length, coming off baseline points 260, 320, and 360 north, respectively. Magnetic measurements were taken at intervals of 5 metres. Minimal fluctuation in base station readings occurred during the time of the survey and a correction of only 10 nT was needed over a two hour period.

6.3.3 Magnetic Intensity Patterns

6.3.3.1 North Diamond Hill Line

Variation along the North Diamond Hill Line ranges between 62133 and 62212 nT. The strongest recordings are exhibited by the Qfb porphyry midway along the line. The magnetic response of the dacitic porphyry has not reached its full potential when recording stopped and would be expected to far overpower any response given by the Qfb porphyry, Figure 6.6.

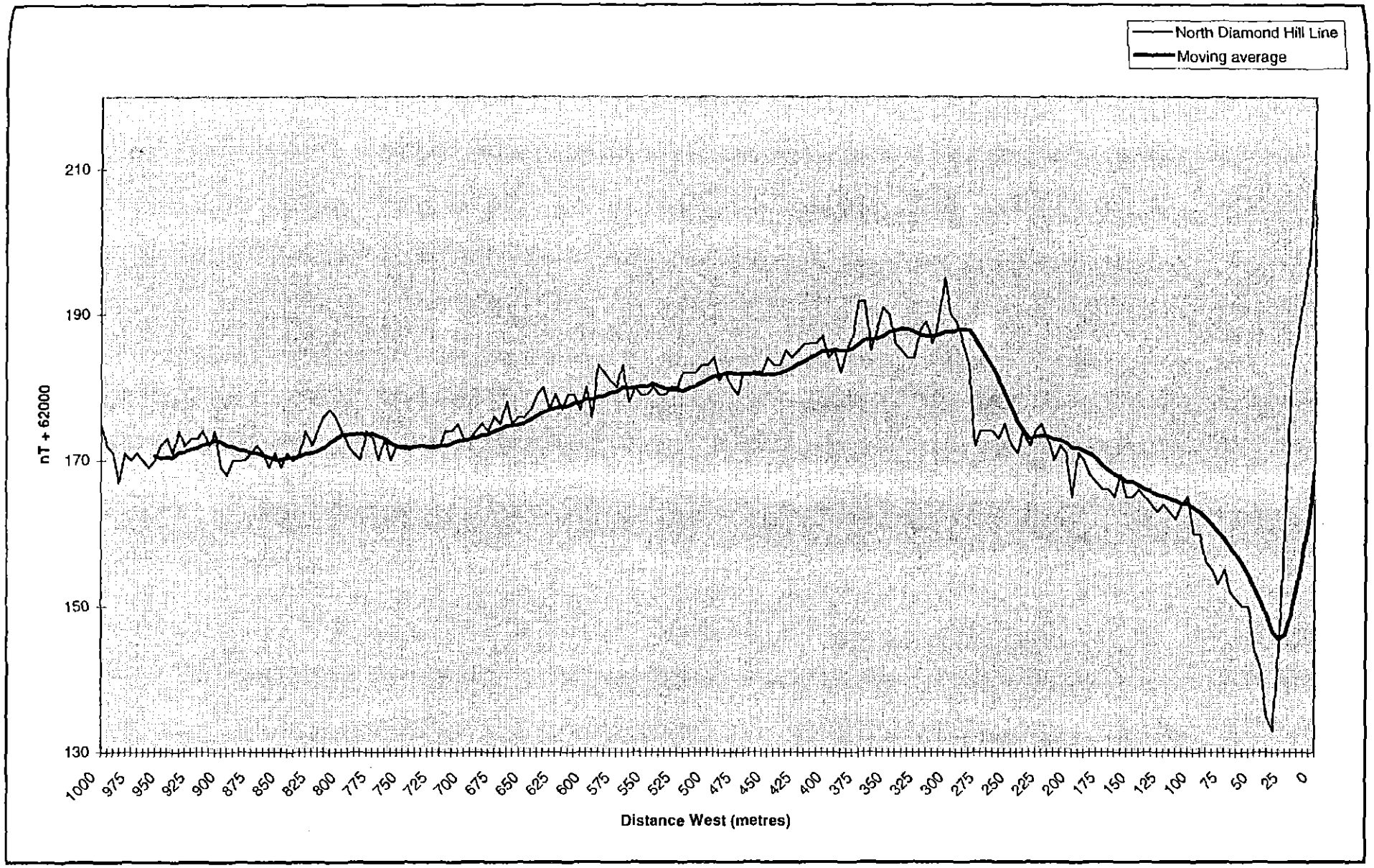

Figure 6.6 - Magnetic profile along North Diamond Hill Line. Magnetic low at 20 metres represents boundary between two units.

6.3.3.2 Diamond Hill Grid

Overall magnetic readings changed in intensity between 62146 and 62262 nT, over the Diamond Hill grid. The Qfb porphyry, which begins at 560 metres on the Diamond Hill Baseline, creates no rise in magnetic response from the level acquired over host rocks (Figure 6.7).

On the three grid lines which drape Diamond Hill there does appear to be some increase in magnetic response (Figures 6.8(a), (b) and (c)). The interpreted increase is shown on Grid Line 360 North (45 to 35 metres), 320 North (90 to 165 metres) and 260 North (30 to 195 metres). This pattern does reflect the underlying position of the Qfb porphyry (Figure 4.2). A larger magnetic response along Grid Line 320 North (270 to 329 metres) does not occur over the Qfb porphyry, but may be due to the Qfh porphyry off to the east.

6.4 MAGNETIC SIGNATURES

6.4.1 Quartz-feldspar-biotite Porphyry

The Qfb porphyry shows differing magnetic responses when comparing the North Diamond Hill magnetic survey and the Diamond Hill Survey. A distinct rise in magnetic response can be seen the North Diamond Hill plot (Figure 6.6). This response is around 62190 nT when at its peak. Similar responses are received over the Diamond Hill Grid, but are perhaps masked by a larger response in host rocks.

6.4.2 Quartz-feldspar-hornblende Porphyry

The can not be examined within ground magnetic surveys conducted for this project. It is known that this porphyry unit exhibits large magnetic responses evident in regional aeromagnetic images. It is assumed that the unit would show similar high responses in ground survey. The one line that traverses a Qfh porphyry, (North Diamond Hill Line, Figure 6.6), shows the beginning of an increased magnetic reading, however the response may continue to climb or fall away after this point.

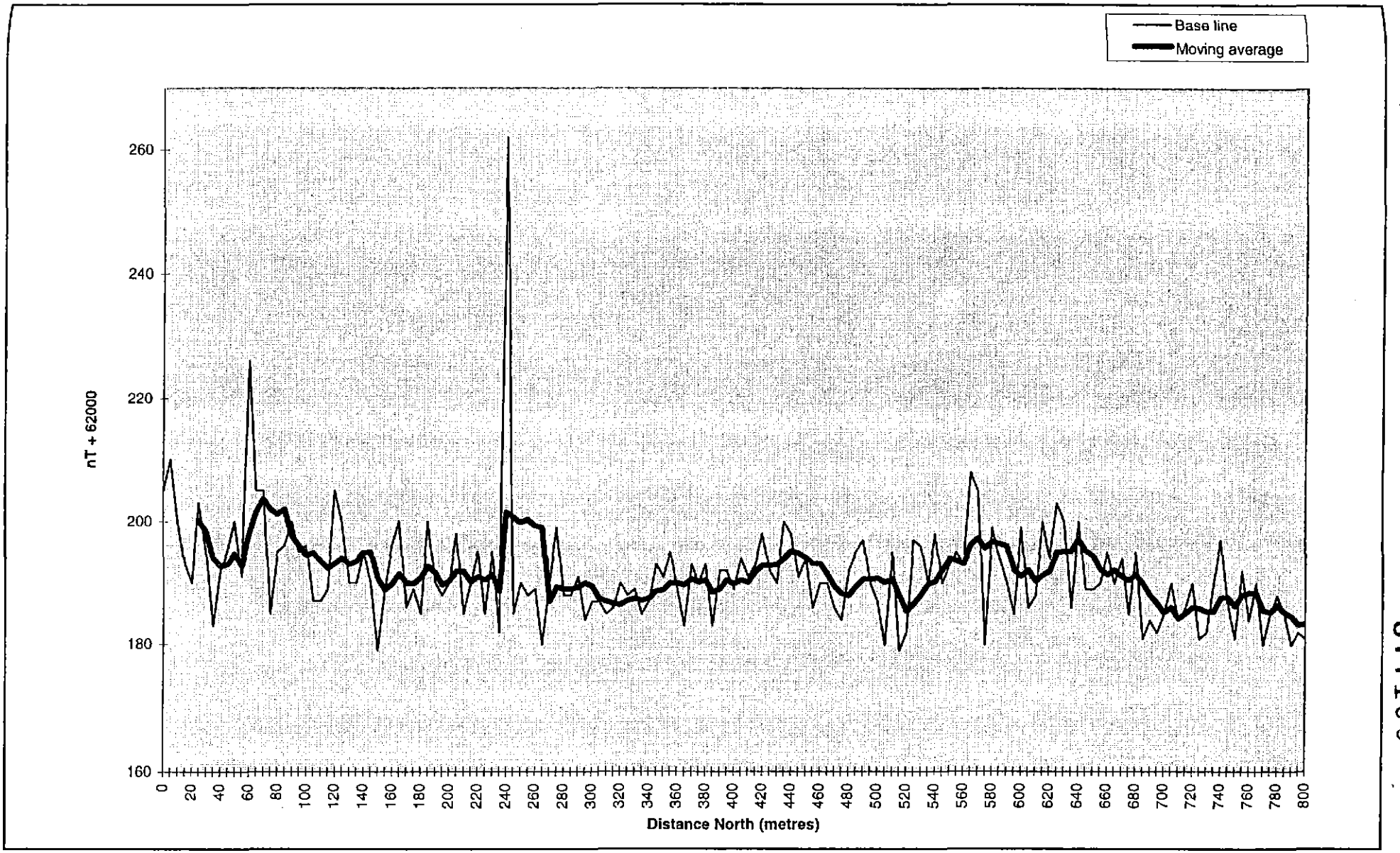

5771106

64

Figure 6.7 - Magnetic profile along the Diamond Hill Baseline. Spike in data at 240 north is due to discarded metal at old adit entrance.

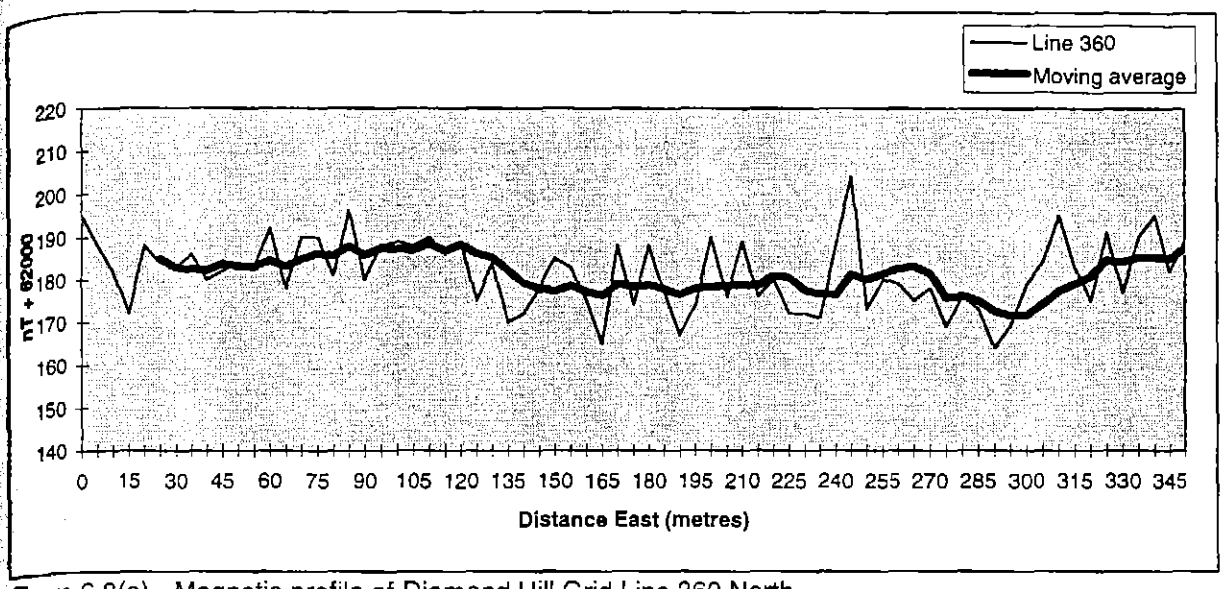

Figure 6.8(a) - Magnetic profile of Diamond Hill Grid Line 360 North

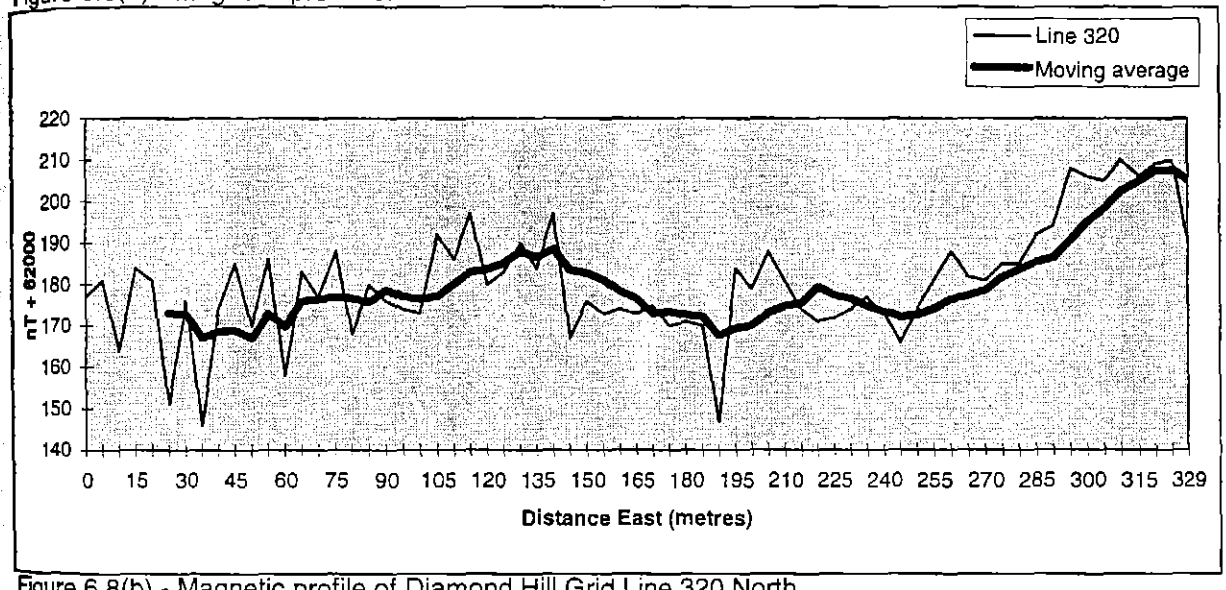

Figure 6.8(b) - Magnetic profile of Diamond Hill Grid Line 320 North.

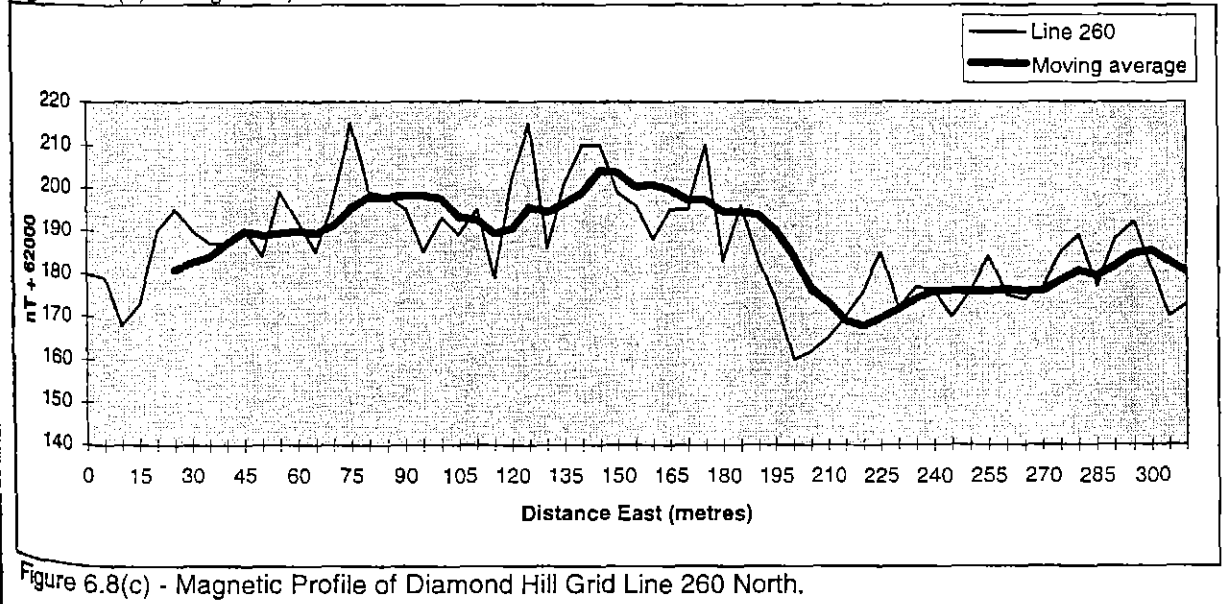

Figure 6.8(c) - Magnetic Profile of Diamond Hill Grid Line 260 North.

6.4.3 Host Sequence

The host sequence which contains Qfb and Qfh porphyritic units shows a general background response of around 62170 nT. This response is much larger (62190 nT) along the Diamond Hill Baseline. Fluctuation in the unit could therefore be in the range of 20 to 30 nT.

6.5 SURFACE ROCK SHIP SAMPLING

6.5.1 Data Acquisition

Rock chip samples of Qfb porphyry and quartz veins, were collected from the Diamond Hill area (Figure 6.9). Samples were assayed for gold (Appendix VII), and represented on Figure 6.9 in ppm.

6.5.2 Gold Patterns

A distinct gold anomaly is indicated by an east-west feature (dashed line on Figure 6.9) which marks assay results above 0.1ppm and corresponds with dominant surface quartz vein direction. Maximum gold assay value of 2.29 ppm is found within this feature. Only one rock chip sample with gold assay levels above 0.1 ppm is found outside this sketched boundary. Sample H1345 lies below Diamond Hill Grid line 260 North and represents an anomalous gold value outside of the designated area.

6.5.3 Results

Values for gold assays around the Diamond Hill area range from <0.01 to 2.29 ppm. Anomalous rock chip gold values (>.1 ppm) occur in a restricted region, with only one other anomalous value occurring to the south of Diamond Hill.

The pattern of gold values shown in Figure 6.9 shows similar orientation to dominant quartz veins cropping out on the surface. The anomalous values may be linked to concentrated gold within these veins.

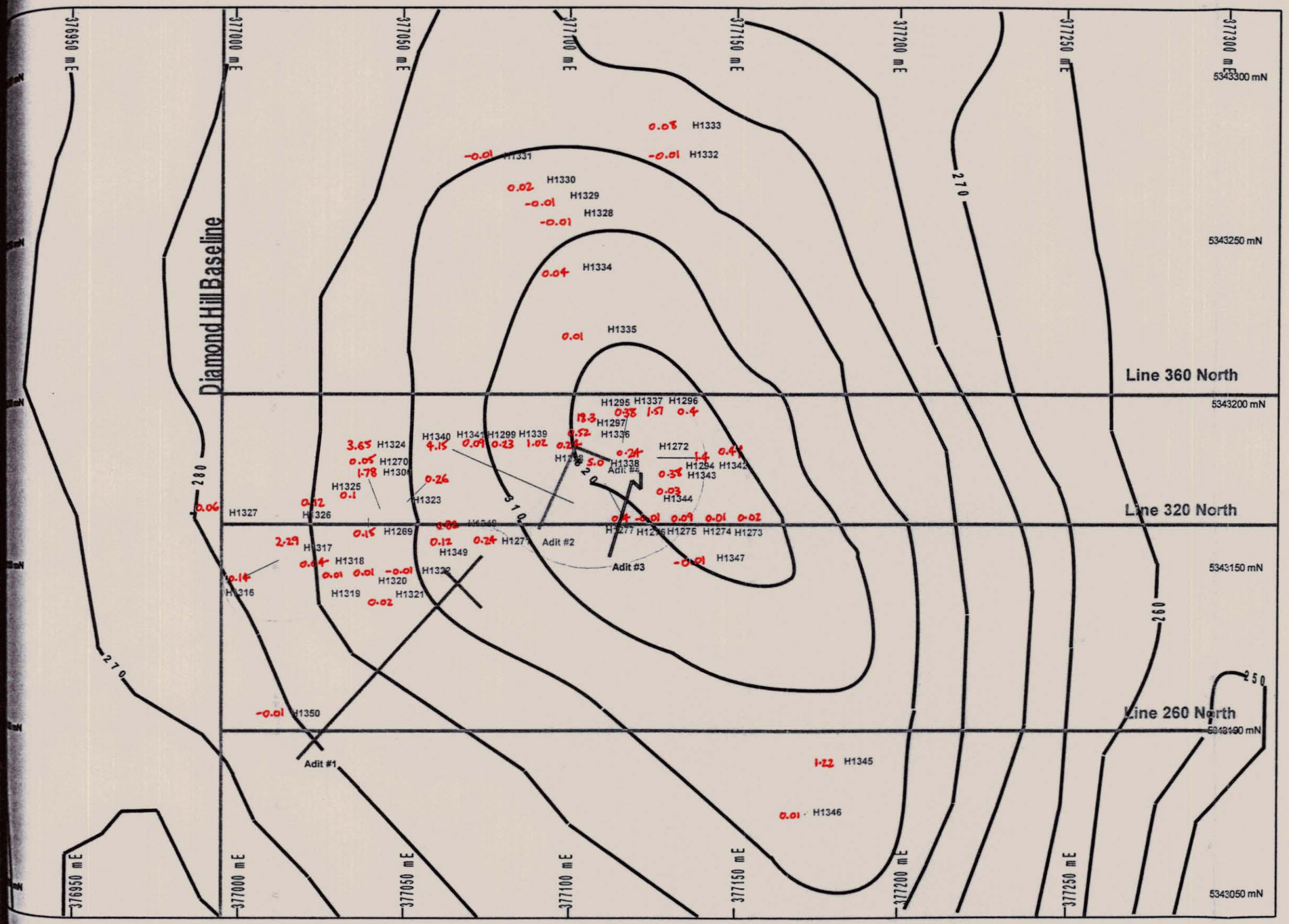

Figure 6.9 - Rockchip samles from Diamond Hill Prospect, with Au assays in ppm (After Morrison and Griffiths, 1998). Figure also shows location of adits and cut grid lines.

6.6 ADIT CHANNEL SAMPLING GEOCHEMISTRY

6.6.1 Sample Program

Rockchip samples were collected from 4 adits located on Diamond Hill (Figure 4.3). A continuous channel sampling technique was utilized so as to capture an adequate sample, which represented the entire length of the adit.

Approximate 1.5 kilogram samples were collected at 2 metre intervals along the entire length of each adit. Samples were assayed for base metals, Au and Arsenic (As), (Figures 6.10, 6.11, 6.12 and 6.13, Map 3, Appendix VIII). Magnetic susceptibility measurements were taken of pulps after assay. These readings have also been plotted on Map 3, and tabulated within Appendix IX.

6.6.2 Results

Quartz veins and porphyritic rocks sampled show elevated levels of gold, above host rock concentration (Map 3). Au values ranged from 0.01 to 0.52 parts per million (ppm) within porphyritic units.

The only elevated gold value within host rocks occurred in and around a major quartz vein in adit number 1.

Low zinc levels are generally recognized where there are increased values of gold within units. No correlation between As and base metals is evident. Copper and Lead also show no distinct patterns throughout any adits.

6.6.3 Analysis

Increased gold values can be attributed to quartz veins or porphyritic rocks found in these adits. The pattern is reflected within surface rock chip sampling (Chapter 6 -6.4) which shows anomalous gold within Qfb porphyry and quartz veins.

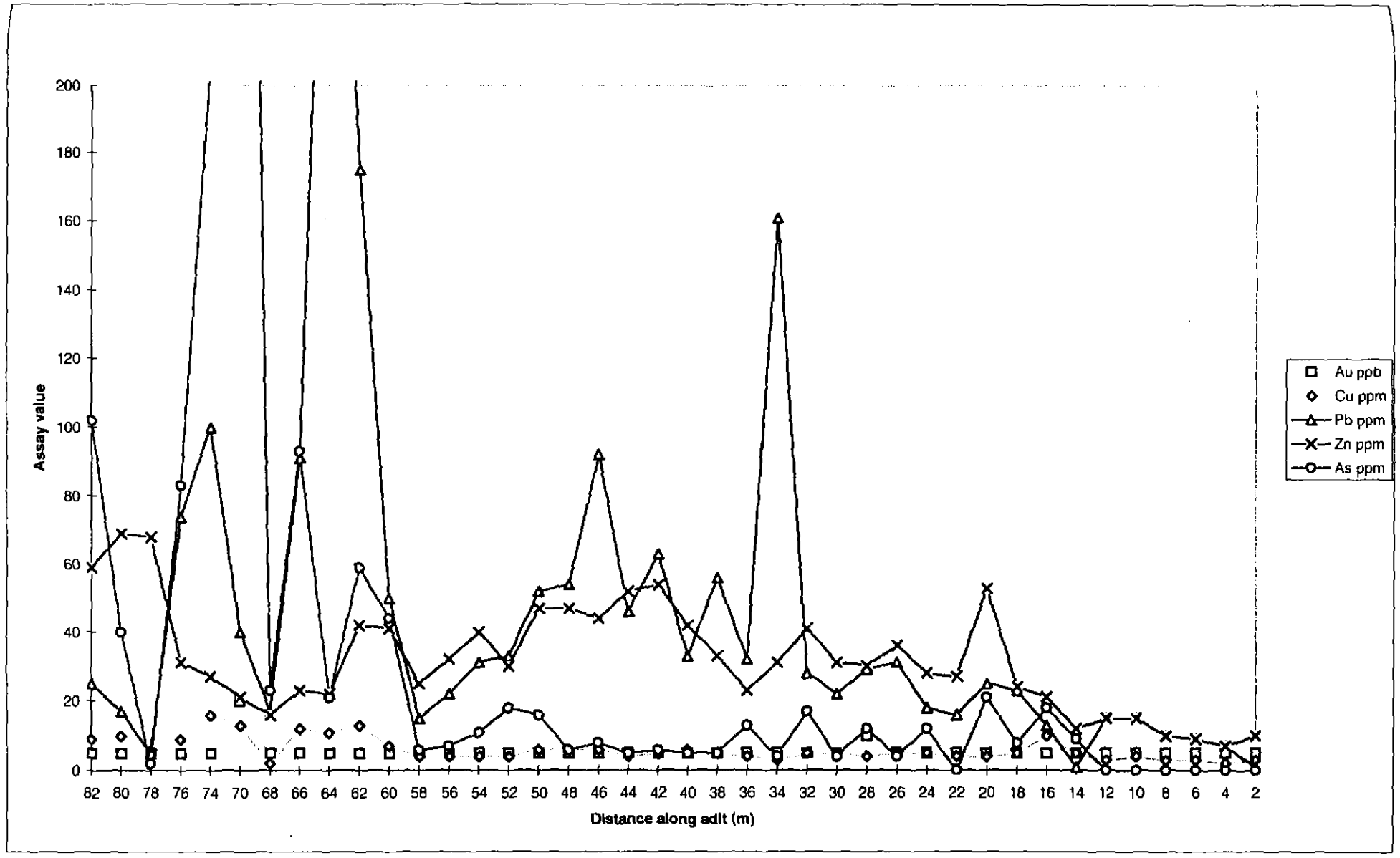

Figure 6.10 - Channel sampling assay results for adit #1 main drive, Diamond Hill. Note: Gold values in ppb, all other elements represented as ppm.

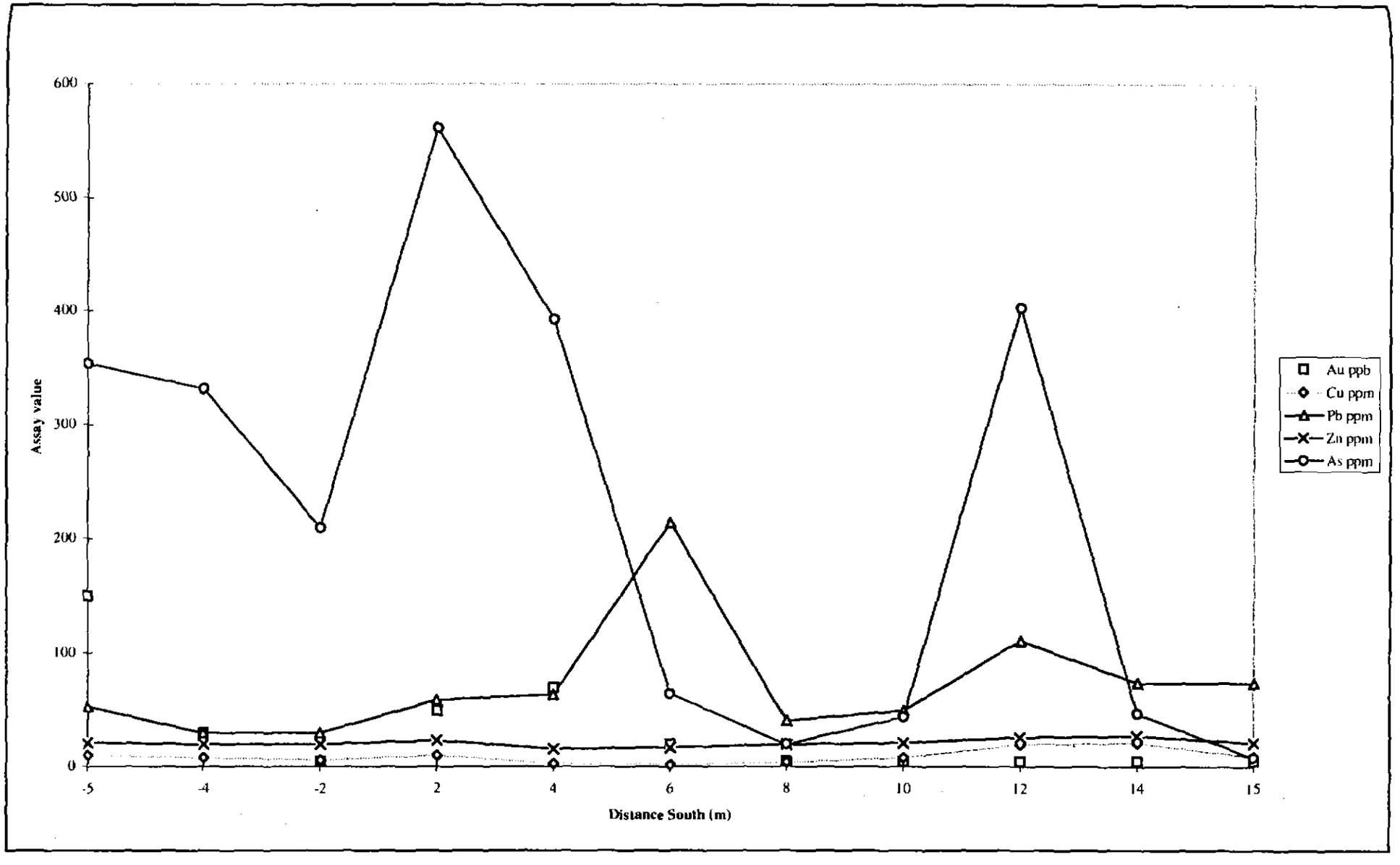

Figure 6.11 - Channel sampling assay results for adit #1cross-cut, Diamond Hill. Note: Au assays in ppb, all other elements represented as ppm.

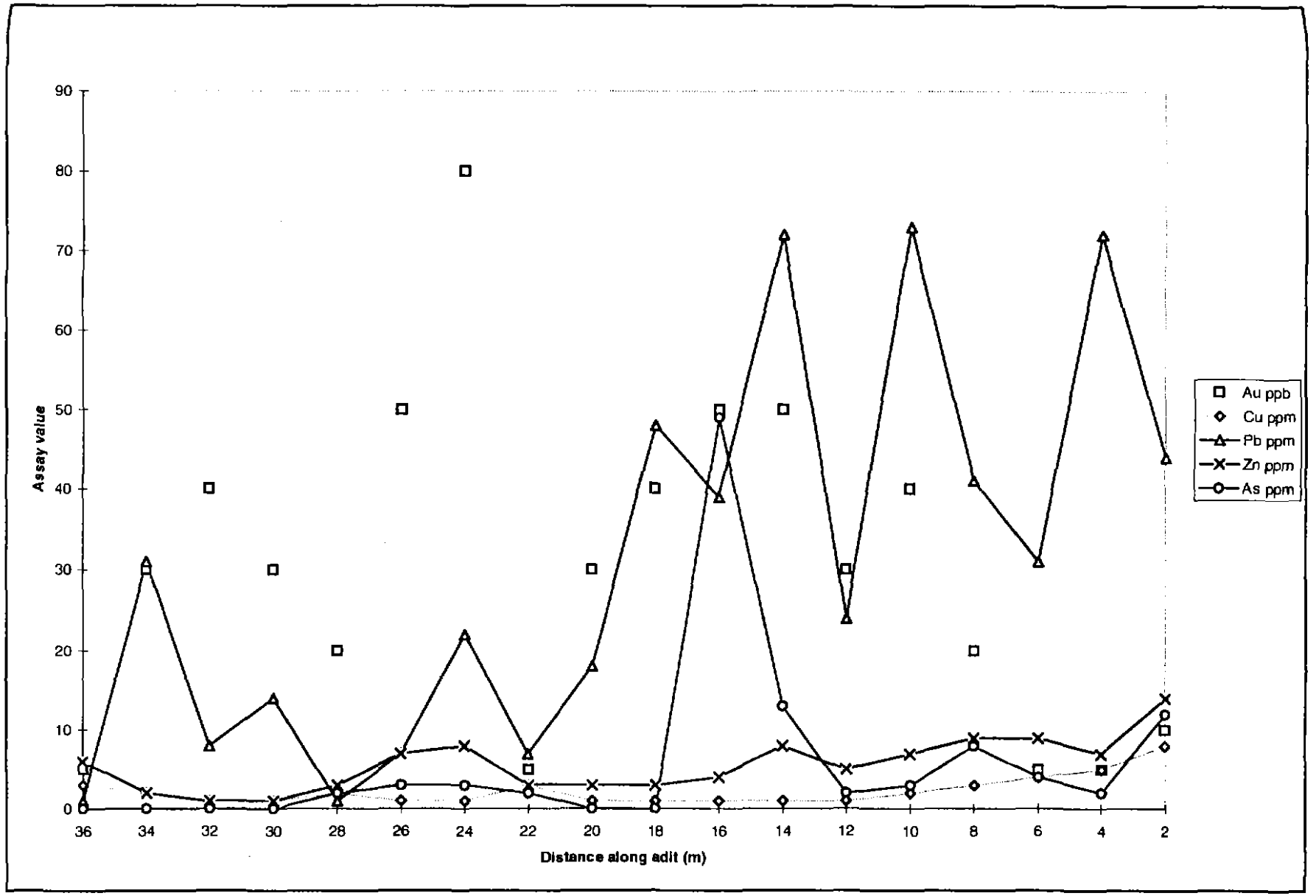

Figure 6.12 - Channel sampling assay results for adit #2, Diamond Hill. Note: Gold assay values in ppb, all other elements represented as ppm.

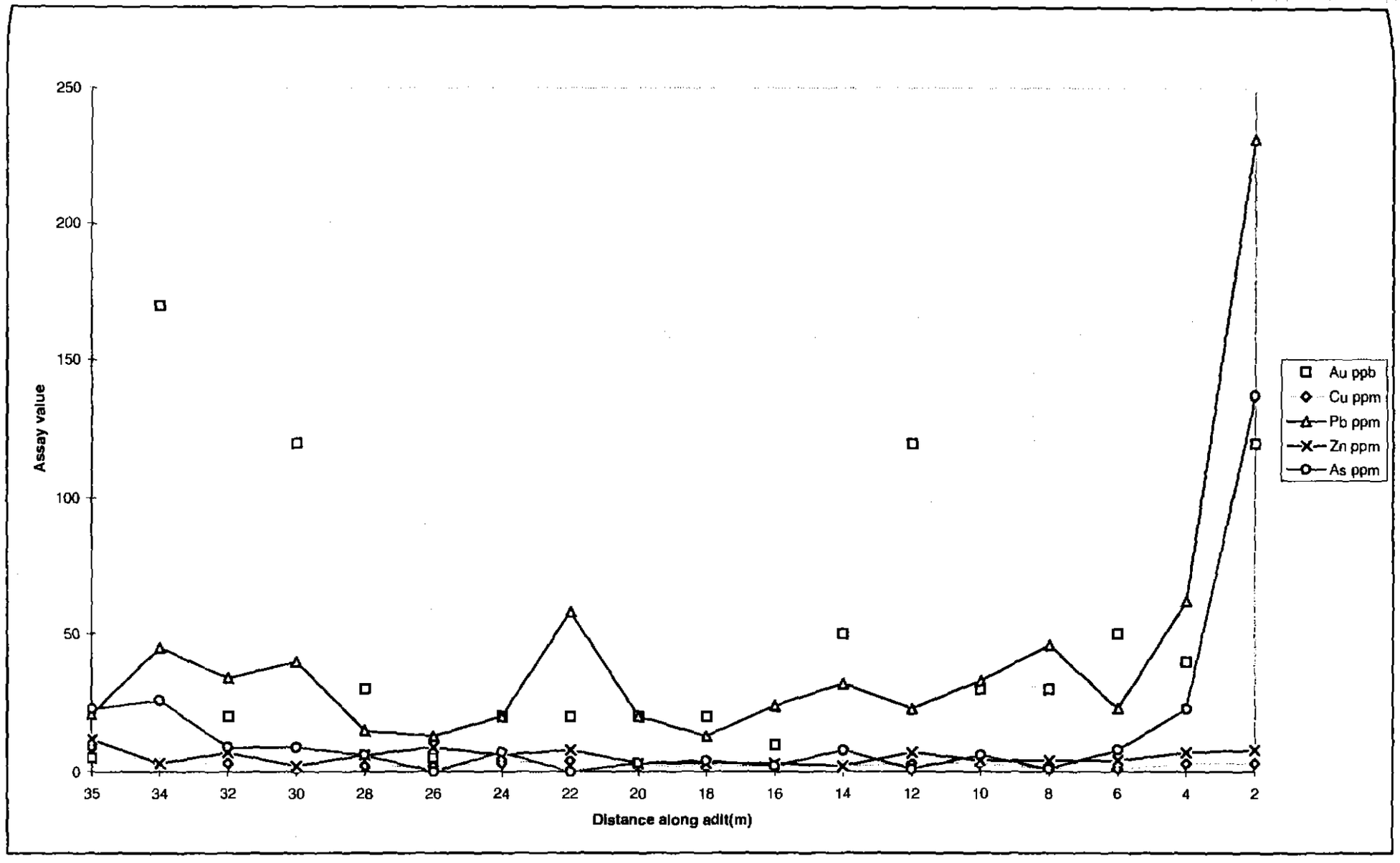

Figure 6.13 - Channel sample assay results for adit #3, Diamond Hill. Note: Gold values in ppb, all other elements represented as ppm.

6.6.4 Analysis of Quartz Veins

Quartz veins within the adits at Diamond Hill are of three main sizes. Alteration surrounding the veins is inferred to be pervasive. Such is the extent of the veining that the entire porphyry host has been intensely altered. Mineral assemblages are not consistent with those exhibited in Porphyry Cu deposits, and no halos of alteration are evident.

Quartz veins are similar in appearance to gold rich quartz veins cropping out south of the Firewood Siding Fault, in Siluro-Devonian aged rocks. Rock units south of the Firewood Siding Fault are younger in age than YRS rocks in the study area. The relationship of veins within both areas therefore assumes quartz veining is post magmatic with respect to porphyries. Some structural control must be inferred, for the veins to be so intense within this porphyry unit and randomly scattered in surrounding host rocks.

6.7 SPECIFIC GRAVITY CALCULATIONS

Proposal to map the Diamond Hill Qfb porphyry through gravity surveys needed preliminary tests to determine gravity differences between different lithologies, and therefore the likelihood of success.

Adit samples were chosen so as to represent all lithologies around the Diamond Hill prospect. Specific gravity (SG) calculations were conducted on twelve samples, representing three dominant lithologies. Tabulated SG results with sample numbers and lithology types are shown in Appendix X.

Host rocks recorded SG values between 2.28 and 2.69 g/cm^3. Porphyry units showed similar results between 2.50 and 2.55 g/cm^3. The variation between units therefore overlapped and would prevent successful gravity surveys being conducted.

CHAPTER 7 : CONCLUSIONS

7.1 SYNTHESIS OF RESULTS

Porphyritic units within the Yolande River Sequence are of two compositions: Rhyolitic, Quartz-Feldspar-Biotite (Qfb) and Dacitic, Quartz-Feldspar-Hornblende (Qfh). Porphyries have been affected by regional feldspar and sericite alteration to different extents, due to primary mineralisation. Qfb porphyries have undergone pseudomorphing of feldspars to muscovite extensively in nearly all specimens. All examined hornblende minerals within Qfh porphyritic units have been selectively altered to chlorite. Similar ground mass of quartz and feldspar phenocrysts, surrounded by muscovite, causing a crude cleavage, is viewed in all porphyry units.

Rhyolitic and dacitic porphyries concur with Suite I and Suite II groups (*Crawford et al.*, 1993) respectively. The divisions of these Suites are best analyzed geochemically through a mixture of whole rock and immobile element determinations, SiO_2, TiO_2, Zr, K_2O, P_2O_5 and Na_2O being the most favourable.
Eight different porphyry units have been studied, with six of these having Suite I characteristics and two having Suite II characteristics. Porphyry 5, is reclassified as Qfb composition, due to thin section analysis and an analyzed signature of Suite I composition.

Lack of regional aeromagnetic and ground magnetic response from Qfb porphyries is contrasted by the large response received from Qfh porphyries. A composite of surface magnetics, mapping and soil geochemistry are the best parameters for locating Qfb porphyries.

7.2 RELATIONSHIP BETWEEN PORPHYRIES AND QUARTZ VEIN-TYPE GOLD MINERALISATION

The most altered Qfb porphyry, Diamond Hill, contains gold enrichment in assay data analysis, which is not reflected within surrounding host rocks. Extensive quartz veining throughout this porphyry also shows anomalous gold assay values.
It is interpreted that this porphyry has been largely altered due to it's brittle nature and the subsequent localization of quartz veining within the unit. Quartz veins are considered to be post magmatic with respect to porphyry units and related to similar Tabberrabberran gold-rich quartz veining, south of the Pearl Creek Fault. Eldon Group Bell Shale, which lies south of the Pearl Creek Fault, is younger than YRS rocks and therefore similar veining would identify post-magmatic timing.

The Diamond Hill porphyry must therefore be located on a structure which has localized the quartz veining to this unit. Strike direction of this porphyry is anomalous with respect to all other porphyries in the area, except for P2. P2 only crops out in three locations and therefore no directional interpretation can be inferred. The Diamond Hill porphyry may be structurally controlled , causing north-west strike direction, rather than dominant north striking of other porphyries. A structural control over this porphyry would accommodate a site for post–magmatic vein emplacement.

The intense quartz veining within the Diamond Hill porphyry is frequent enough to cause intense alteration. This is the most likely conclusion for the anomalous alteration of this porphyry.

Quartz veins are interpreted not to relate to porphyry bodies, but rather to localize on structures which allow fluid movement. Exploration for quartz vein-type gold mineralisation should be focussed on areas where localizing structures are present.

REFERENCES

Banks M.R. and Baillie P.W., 1989. Late Cambrian to Devonian, In Burrett C.F. and Martin E.L. (Eds.), Geology and mineral resources of Tasmania. *Geol. Soc. Aust. Spec. Publ.*, 15: 182-237.

Berry R.F., 1989. The history of fault movement on the Henty Fault Zone, Western Tasmania: an analysis of fault striations. *Aust. Jour. Sci.*, 36: pp 189-205.

Berry R.F., 1990. Structure of the Queenstown area and its relationship to mineralisation. Interim Report. *CODES:Amira Project P291 - Structure and Mineralisation of Western Tasmania.* pp 27-67.

Bishop J.R., 1981: A reinterpretation of the Dighem surveys over the Henty-Yolande, Selina and Lynch Ck. Areas. Mitre Geophysics Pty. Ltd. (unpubl.) TCR 84-2258

Brophy P. & Stevens-Hoare N.P., 1976: Annual report EL 41/71 (Henty-Yolande area) 1975-76. Mt Lyell Mining and Railway Co. Ltd. (unpubl.) TCR 76-1176.

Burrett C. F. & Martin E. L. 1989. Geology and mineral resources of Tasmania. *Special Publication Geological Society of Australia* 15.

Calver C.R., 1995. ETA 389 Notes – Yolande River. Tasmania Development and Resources Notes.

Corbett K. D., 1992. Stratigraphic-Volcanic Setting of Massive Sulfide Deposits in the Cambrian Mount Read Volcanics, Tasmania. *Economic Geology and the Bulletin of the Society of Economic Geologists* (ISSN 0361 - 0128) Vol 87 May 1992 No. 3.

Corbett K.D. & Lees T.C., 1987. Stratigraphic and structural relationships and evidence for Cambrain deformation at the western margin of the Mt Read Volcanics, Tasmania. *Aust. Jour. Earth Sci.*, 34(1); pp 45-67

Corbett K.D & Solomon M., 1989. Cambrian Mt. Read Volcanics and associated mineral deposits, In Burrett C.F. and Martin E.L. (Eds), Geology and mineral resources of Tasmania. *Geol. Soc. Aust. Spec. Pub.*, 15: 154-181.

Corbett K.D. and Turner N.J., 1989. Early Proterozoic deformation and tectonics. In Burrett C.F. and Martin E.L. (Eds.), Geology and mineral resources of Tasmania. *Geol. Soc. Aust. Spec. Pub.*, 15: 154-181.

Corbett K.D., Pemberton J. and Vicary M.J., 1993. Map 13. Geology of the Mt Jukes Mt. Darwin area. Scale 1:25 000. *Geol. Surv. Tasm.*

Copper Mines of Tasmania Pty. Ltd. Arc Info digital basemap for EL 27/95 Yolande River

Crawford A.J., Corbett K.D. & Everard J.L., 1992. Geochemistry of the Cambrian Volcanic-Hosted Massive Sulphide-Rich Mount Read Volcanics, Tasmania and Some Tectonic Implications. *Economic Geology & the Bulletin of the Society of Economic Geologists*, Vol. 87, 3, pp 597-619.

Fitzgerald F.G. & Poltock R., 1991: EL 11/85 Yolande Joint Venture Relinquishment Report August 1985-January 1991. Pasminco Exploration. (unpubl.) TCR 91 – 3222.

Geological Survey of Tasmania. Queenstown Map, 1:25000 & Mt Read Volcanics Project, Map 6, 1:1000.

Groves, D.I., 1964. Madam Howard Plains Barite Deposit. *Tas. Dept. Mines Tech. Rep. No. 8*, 73-81.

Herrmann W., 1998. Use of immobile elements and chemostratigraphy to determine precursor volcanics. CODES: AMIRA / ARC Project (Unpublished).

Howland-Rose A. W., 1974: A report on electrical induced polarisation reconnaissance survey over the Madam Howards grid, Henty-Yolande area, EL 41/71 Queenstown. Scintrex Pty. Ltd. (unpubl.) TCR 84-2233.

Ishikawa Y., Sawaguchi T., Iwaya S., and Horiucihi M., 1976. Delineation of prospecting targets for Kuroko deposits based on modes of volcanism of underlying dacite and alteration haloes. *Mining Geol.* 19: pp 379-382

Jago J.B., Reid K.O., Quilty P.G., Green G.R. and Daly B., 1972. Fossiliferous Cambrian limestone from within the Mt Read Volcanics, Mt Lyell Mine area, Tasmania. *Jour. Geol. Soc. Aust.*, 19: pp 379-382.

Large R. R., 1998. Development and use of the alteration box plot. CODES: AMIRA / ARC Project (Unpublished).

MacClean W.H. & Barrett T.J., 1993. Lithogeochemical techniques using immobile Elements. Journal of Geochemical Exploration, V48, pp. 109-133.

McPhie J. & Allen R.L., 1992. Facies Architecture of Mineralized Submarine Volcanic Sequences: Cambrian Mount Read Volcanics, Western Tasmania. *Economic Geology*, Vol. 87, pp. 587-596.

McPhie J. & Gemmell J.B., 1992. Mount Read Volcanics : host sequences to Cambrian massive sulphide deposits in western Tasmania. *Bull. Geol. Surv. Tasm.*, 70: pp 161-166

Meares R.M.D., Purvis J.G., Hutton M.J. & Komyshan P., 1982: EL 9/66 Tasmania Annual Report 1981-1982. Gold Fields Exploration Pty. Ltd. (unpubl.) TCR 82-1791.

Morrison K. C. and Griffiths A. G., 1998. Annual Report Year 2 (24/05/97 - 4/05/98), EL 27/95 Yolande River (Unpublished). Copper Mines of Tasmania Pty. Ltd. T1998-005.

Pemberton J. and Corbett K.D., 1992. Stratigraphic-facies associations and their relationship to mineralisation in the Mount Read Volcanics. *Bull. Geol. Surv. Tasm.*, 70: pp. 167-176.

Purvis J.G., Jones M.T., Fitzgerald F.G., Komyshan P., & Bishop J.R., 1983: Relinquishment Report Henty-Yolande and West Huxley areas, Tyndall EL 9/66 western Tasmania. Gold Fields Exploration Pty. Ltd. (unpubl.) TCR 83-2029

Purvis J.G., Jones M.T., Fitzgerald F.G. & Poltock R., 1983: A Geological Review of the Tyndall EL 9/66, western Tasmania Gold Fields Exploration Pty. Ltd. (unpubl.) TCR 83-1995

Quayle, P.M., 1995: Pasminco Exploration Yolande River EL 25/91 Annual Report July 1994-June 1995 and Final Report November 1991 – August 1995. Pasminco Exploration. (unpubl.) TCR 74-1054

Rollinson H., 1993. Using geochemical data: evaluation, presentation, interpretation: *Longman Scientific & Technical*, England.

Sheppard N.W., 1974: Report on EL 41/71 (Henty-Yolande area) 1973-74. Mt Lyell Mining and Railway Co. Ltd. (unpubl.) TCR 74-1054

Sheppard N.W., 1974: Report on EL 41/71 (Henty-Yolande area) 1974-75. Mt Lyell Mining and Railway Co. Ltd. (unpubl.) TCR 75-1093

White N.C., 1975. Cambrian volcanism and mineralisation, south-west Tasmania. *PhD Thesis (Unpublished), University of Tasmania*. pp. 264.

APPENDICES

APPENDIX I

Literature Review

The form, contact relationships, and modes of emplacement of porphyry bodies in subaqueous sedimentary sequences

Ashley Griffiths (B.Sc.)

University of Tasmania

A literature review submitted in partial fulfilment of the requirements of the Degree of Bachelor of Science with Honours.

Centre for Ore Deposit Research (CODES SRC)

School of Earth Sciences

University of Tasmania

November 1998

Abstract

Porphyritic bodies are created by disruption of deep cooling magmatic chambers. These magmas rise through the above sediment rapidly when changes in pressure occur. Cooling quickly once near the surface, this quenching of the magmatic body preserves dominant textures providing large porphyritic bodies.

The uprising magma which creates porphyry bodies, will only rise to a certain level. The extent of this rising depends greatly on the density of the magma and the density of the rock or sediments it is intruding into. Other factors include the amount of water present in the host unit and the amount of compaction the host has undergone.

Once uprising magma reaches rocks or sediments which are less dense than itself, then it will cease to rise further. If the magma does not intrude sediments of lower density then it will continue upward until it extrudes to the surface. Lowe density rocks or unconsolidated sediments will therefore be intruded by bodies such as sills, dykes and cryptodomes. Consolidated sediments and rock will be hosts to extrusive domes and lava flows.

Although these intrusive and extrusive bodies appear to be vastly different, they tend to cause similar contacts and reactions with hosts. Peperite, hyaloclastite and autobreccia are common productions from both intrusive and extrusive magmatic bodies.

Detailed study of contact relationships and modes of emplacement provide information for the identification of different porphyritic bodies.

Table of Contents

List of Figures

List of Tables

Acknowledgments

Thanks must go to:

Wally Herrmann for his initial outline and construction of this literature review, and his overall supervision.

Dr. Jocelyn McPhie for her aid in the finding of suitable references to be studied.

Ken Morrison for his input into current and interesting papers relating to the literature review topic.

Copper Mines of Tasmania Pty Ltd and employees for their support throughout my honours year.

Chapter I1 : Introduction

I1.1 Definitions

Porphyry is used for hypabyssal rocks containing phenocrysts of, in the original sense, alkali-feldspar composition. In many cases, the ground mass of a porphyry is made up of similar composition crystals to those that comprise the phenocrysts (Turner 1960).

The word hypabyssal indicates a rock that has crystallised at an intermediate level, between plutonic and volcanic, ie, a shallow intrusive. Dykes and sills are typical hypabyssal rock forms. Porphyritic texture may also be found in lavas, lava-like ignimbrites and clasts derived from such deposits (McPhie & Allen 1992).

Porphyritic rocks are generally thought to have formed as coherent facies. This means they have formed directly as a result of the cooling and solidification of molten lava or magma. This means that they have formed directly as a result of the cooling and solidification of molten lava or magma. The classification scheme for general volcanic facies can be seen in figure I1.1.

Porphyries are characterised by crystals that are euhedral, evenly distributed and have narrow size ranges (McPhie & Allen 1992).

The distinction between phenocrysts and smaller crystals of the groundmass in porphyries is attributed to a change in conditions during the cooling of the rock. At depth, cooling and crystallisation are disrupted by the uprising of the magma, and either injection into cold sediments, extrusion onto the surface or injection into solid rock. Such changes in temperature and pressure cause rapid crystallisation or quenching of the magma and subsequent trapping of dominant textures formed during cooling at depth (Turner 1960).

The crystals found in porphyries can be attributed to crystallisation during cooling at depth, because of the high temperature types that are common. It is not right, however, to assume that all crystals found within porphyries have developed in such an environment (Turner 1960), because common porphyry crystals such as alkali feldspar, are low temperature minerals. Such crystals are formed after some movement of magma to the surface and subsequent crystalisation during lower temperatures.

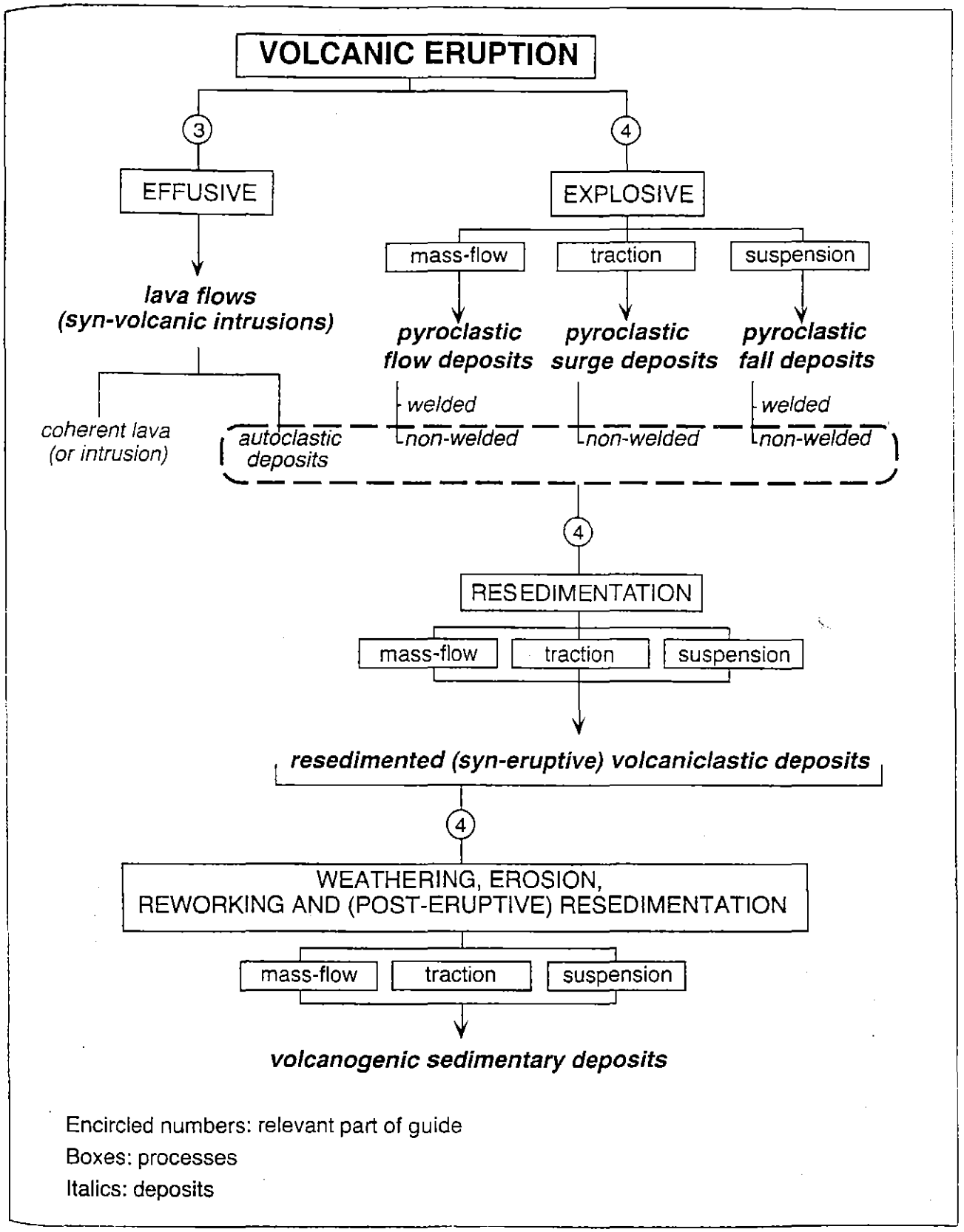

Figure I1.1 - A genetic cclassification for volcanic deposits (McPhie *et al.*, 1993).

I1.2 Aims

The aims of this literature review are

1. to examine different forms of porphyry
2. to understand the processes which develop porphyry bodies
3. to recognise the characteristics of each form of porphyry

Chapter I2: Porphyry Forms

I2.1 Introduction

The rise of magma is determined by its density and hydrostatic pressure in comparison to the density and lithostatic pressure produced by the surrounding sediment or rock type (Figure I2.1).

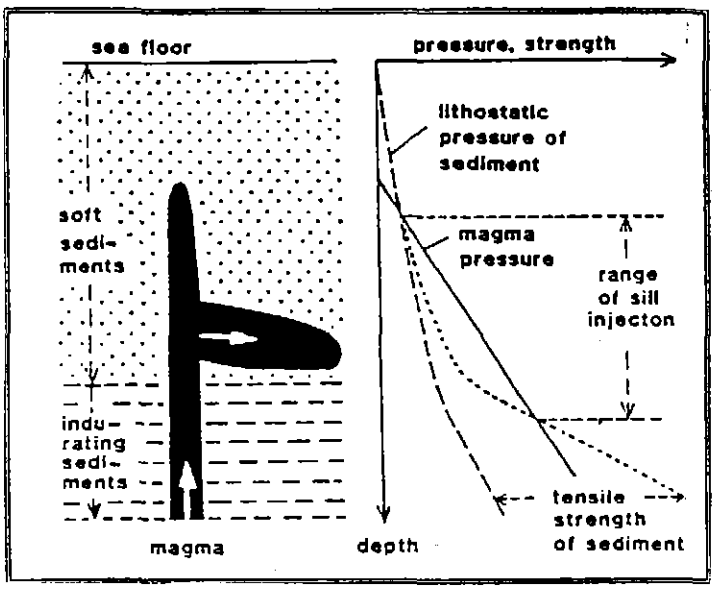

Figure I2.1 - Pressures which affect the rise of magma through sediment (Hine, 1994).

Dense magma will tend to remain under the surface of less dense host lithologies. The subaqueous environment is therefore perfect for the formation of intrusive bodies, due to the fact that it mostly contains unconsolidated thick sediments (McPhie & Allen 1992), and therefore low density material.

A large proportion of magmatism, especially in subaqueous settings may in fact comprise syn-volcanic, high-level intrusions rather than surface flows (McBirney 1963). Other porphyry forms which may occur within subaqueous settings include syn-volcanic sills, feeder dykes, cryptodomes and lavas (McPhie & Allen 1992) (Figure I2.2).

Rock Type	Range (g/cm3)	Average (g/cm3)
Sediments (wet)		
Overburden		1.92
Soil	1.2 - 2.4	1.92
Clay	1.63 - 2.6	2.21
Gravel	1.7 - 2.4	2.0
Sand	1.7 - 2.3	2.0
Sandstone	1.61 - 2.76	2.35
Shale	1.77 - 3.2	2.40
Limestone	1.93 - 2.90	2.55
Dolomite	2.28 - 2.90	2.70
Sedimentary rocks (av.)		2.70
Igneous Rocks		
Rhyolite	2.35 - 2.70	2.52
Andesite	2.4 - 2.8	2.61
Granite	2.50 - 2.81	2.64
Granodiorite	2.67 - 2.79	2.73
Porphyry	2.60 - 2.89	2.74
Quartz diorite	2.62 - 2.96	2.79
Diorite	2.72 - 2.99	2.85
Lavas	2.80 - 3.00	2.90
Diabase	2.50 - 3.20	2.91
Basalt	2.70 - 3.30	2.99
Gabbro	2.70 - 3.50	3.03
Peridotite	2.78 - 3.37	3.15
Acid igneous	2.30 - 3.11	2.61
Basic igneous	2.09 - 3.17	2.79

Table I2.1 - Wet sediment densities and magma densities. (Telford in Hine, 1994).

LAVAS AND SYN-VOLCANIC INTRUSIONS

coherent facies

- porphyritic texture (evenly distributed euhedral crystals) or aphanitic
- high T devitrification textures common in groundmass (spherulites, lithophysae, micropoikilitic texture)
- internally massive or flow foliated
- non-vesicular ↔ vesicular { *pumiceous*, scoriaceous

autoclastic facies

- monomict
- clasts with porphyritic texture or aphanitic texture
- abundant jigsaw-fit texture

autobreccia

- slabby, flow foliated clasts with jagged ends; ragged or blocky, massive clasts
- clast margins not quenched
- pumiceous or scoriaceous clasts common
- low proportion of clasts finer than 2 mm
- separate crystal fragments uncommon

hyaloclastite breccia

- blocky clasts with curviplanar surfaces
- clast margins have (or had) glassy groundmass; clast interiors glassy or crystallised
- "tiny normal joints" along clast margins
- very coarse sand to granule size (1–4 mm) matrix may be abundant
- separate crystal fragments can be abundant
- pumiceous or scoriaceous clasts may be present

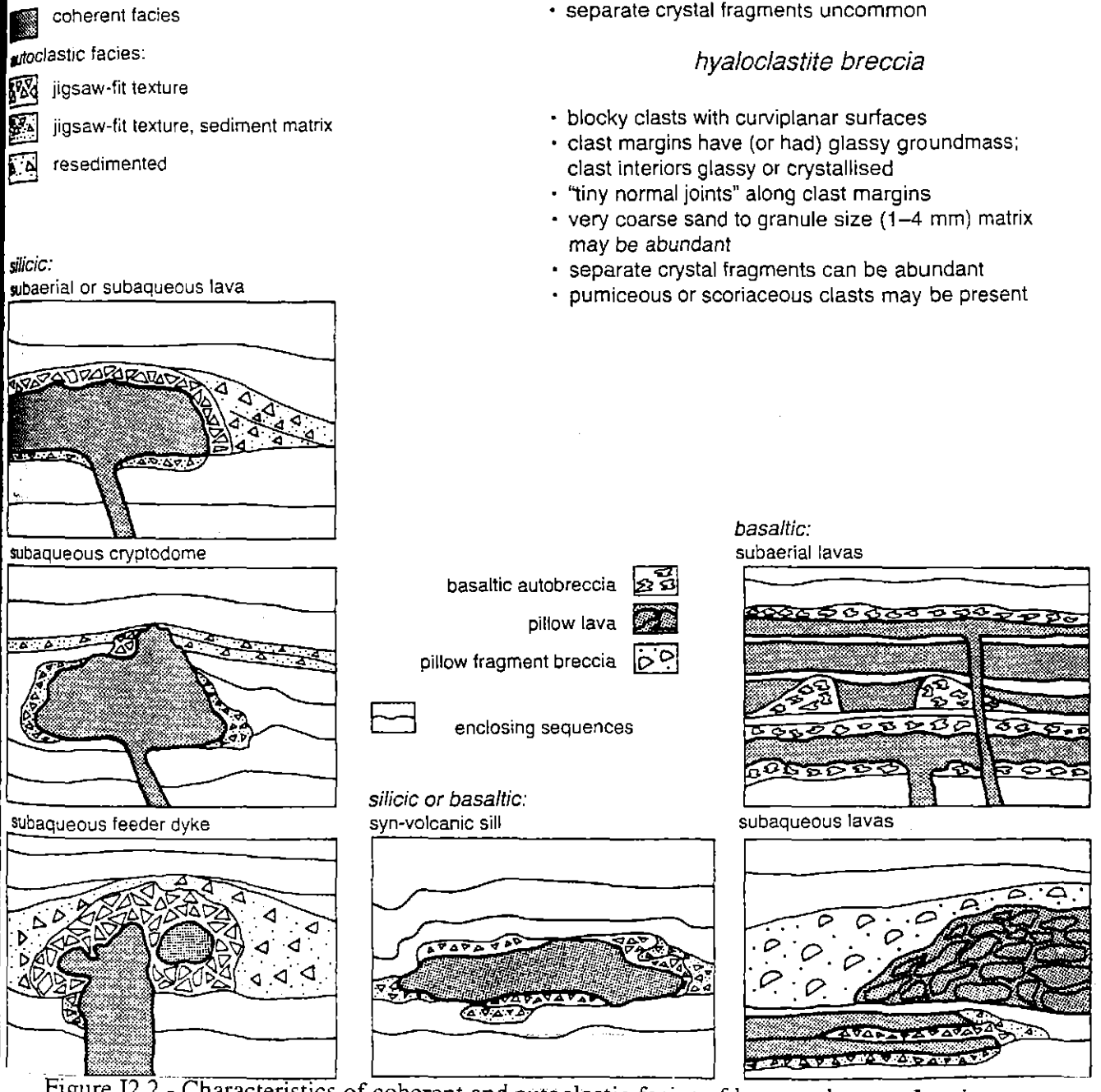

Figure I2.2 - Characteristics of coherent and autoclastic facies of lavas and syn-volcanic intrusions (McPhie *et al.*, 1993).

I2.2 Sills

Sills are characterised as bodies of igneous rock which intrude through host rocks , but conform with the local bedding or structural planes of their host lithology. They may be hundreds of metres thick and extend laterally for many kilometres (Turner 1989).

Sills are normally medium-grained, but can be found to be coarser or glassy in some instances. Sills may be characterised as composite, ie. an original sill of certain character may be intruded by a subsequent sill of different composition. They may also be multiple, which infers that there have been several occurrences of similar material of the same composition, which together make up a single unit (McBirney 1963; Walker 1989).

I2.3 Dykes

A dyke is characterised as a body of igneous rock which is discordant, or crosscuts bedding or other structural planes in the host rock. Dykes usually occur in association with larger igneous bodies and are vertically aligned or steeply dipping. Dykes may link up to other bodies such as cryptodomes, as in figure I2.3.

Although rocks of this kind are normally medium-grained, they may occur as coarse and fine grained rocks in some instances. The grain size will depend on the width and cooling time of each unit (McBirney 1963; Walker 1989). Dykes in general tend to be singularily, much less extensive than sills and may occur in dyke swarms.

There may be a glassy fabric along the outside of some smaller dykes. This indicates that the magma had a very low viscosity and was injected primarily as a liquid. Phenocrysts in such a case are developed after intrusion, whilst the outer groundmass is essentially quenched.

I2.4 Cryptodomes

Cryptodomes are intrusions that cause up-doming of overlying sediments or rocks (Minakami in McPhie 1992). These may also be known as high-level domes. They intrude the overlying sediment, but seldom break the surface (Cas 1992) (Figure I2.3).

Most cryptodomes have intermediate or felsic composition. They have a coherent centre with hyaloclastite composition around the extremities of the dome (Hall 1987). Domes rise up to the surface through pressure changes like other intrusions. If they reach the surface they do not flow, due to the usual viscosity of the magma type.

I2.5 Lava Flows

Lava flows consist of molten or partly-molten silicate materials which are extruded from fissures or vents (McBirney 1963; Walker 1989). They exist as pillow lavas or large extensive lava-sheets and occur as baslatic, andesitic or acid-felsic compositions (Cas 1992).

The mineralogy, abundance and distribution of phenocrysts normally remain fairly consistent within lava flows. This factor thererfore provides useful means for distinguishing between different flows (McPhie et al. 1993).

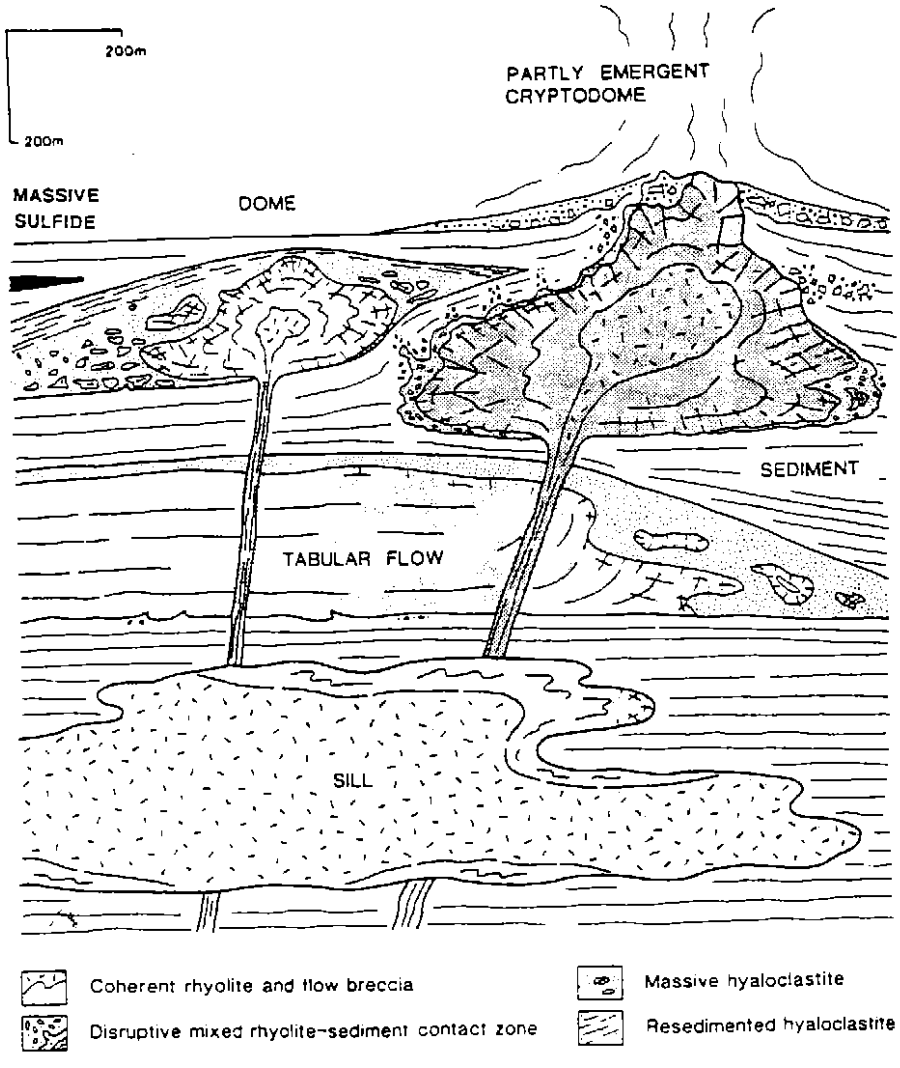

Figure I2.3 - Examples of typical volcanic units found in subaqueous settings (Allen, 1992).

I2.6 Summary

The density of a magma, and the density of the surrounding sediments or rock type within which it lies, will determine whether the magma intrudes or extrudes on to the surface.

Different forms of porphyry bodies are developed due to these properties. Intrusive bodies such as sills and dykes form from magma which is denser than its surrounding host sediments, and therefore does not continue to rise through to the surface.

Bodies such as cryptodomes are generally intrusive, but may have slight effects on the surface, including baking and doming. This indicates an environment where the intrusive magma is close to the density of the surrounding host sediment or rock. Densities of sediment and magma must be similar when there is extrusion of lava domes.

Lavas may represent fully extrusive forms of porphyritic rock. Due to their low density, they will penetrate up to the sediment surface. Subsequent subaqueous flows of lava are emplaced along the ocean or basin floor..

Chapter I3 : Contact Relationships

I3.1 Introduction

Settings such as volcano-tectonic rift basins and submarine volcaniclastic aprons around island-arc volcanoes, are regions interaction between magma and wet, unconsolidated sediment occurs. Such settings are where volcanism and the accumulation of sediments occur simultaneously (Hanson and Wilson 1991).

Interaction between volcanism and accumulating sediment will cause the development of certain contacts and facies types which indicate the processes occurring around porphyry rocks.

I3.2 Passive Porphyry Contacts

Passive margins or contacts can be described as the margins between units which pre-tectonically, show no deformation or mixing of sediments (Allen, 1992).

Passive margin contacts are indicative of easy intrusion of magmatic bodies through sediment host. Due to the ease of intrusion, the host is not deformed and there appear to be clear, undisturbed contacts. This is also characteristic of some intrusions into solid rock.

I3.3 Disruptive Contacts

Disruptive contacts are identified by the intermixing of volcanic rock and sedimentary rocks. This relationship indicates formation of contacts through quenching of magma and wet sediment (Allen, 1992).

The disruptive contact is caused by deformation of original lithology when intrusion and reaction occurs. Factors affecting the behaviour of the intrusion may be "magma viscosity and rate of supply, pore-water volume in the host sediments, and degree of sediment consolidation." (Hanson and Wilson, 1991, pp.262).

I3.4 Peperite

Peperite is a rock generated by mixing of coherent lava or magma with unconsolidated wet sediment (McPhie, 1993), and characterised by a clastic texture in which either component may form the matrix. Primary formation is caused by the fragmentation of the lava or magma. Magmas involved in the formation of peperite may range between basaltic and rhyolitic in composition (McPhie et al., 1993).

Four processes have been suggested by Kokelaar (1986), which may allow the formation of peperite, through the fragmentation of magma: (1) explosive release of magmatic volatiles; (2) steam explosivity; (3) bulk interaction; and (4) cooling contraction granulation.

These processes cause the development of two different peperite forms on the basis of the shape of the igneous component. These are referred to as fluidal and blocky peperites (Busby-Spera and White 1987) (Table I3.1).

Peperitic boundaries indicate strong evidence for an intrusion (McPhie 1993) although subaqueous lavas may also develop peperitic bases and non-peperitic upper margins. Peperite occurs at the contacts between intrusions and wet sediments (Hanson and Schweickert 1982), and a long the basal contacts of lava flows that override or burrow into unconsolidated sediments (Schmincke 1967, Bull and Cas 1989).

Peperitic contacts are often very complex, with planarand mixed contacts often found together in one body.

The preservation of in situ fragmentation textures is an important feature of peperites. Jigsaw fit texture occurs where clasts separated by sediment can be matched back to there original locations before quenching (Hanson, 1991) the outlines of individual clasts separated by sediment can be closely matched like pieces of jigsaw puzzle, are commonly produced by quench fragmentation of magma (Hanson and Wilson 1991)

577145

	Fluidal peperites		Blocky, hydroclastic peperites	
Host	unconsolidated micrite, very fine grained	unconsolidated micrite, very fine grained	lithic lapilli tuff breccia, poorly sorted but generally ash-poor	lithic lapilli tuff breccia, poorly sorted but generally ash-poor
Host permeability	very low (millidarcys?)	very low (millidarcys?)	very high (tens of darcys	very high (tens of darcys)
Host water content	high (40%), diffuse	high (40%), diffuse	high (30%), localized	high (30%), localized
Morphology	Micro-globular	Globular	Blocky	Dispersed
Peperite fragment shape	small (mm-scale) micro-fluidal	medium (cm-dm scale) macro-fluidal	small (mm scale) angular fragments	large (dm-m scale) angular fragments
Peperite fragment-forming mechanism	fluid interface instabilities	fluid interface instabilities (?)	dynamic stressing granulation	steam explosions
Fluidization pipes	mm-scale only	mm-scale only	meter-scale pipes	meter-scale pipes
Mixing mechanisms	immiscibility, fluidization "oscillation-pumping"	immiscibility, fluidization, fluid density differences	dynamic, or unmixed	steam explosions, fluidization

Table I3.1 - Summary of the critical properties of host sediment characteristics which influence peperite formation (Hine, 1997).

I3.5 Hyaloclastite

Hyaloclastite is formed by the non-explosive fracturing of lavas and intrusions in contact with wet sediment (McPhie et al., 1993). The typical composition of hyaloclastite is a material called palagonite, usually in fragments sized from a few millimetres to a few centimetres.

A relationship is evident between fluidal peperite and in situ hyaloclastite, where the two represent distinct end members. The intermediate phase between these two end members may be referred to as intrusive hyaloclastite or blocky peperite (Hine 1994). The fluidal peperitic end member indicates fluidization of magma, blocky peperite indicates brittle fracture and mixing with sediment, and intrusive hyaloclastite representing solely quench fragmentation (Hine, 1994).

Subsequently it can be indicated that different environments may derive different end members. Surface quenching will form an in situ hyaloclastite, sub-surface reactions will cause blocky peperite, and fluidal peperite will form from low viscosity magmas also in the sub-surface environment (Hine, 1994).

I3.6 Autobreccia

"Autobrecciation involves the non-explosive fragmentation of flowing lava" (McPhie et al, 1993). Cooler parts of flowing lava are subjected to different amounts of strain than warmer areas. The response to this increased amount of strain, is brittle fragmentation. The resultant deposit of fragmental or refused brecciated blocks and shards, is known as autobreccia (McPhie et al., 1993).

I3.7 Summary

Peperite, hyaloclastite and autobreccia may be formed from all magmas through the range from basaltic to rhyolitic composition (McPhie et al,. 1993).

Contacts between volcanic rocks and unconsolidated host rocks in subaqeous, volcano-sedimentary sequences generally produce varying amouints of each of these diagnostic rock types.

The contact relationships evident between sills, dykes, cryptodomes and lavas, and their host rocks allow determinations of the type of body present.

The typre of magma intruding or extruding, the rate of lfow of the magma, the amount of water in the host rock and the lithology of the host rock, are all important factors which contribute to the final product produced during contact between volcanic and valcano-sedimentary facies.

Chapter I4 : Modes of Emplacement

I4.1 Introduction

The mode of emplacement of various bodies such as domes, sills, dykes and flows can be determined from characteristic contacts. The basis for determining the mode of emplacement comes from the distribution and relationships between lava, peperite and hyaloclastite (McPhie etal., 1993).

I4.2 Sills

The margins of intrusive sills may be passive contacts or disruptive contacts. The internal structure of these sills is coherent and may have a chilled margin (Allen 1992). The degree of consolidation and grain size of sediment that the sill intruded into, will determine the complexity of the contact relationships. Typical facies character and distribution created during sill emplacement are shown in figure I4.1.

Fine-grained, perlitic and amygdaloidal textures indicate that a sill may have intruded into wet sediments at a moderately shallow level (Allen 1992). Large amounts of hyaloclastite and many disruptive surfaces indicate that a sill may have intruded into unconsolidated and water-saturated sediments. A low amount of hyaloclastite and few disruptive surfaces, indicates that a sill may have intruded into sediments that were more consolidated and less saturated with water (Allen 1992).

Evidence for syn-sedimentary sills primarily lies in the upper contact of the sill, in particular the amount of consolidation of the sediments (McPhie & Allen, 1992). The intrusion of small lobes from the surface of the sill, peperite formation and induration of the host are all important factors for identification (Kokelaar, 1982; Branney & Suthren, 1988). intrusions include variable amounts of hyaloclastite and intrusive hyaloclastite (peperite) breccia, whereas the cores are largely coherent."

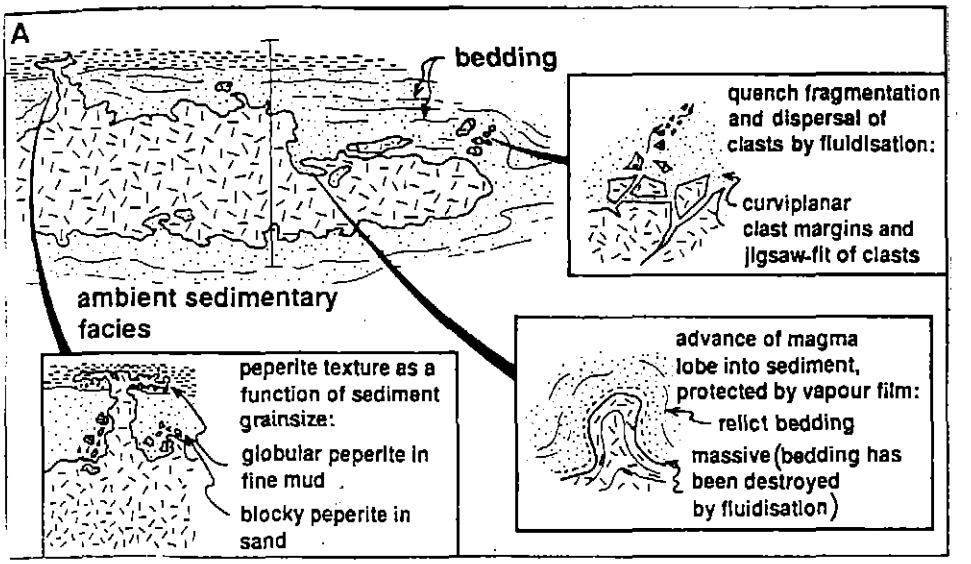

Figure I4.1 - Facies character and distribution formed during emplacement of sills, and the processes involved in the formation of peperite (McPhie *et al.*, 1993).

I4.3 Dykes

Dykes have essentially the same characteristics of sills, in that their boundaries may be passive or disruptive. Due to the fact that dykes crosscut unit boundaries in unconsolidated sediment, it is far more likely that their contacts will be disruptive. Different host rocks will react differently to intrusive bodies, relative to their consolidation and amount of water contained within.

Dykes, may be in many cases, feeders to lava domes and flows, (figure I4.2). Quenching in the near-surface, water-unsaturated enviroinment is evidence of syn-volcanic dykes (McPhie et al., 1993).

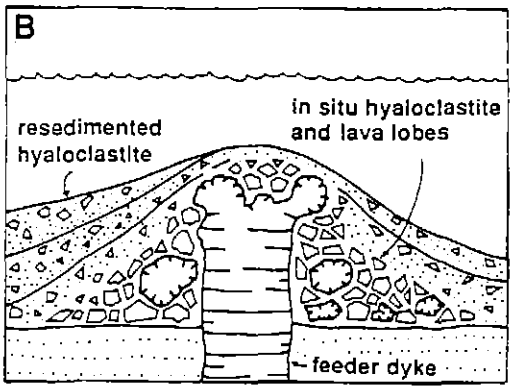

Figure I4.2 Feeder dyke and resultant sedimentation (McPhie *et al.*, 1993).

I4.4 Cryptodomes

577150

Cryptodomes or extrusive domes are characterised by coherent cores of massive coherent volcanic rock. The outer boundary of this solid coherent core is surrounded by hyaloclastite. Generally the hyaloclastite will be massive, however some sedimented hyaloclastite may be present due to the instability of extruding rock. The resedimentation of unstable hyaloclastite may form a volcaniclastic layer directly above extrusive cryptodomes (Allen 1992).

The distribution of facies related to cryptodomes and extrusive domes is shown in figures I4.3 and I4.4 respectively.

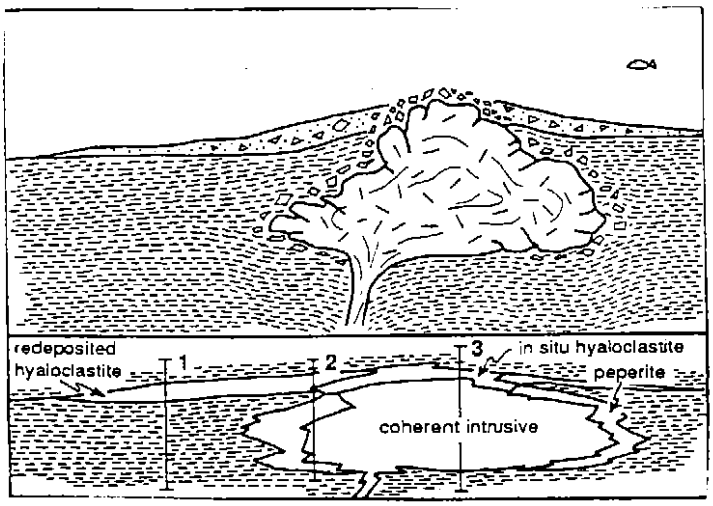

Figure I4.3 - Relationships between facies which develop due to emplacement of subaqueous cryptodomes (McPhie *et al.*,1993).

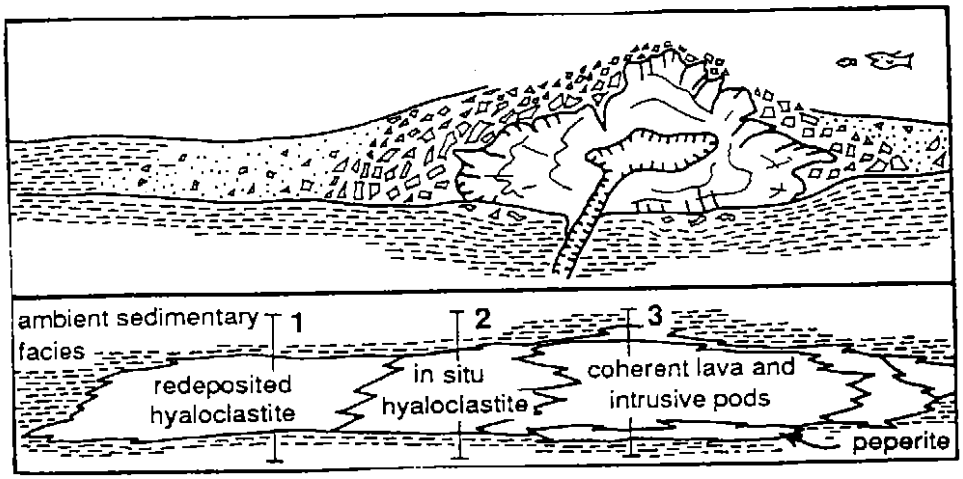

Figure I4.4 - Facies relationships around extrusive lava domes (McPhie *et al.*,1993).

I4.5 Lavas

Lava flows may exhibit the same general internal characteristics as cryptodomes of the same composition. The lateral extent of the coherent centre will however be larger, due to the higher discharge rate exhibited by flows (Allen 1992).

The base of a lava may be peperitic or coherent. If the lava has burrowed into the surrounding sedimentary facies whilst flowing both of these boundary types may form. Peperitic contacts will occur on the basal plane of a lava flow that is relatively passive. If the rate of discharge of the lava is intense and forceful, then the extruding lava may tear away and remove the peperitic or hyaloclastite layer that was formed upon contact with surrounding sediment (Allen 1992).

"If preservation of the flow-top and exposure of the flow-base are both poor, conclusive determination of a unit's physical state at eruption may not be possible"(Manly 1992).

Lateral intrusion may occur where the pressure of the magma intruding overcomes the lithostatic pressure and the tensile strength of sediments (Einsele 1986). Sill intrusion therefore occurs in soft sediment , several metres below the sea floor. During intrusion of sills, the surrounding sediment becomes indurated and therefore further intrusions are most likely to occur above previous intrusions and their upper contacts (Einsele 1986). "If the time intervals between magmatic pulses that form sills are approximately equal, decreasing sediment accumulation will reduce the spacing of the sills and eventually cause the magma to extrude onto the sea floor, whereas increasing sedimentation would magnify the vertical spacing of the sills and prevent magma extrusions" (Einsele 1986).

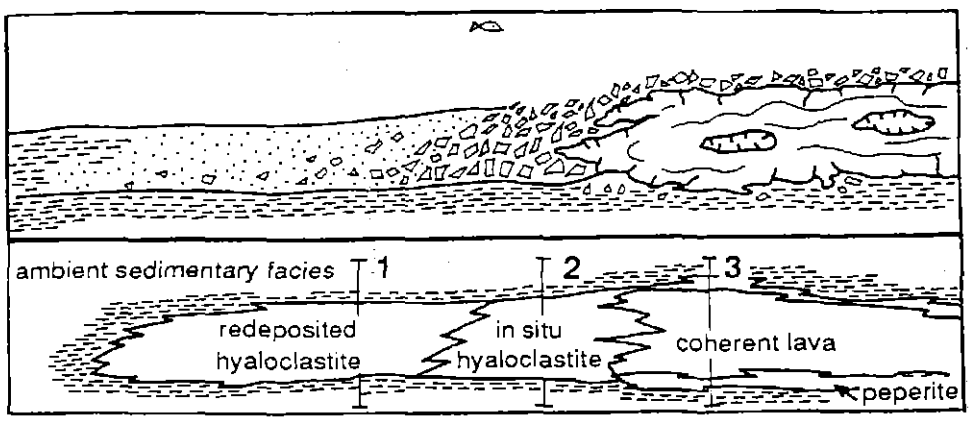

Figure I4.5 - Facies associations around subaqueous lava flows (McPhie et al., 1993).

I4.6 Summary

Sills, dykes, cryptodomes and lavas, all must rise through underlying rocks inorder to reach their final placement in a sequence. It is important to study the rock types formed during intrusion or extrusion of each of these untis.

Dykes and sills, which are differentiated by their relationship to predominant bedding and structural orientation with a host unit, essentially form similar contact relationships.

Dykes may feed cryptodomes and also lava flows, which would indicate similar production of rock forms along boundaries. Similarities in all four units cause difficulty in interpretation of emplacement mode.

It is important to take into account tyhe development of peperitic, hyaloclastite and autobrecciated areas around volcanic bodies. Quenching and fragmentation, as well as the level at which the body sits in the volcano-sedimentary sequence also determiune the mode of emplacement.

Chapter I5 :Conclusions

Subaqueous volcano-sedimentary sequences occur with porphyritic bodies of four main forms; sills, cryptodomes, dykes and lava flows. All four bodies may range from basaltic to rhyolitic in composition. The criteria used for distinguishing submarine volcanic units, as derived by Allen (1992), is provided in table I5.1.

Density and water content of host rocks have a large effect on whether the magma body will remain intrusive or become extrusive. If the magma is less dense than surrounding sediments it will extrude to the surface, creating lava flows and feeder dykes. More dense magmas will remain below sediments or rocks of less density, creating sills and domes.

All four types of intrusive and extrusive bodies tend to develop similar products during reaction with host sediments. Peperite, hyaloclastite and autobreccia are common products of intrusion and extrusion of volcanic bodies. The relative amounts of these three products, as well as their distribution around the porphyritic body provide conclusive evidence for the form, and mode of emplacement of fidderent porphyry bodies.

577154

Type of unit	Contacts with sediments or other volcaniclastics: Upper contact	Lower contact	Internal facies
Extrusive dome (rhyolite)	Mainly passive Lava top hyaloclastic Sediment not baked or bleached	Passive + disruptive Lava base coherent or hyaloclastic	Central facies: thick coherent (massive and flow-banded) core, thin in situ (massive, jigsaw-textured) hyaloclastite base, thick or thin in situ hyaloclastite top capped by thin or absent resedimented (stratified) hyaloclastite Lateral margin facies: mainly in situ + resedimented hyaloclastite
Extrusive tabular flow (rhyolite-basalt)			Central facies: mainly coherent (massive and flow-banded) core, thin in situ (massive, jigsaw-textured) ± resedimented (stratified) hyaloclastite top, ± pillow or minipillow fragments within hyaloclastite in basalt units; hyaloclastite very thin or absent at base Lateral margin facies: mainly in situ + resedimented hyaloclastite
Partially emergent cryptodome or sill (rhyolite-basalt)	Disruptive ± locally passive Top hyaloclastic Sediments locally baked and bleached Resedimented hyaloclastite within overlying sediment sequence	Disruptive ± locally passive Base hyaloclastic or coherent	Beds of resedimented (stratified) hyaloclastite, or resedimented-slumped mixed hyaloclastite-sediment, or mass-flow sediments with included rip-up clasts of hyaloclastite occur within overlying sediment sequence and locally directly on top of volcanic unit Central and lateral margin facies same as for shallow sill
Shallow sill (rhyolite-basalt)	Disruptive ± locally passive Top hyaloclastic or coherent Sediment baked and bleached		Central facies: coherent (massive or flow-banded) core ± thin hyaloclastite top and base, including sediment-matrix intrusive hyaloclastite Lateral margin facies: mainly sediment-matrix intrusive hyaloclastite + in situ (massive, jigsaw-textured) hyaloclastite; subordinate coherent intervals; multiple layers of the sill separated by thin sediment screens common No pillow or minipillow fragments in basalt units
Deeper sill (rhyolite-basalt)	Mainly passive, but locally transgressive, interfingering or slightly disruptive Top mainly coherent Sediment baked and bleached	Mainly passive ± locally slightly disruptive Base coherent	Coherent massive or faintly flow banded, ± coherent fine-grained chilled margin or very thin hyaloclastite margin; no pillow or minipillow fragments in basalt units
Pyroclastic debris (rhyolite)	Sharp sedimentary contacts		Entirely clastic, no gradations into in situ (jigsaw-textured) breccia, pyroclastic clast morphologies, shards, bed forms of subaqueous granular mass-flow deposits ± subaqueous suspension fallout

Table I5.1 - Criteria used for distinguishing submarine volcanic units (domes, flows, sills) (Allen, 1992).

References

ALLEN R. 1992. Reconstruction of the Tectonic, Volcanic, and Sedimentary Setting of Strongly Deformed Zn-Cu Massive Sulfide Deposits at Benambra, Victoria. *Economic Geology* **5**, 825-854.

BRANNEY M. J. & SUTHREN R., 1988. High-level peperitic sills in the English Lake district: Distinction from block lavas, and implications for Borrowdale Volcanic Group Stratigraphy. Geological Journal, **23**, 171-187.

BULL S. W. & CAS R. A. F. 1991. Depositional controls and characteristics of subaqueous bedded volcaniclastics of the Lower Devonian Snowy River Volcanics. *Sedimentary Geology* **74**, 189-215.

BUSBY-SPERA C. J. & WHITE J. D. L. 1987. Variation in peperitic textures associated with differing host-sediment properties. *Bulletin of Volcanology* **49**, 765-775.

CAS R. A. F. 1992. Submarine Volcanism: Eruption Styles, Products, and Relevance to Understanding the Host-Rock Successions to Volcanic-Hosted Massive Sulfide Deposits. *Economic Geology* **87**, 511-541

EINSELE G. 1986. Interaction between sediments and basaltic injections in young Gulf of California-type spreading centers. *Geologisches Rundschau* **75**, 197-208

HALL A. 1987. *Igneous Petrology*. Longman Scientific & Technical, Longman Group UK Limited, Essex, England.

HANSON R. E., 1991. Quenching and Hydroclastic disruption of andesitic to rhyolitic intrusions in a submarine island-arc sequence, northern Sierra Nevada, California. *Geological Society of America Bulletin* **103**, 804-816.

HANSON R. E. & SCHWEICKERT R. A. 1982. Chilling and brecciation of a Devonian rhyolitic sill intruded into wet sediments, northern Sierra Nevada, California. *Journal of Geology* **90**, 717-724.

HANSON R. E. & WILSON T. J. 1993. Large-scale rhyolite peperites (Jurassic, southern Chile). *Journal of Volcanology and Geothermal Research* **54**, 247-264.

HINE R. D. 1994. Peperite: Definition, characteristics, origin and implications. Literature Review, CODES Department of Earth Sciences, University of Tasmania.

KOKELAAR B. P., 1982. Fluidization of wet sediments during emplacement and cooling of various igneous bodies. *Journal of Geological Society of London* **139**, 21-33.

MANLY C. R. 1992. Extended cooling and viscous flow of large, hot rhyolite lavas: implications of numerical modelling results. *Journal of Volcanology and Geothermal Research* **53**, 27-46.

MCBIRNEY A. R. 1963. Factors governing the nature of submarine volcanism. *Bulletin of Volcanology* **26**, 455-469.

MCPHIE J. 1993. The Tennant Creek porphyry revisited: A syn-sedimentary sill with peperite margins, Early Proterozoic, Northern Territory. *Australian Journal of Earth Sciences* (1993) **40**, 545-558

MCPHIE J. & ALLEN R.L.1992. Facies Architecture of Mineralised Submarine Volcanic Sequences: Cambrian Mount Read Volcanics, Western Tasmania. *Economic Geology* **87**, 587-596

MCPHIE J., DOYLE M. & ALLEN R. 1993 *Volcanic Textures* A guide to the interpretation of textures in volcanic rocks. Centre for Ore Deposit and Exploration Studies, University of Tasmania.

MCPHIE J., GEMMELL B. & HOUGHTON B. 1998 VOLCANOLOGY An outline of eruption processes and products, volcanic facies and facies associations in modern volcanic terrains. Master of Economic Geology, Course Work Manual 7, 5th Ed.

SCHMINCKE H. -U., 1967. Fused tuff and peperites in south-central Washington. *Geological Society of America Bulletin* **78**, 319-330.

SUTHERLAND BROWN A. & CATHRO R. J., 1976. Porphyry deposits of the Canadian Cordillera. A volume dedicated to Charles S.Ney *The Canadian Institute of Mining and Metallurgy*. Spec. Vol. **15**., 1976.

TURNER F. J., 1960 *Igneous and Metamorphic Petrology*. Dept. Of Geology University of California, Berkeley. Second Ed. McGraw-Hill Book Company Inc.

WALKER G. P. L. 1989. Gravitational (density) controls on volcanism, magma chambers and intrusions. *Australian Journal of Earth Sciences* **36**, 149-165.

APPENDIX II

Assay Data

Element	B4	Y586	B5	B7	B8	Y344A	Z488	Z208	Y549
SiO_2	71.1	72.03	65	65.5	66.12	76.11	65.56	71.02	69.77
TiO_2	0.45	0.46	0.6	0.58	0.71	0.29	0.6	0.38	0.33
Al_2O_3	13	13.41	12.3	13.1	14.19	13.28	13.91	14.18	14.14
Fe_2O_3	2.556	2.778	5.934	3.89	6.52	1.34	3.9	2.59	2.78
MnO	0.05	0.06	0.2	0.2	0.3	0.02	0.2	0.06	0.09
MgO	1.3	1.77	4.05	3	3.36	0.85	3.03	0.72	0.72
CaO	0.28	0.31	3.72	2	1.74	0.06	1.87	0.58	1.08
Na_2O	3.5	3.5	3.05	3	2.84	1.02	2.46	3.78	3.86
K_2O	4.2	3.44	3.59	4.1	4.17	3.6	4.4	3.92	4.32
P_2O_5	0.07	0.08	0.65	0.11	0.41	0.03	0.11	0.09	0.11
Ti	0.27	0.28	0.36	0.35	0.43	0.17	0.36	0.23	0.20
Zr	302	250	250	257	260	175	230	230	230
P2O5/TiO2	0.16	0.17	1.08	0.19	0.58	0.10	0.18	0.24	0.33
Ti/Zr	8.93	11.03	14.39	13.53	16.37	9.93	15.64	9.90	8.60
FeO	1.15	1.25	2.67	1.75	2.93	0.60	1.75	1.17	1.25
CCPI	24.14	30.32	50.30	40.09	47.31	23.92	41.09	19.67	19.41
AI	59.27	57.76	53.02	58.68	62.18	80.47	63.18	51.56	50.50
FMA	54.55	49.57	54.07	57.75	59.49	77.92	64.14	50.91	52.81
FCA	82.28	85.10	52.12	60.00	65.88	93.41	61.84	55.38	40.00

5771159

H-1

Element	H4503	H4513	H4514	H4610	H4612	H4613	H4614
SiO_2	65.31	73.9	71.96	63.85	75.34	75.41	76.65
TiO_2	0.58	0.50	0.43	0.65	0.38	0.28	0.28
Al_2O_3	17.34	12.05	15.35	14.86	14.81	14.04	13.14
Fe_2O_3	4.76	3.25	0.69	6.49	1.49	0.98	1.84
MnO	0.03	0.02	0	0.1	0	0	0.04
MgO	1.07	0.81	0.25	2.78	0.45	0.36	0.34
CaO	0.18	0	0.06	0.1	0.01	0.02	0.02
Na_2O	5.19	0.16	1.69	2.1	1.38	1.53	1.07
K_2O	2.54	5.43	3.62	4.29	3.41	5.19	5.05
P_2O_5	0.09	0.02	0.01	0.11	0.03	0.03	0.04
Ti	0.35	0.30	0.26	0.39	0.23	0.17	0.17
Zr	314	190	289	245	268	186	181
P2O5/TiO2	0.15	0.04	0.02	0.17	0.08	0.11	0.14
Ti/Zr	11.15	15.79	9.00	15.92	8.58	9.14	9.39
FeO	2.14	1.46	0.31	2.92	0.67	0.44	0.83
CCPI	29.35	28.90	9.55	47.15	18.96	10.65	16.02
AI	40.20	97.50	68.86	76.27	73.52	78.17	83.18
FMA	32.86	97.14	68.17	67.14	71.19	77.23	82.52
FCA	85.60	100.00	80.65	96.53	97.83	94.74	94.44

577160

II-2

Element	H4724	H4725	H4726	H4732	H4733	H4735	H4736	H4737	H4740
SiO_2	78.73	69.7	72.56	65.48	73.99	73.28	75.64	63.31	76.88
TiO_2	0.30	0.43	0.45	0.70	0.32	0.36	0.3	0.71	0.29
Al_2O_3	10.41	14.27	11.57	14.73	15.9	16.74	13.13	16.15	12.33
Fe_2O_3	2.69	3.72	3.36	5.31	1.33	1.18	2.07	6.41	1.24
MnO	0.04	0.12	0.1	0.05	0	0	0.02	0.14	0
MgO	0.76	0.85	1.11	2.78	0.46	0.47	0.96	1.93	0.39
CaO	0.52	1.48	1.89	0.08	0	0	0.26	0.08	0.05
Na_2O	0	1.32	1.29	2.41	0.06	0	1.57	1.8	2.15
K_2O	3.69	4.29	3.7	4.19	5.06	5.36	4.02	3.66	5.56
P_2O_5	0.04	0.08	0.07	0.07	0.04	0.03	0.05	0.07	0.02
Ti	0.18	0.26	0.27	0.42	0.19	0.22	0.18	0.43	0.17
Zr	181	248	216	252	198	201	192	247	181
P2O5/TiO2	0.13	0.18	0.16	0.10	0.13	0.08	0.17	0.10	0.07
Ti/Zr	9.94	10.48	12.50	16.67	9.60	10.95	9.38	17.41	9.39
FeO	1.21	1.67	1.51	2.39	0.60	0.53	0.93	2.88	0.56
CCPI	34.81	31.03	34.44	43.92	17.13	15.74	25.28	46.86	10.95
AI	89.54	64.74	60.20	73.68	98.92	100.00	73.13	74.83	73.01
FMA	100.00	76.47	74.15	63.48	98.83	100.00	71.91	67.03	72.11
FCA	59.38	36.48	37.00	97.20	100.00	100.00	78.69	96.02	88.64

5771191

II-3

APPENDIX III

Rock Specimen Identification and Location

III-1

Ashley Griffiths | Yolande River Sequence porphyries, N of Queenstown | Honours 1998

Catalog#	Field#	Rock Name	Rock description	Associated with	AMGNorth	AMGEast	Preps
138287	H4503	volcaniclastic	sand sized particles	igneous body	5450500N	377600E	R
138288	H4510	breccia	Calcite, quartz, volcanics	fault zone	5472000N	377190E	R
138289	H4513	volcaniclastic	fine grained	igneous body	5428600N	377000E	R
138290	H4514	breccia	pumice, feldspar	igneous body	5446700N	376490E	R
138291	H4610	porphyry	feldspar, quartz, hornblende, magnetite		5450000N	377570E	R
138292	H4612	volcaniclastic	sand sized particles	igneous body	5468400N	376350E	R
138293	H4613	porphyry	quartz, feldspar		5469100N	376710E	R
138294	H4724	ash tuff	layered with rare pyrite cubes	igneous body	5428600N	377000E	R
138295	H4725	volcaniclastic	fine grained	igneous body	5427000N	376940E	R
138296	H4726	volcaniclastic	sand sized particles	igneous body	5426600N	376900E	R
138297	H4732	porphyry	feldspar, quartz, hornblende, magnetite		5438100N	378170E	R
138298	H4733	porphyry	quartz, feldspar		5431300N	377135E	R
138299	H4734	quartz vein*	chlorite pieces abundant	igneous body	5431300N	377130E	R
138300	H4735	porphyry	quartz, feldspar		5431300N	377131E	R
138301	H4736	porphyry	quartz, feldspar		5469300N	376560E	R
138302	H4737	porphyry	feldspar, quartz, hornblende, magnetite		5449800N	377570E	R
138303	H4738	porphyry	quartz, feldspar		5469300N	376560E	R
138304	H4739	porphyry	quartz, feldspar		5431300N	377130E	R
138305	H4740	porphyry	quartz, feldspar		5447700N	377080E	R
138306	H4741	breccia	pumice, feldspar	igneous body	5430600N	377030E	R
138307	H4742	basalt*	plagioclase, pyroxene	fault zone	5342500N	379010E	R
138308	H4743	basalt*	plagioclase, pyroxene	fault zone	5342500N	379010E	R
138309	H4744	basalt*	plagioclase, pyroxene	fault zone	5342250N	378000E	R

5771163

Cambrian (*=Siluro-Devonian)
Yolande River Sequence

138287-138309

577164

APPENDIX IV

Stream Sediment Assay Data

Stream sediment sample numbers and assayed gold values

Sample Number	Au Assay Value (ppb)		Sample Number	Au Assay Value (ppb)	
H1407	<0.05		H1449	930	
H1408	10		H1450	16	
H1409	66		H1451	<0.05	
H1410	8		H1452	51	
H1411	108		H1453	8	
H1412	233		H1454	<0.05	
H1413	14		H1455	<0.05	
H1414	13		H1456	<0.05	
H1415	<0.05		H1457	<0.05	
H1416	<0.05		H1458	14	
H1417	213		H1459	<0.05	
H1418	6		H1460	<0.05	
H1419	1090		H1461	<0.05	
H1420	10		H1462	<0.05	
H1421	<0.05		H1463	<0.05	
H1422	27		H1464	42	
H1423	<0.05		H1465	<0.05	
H1424	175		H1466	3	
H1425	<0.05		H1467	<0.05	
H1426	21		H1468	<0.05	
H1427	<0.05		H1469	4	
H1428	<0.05		H1472	<0.05	
H1429	<0.05		H1473	14	
H1430	810		H1474	18	
H1431	202		H1475	<0.05	
H1432	32				
H1441	14				
H1442	<0.05				
H1443	<0.05				
H1445	<0.05				
H1446	7				
H1447	<0.05				
H1448	29				

577165

APPENDIX V

Soil Sampling Assay Results

577166

Sample	Au	Au(R)	Cu	Pb	Zn	As	As_R	Rock type	Distance	Line	Horizon
H4615	<0.01	<0.01	19	36	26	<50	11	Volcaniclastic Sand/Siltstone	1000 metres	North Diamond Hill	B/C
H4616	<0.01	-	3	8	18	<50	<1	Volcaniclastic Sand/Siltstone	975 metres	North Diamond Hill	B/C
H4617	<0.01	-	3	5	18	<50	<1	Volcaniclastic Sand/Siltstone	950 metres	North Diamond Hill	B/C
H4618	<0.01	<0.01	10	25	18	<50	<1	Volcaniclastic Sand/Siltstone	925 metres	North Diamond Hill	B/C
H4619	<0.01	-	3	4	13	<50	2	Volcaniclastic Sand/Siltstone	900 metres	North Diamond Hill	B/C
H4620	<0.01	-	3	5	14	<50	<1	Volcaniclastic Sand/Siltstone	875 metres	North Diamond Hill	B/C
H4621	<0.01	<0.01	5	5	14	<50	1	Quartz-feldspar porphyry	850 metres	North Diamond Hill	B/C
H4622	<0.01	-	5	11	16	<50	1	Quartz-feldspar porphyry	825 metres	North Diamond Hill	B/C
H4623	<0.01	<0.01	4	7	18	<50	<1	Quartz-feldspar porphyry	800 metres	North Diamond Hill	B/C
H4624	<0.01	-	2	3	12	<50	1	Quartz-feldspar porphyry	775 metres	North Diamond Hill	B/C
H4625	<0.01	-	3	<3	8	<50	<1	Quartz-feldspar porphyry	750 metres	North Diamond Hill	B/C
H4626	<0.01	<0.01	3	8	10	<50	1	Quartz-feldspar porphyry	725 metres	North Diamond Hill	B/C
H4627	<0.01	<0.01	4	7	21	<50	1	Quartz-feldspar porphyry	700 metres	North Diamond Hill	B/C
H4628	<0.01	-	4	4	22	<50	<1	Quartz-feldspar porphyry	675 metres	North Diamond Hill	B/C
H4629	<0.01	-	3	<3	19	<50	1	Quartz-feldspar porphyry	650 metres	North Diamond Hill	B/C
H4630	<0.01	-	4	4	19	<50	<1	Quartz-feldspar porphyry	625 metres	North Diamond Hill	B/C
H4631	0.04	-	4	3	17	<50	<1	Quartz-feldspar porphyry	600 metres	North Diamond Hill	B/C
H4632	<0.01	-	3	3	16	<50	<1	Quartz-feldspar porphyry	575 metres	North Diamond Hill	B/C
H4633	<0.01	<0.01	4	6	16	<50	1	Quartz-feldspar porphyry	550 metres	North Diamond Hill	B/C
H4634	<0.01	-	3	4	15	<50	<1	Quartz-feldspar porphyry	525 metres	North Diamond Hill	B/C
H4635	<0.01	<0.01	4	3	16	<50	<1	Quartz-feldspar porphyry	500 metres	North Diamond Hill	B/C
H4636	<0.01	-	<2	4	15	<50	<1	Quartz-feldspar porphyry	475 metres	North Diamond Hill	B/C
H4637	<0.01	-	6	6	17	<50	1	Quartz-feldspar porphyry	450 metres	North Diamond Hill	B/C
H4638	<0.01	-	2	4	18	<50	<1	Quartz-feldspar porphyry	425 metres	North Diamond Hill	B/C
H4639	<0.01	-	6	8	31	<50	1	Quartz-feldspar porphyry	400 metres	North Diamond Hill	B/C
H4640	<0.01	<0.01	4	5	19	<50	<1	Quartz-feldspar porphyry	375 metres	North Diamond Hill	B/C
H4641	<0.01	-	3	4	10	<50	<1	Quartz-feldspar porphyry	350 metres	North Diamond Hill	B/C
H4642	<0.01	-	2	<3	11	<50	<1	Quartz-feldspar porphyry	325 metres	North Diamond Hill	B/C
H4643	<0.01	-	2	4	11	<50	1	Quartz-feldspar porphyry	300 metres	North Diamond Hill	B/C
H4644	<0.01	-	2	3	13	<50	1	Quartz-feldspar porphyry	275 metres	North Diamond Hill	B/C
H4645	<0.01	-	4	8	16	<50	<1	Volcaniclastic Sand/Siltstone	250 metres	North Diamond Hill	B/C
H4646	<0.01	<0.01	4	5	15	<50	<1	Volcaniclastic Sand/Siltstone	225 metres	North Diamond Hill	B/C
H4647	<0.01	-	2	4	12	<50	2	Volcaniclastic Sand/Siltstone	200 metres	North Diamond Hill	B/C
H4648	<0.01	<0.01	2	<3	21	<50	<1	Feldspar-Hornblende porphyry	175 metres	North Diamond Hill	B/C
H4649	<0.01	-	21	69	72	<50	<1	Feldspar-Hornblende porphyry	150 metres	North Diamond Hill	B/C
H4650	<0.01	<0.01	4	8	24	<50	<1	Feldspar-Hornblende porphyry	125 metres	North Diamond Hill	B/C

H4651	<0.01	-	9	15	26	<50	3	Feldspar-Hornblende porphyry	100 metres	North Diamond Hill	B/C
H4652	<0.01	-	9	21	35	<50	6	Feldspar-Hornblende porphyry	75 metres	North Diamond Hill	B/C
H4653	<0.01	-	75	261	64	<50	2	Feldspar-Hornblende porphyry	50 metres	North Diamond Hill	B/C
H4654	<0.01	-	21	7	32	<50	1	Feldspar-Hornblende porphyry	25 metres	North Diamond Hill	B/C
H4655	<0.01	-	5	9	40	<50	1	Feldspar-Hornblende porphyry	0 metres	North Diamond Hill	B/C
H4674	<0.01	-	6	5	18	<50	1	Volcaniclastic Sand/Siltstone	0 metres	Diamond Hill 000E	B/C
H4675	<0.01	<0.01	4	4	12	<50	<1	Volcaniclastic Sand/Siltstone	20 metres	Diamond Hill 000E	B/C
H4676	<0.01	-	4	8	12	<50	1	Volcaniclastic Sand/Siltstone	40 metres	Diamond Hill 000E	B/C
H4677	<0.01	-	3	<3	7	<50	3	Volcaniclastic Sand/Siltstone	60 metres	Diamond Hill 000E	B/C
H4678	<0.01	-	2	16	12	<50	2	Volcaniclastic Sand/Siltstone	80 metres	Diamond Hill 000E	B/C
H4679	<0.01	-	2	<3	7	<50	2	Volcaniclastic Sand/Siltstone	100 metres	Diamond Hill 000E	B/C
H4680	<0.01	<0.01	3	7	7	<50	1	Volcaniclastic Sand/Siltstone	120 metres	Diamond Hill 000E	B/C
H4681	<0.01	-	10	25	13	<50	3	Volcaniclastic Sand/Siltstone	140 metres	Diamond Hill 000E	B/C
H4682	<0.01	-	4	17	13	<50	2	Volcaniclastic Sand/Siltstone	160 metres	Diamond Hill 000E	B/C
H4683	<0.01	-	5	12	16	<50	3	Volcaniclastic Sand/Siltstone	180 metres	Diamond Hill 000E	B/C
H4684	<0.01	-	4	<3	11	<50	2	Volcaniclastic Sand/Siltstone	200 metres	Diamond Hill 000E	B/C
H4685	<0.01	0.02	2	3	10	<50	2	Volcaniclastic Sand/Siltstone	220 metres	Diamond Hill 000E	B/C
H4686	<0.01	<0.01	<2	4	8	<50	1	Volcaniclastic Sand/Siltstone	240 metres	Diamond Hill 000E	B/C
H4687	<0.01	-	6	<3	7	<50	3	Volcaniclastic Sand/Siltstone	260 metres	Diamond Hill 000E	B/C
H4688	<0.01	-	4	6	10	<50	1	Volcaniclastic Sand/Siltstone	280 metres	Diamond Hill 000E	B/C
H4689	<0.01	<0.01	4	6	9	<50	1	Volcaniclastic Sand/Siltstone	300 metres	Diamond Hill 000E	B/C
H4690	<0.01	0.03	<2	3	<2	<50	1	Volcaniclastic Sand/Siltstone	320 metres	Diamond Hill 000E	B/C
H4691	<0.01	<0.01	3	4	4	<50	2	Volcaniclastic Sand/Siltstone	340 metres	Diamond Hill 000E	B/C
H4692	<0.01	-	6	74	17	<50	8	Volcaniclastic Sand/Siltstone	360 metres	Diamond Hill 000E	B/C
H4693	<0.01	-	5	5	10	<50	<1	Volcaniclastic Sand/Siltstone	380 metres	Diamond Hill 000E	B/C
H4694	<0.01	-	5	9	14	<50	3	Volcaniclastic Sand/Siltstone	400 metres	Diamond Hill 000E	B/C
H4695	<0.01	-	5	9	12	<50	8	Volcaniclastic Sand/Siltstone	420 metres	Diamond Hill 000E	B/C
H4696	<0.01	-	7	7	11	<50	3	Volcaniclastic Sand/Siltstone	440 metres	Diamond Hill 000E	B/C
H4697	<0.01	-	4	6	11	<50	<1	Volcaniclastic Sand/Siltstone	460 metres	Diamond Hill 000E	B/C
H4698	<0.01	-	10	14	16	<50	2	Volcaniclastic Sand/Siltstone	480 metres	Diamond Hill 000E	B/C
H4699	<0.01	<0.01	7	3	13	<50	1	Quartz-feldspar porphyry	500 metres	Diamond Hill 000E	B/C
H4700	<0.01	<0.01	3	<3	11	<50	1	Quartz-feldspar porphyry	520 metres	Diamond Hill 000E	B/C
H4701	<0.01	-	4	39	22	<50	1	Quartz-feldspar porphyry	540 metres	Diamond Hill 000E	B/C
H4702	<0.01	-	2	7	10	<50	2	Quartz-feldspar porphyry	560 metres	Diamond Hill 000E	B/C
H4703	<0.01	-	3	11	16	<50	1	Quartz-feldspar porphyry	580 metres	Diamond Hill 000E	B/C
H4704	<0.01	-	2	3	7	<50	1	Quartz-feldspar porphyry	600 metres	Diamond Hill 000E	B/C
H4706	<0.01	-	4	<3	12	<50	2	Quartz-feldspar porphyry	640 metres	Diamond Hill 000E	B/C

H4708	<0.01	-	3	<3	13	<50	5	Quartz-feldspar porphyry	680 metres	Diamond Hill 000E	B/C
H4709	<0.01	-	2	<3	11	<50	3	Quartz-feldspar porphyry	700 metres	Diamond Hill 000E	B/C
H4710	<0.01	<0.01	3	<3	9	<50	1	Quartz-feldspar porphyry	720 metres	Diamond Hill 000E	B/C
H4711	<0.01	-	4	<3	11	<50	2	Quartz-feldspar porphyry	740 metres	Diamond Hill 000E	B/C
H4712	<0.01	-	3	<3	11	<50	3	Quartz-feldspar porphyry	760 metres	Diamond Hill 000E	B/C
H4713	<0.01	-	3	3	9	<50	2	Quartz-feldspar porphyry	780 metres	Diamond Hill 000E	B/C
H4714	<0.01	<0.01	3	3	10	<50	5	Quartz-feldspar porphyry	800 metres	Diamond Hill 000E	B/C
H4715	<0.01	0.01	8	312	11	<50	4	Quartz-feldspar porphyry	120 metres	Diamond Hill 360N	B/C
H4716	<0.01	0.01	7	9	11	<50	20	Weathered clay	200 metres	Diamond Hill 360N	B/C
H4717	<0.01	<0.01	7	18	25	<50	2	Volcaniclastic Sand/Siltstone	300 metres	Diamond Hill 360N	B/C
H4718	<0.01	<0.01	6	18	30	<50	2	Volcaniclastic Sand/Siltstone	320 metres	Diamond Hill 360N	B/C
H4719	<0.01	<0.01	10	22	22	<50	3	Volcaniclastic Sand/Siltstone	340 metres	Diamond Hill 360N	B/C
H4720	<0.01	<0.01	8	24	22	<50	17	Weathered clay	180 metres	Diamond Hill 260N	B/C
H4721	<0.01	-	3	<3	19	<50	<1	Volcaniclastic Sand/Siltstone	40 metres	Diamond Hill 260N	B/C
Method	F650	F650	A102	A102	A102	A102	4102				
Units	ppm	ppm	ppm	ppm	ppm	ppm	ppm				
ction Limit	0.01	0.01	2	3	2	50	1				

Sample	Au	As(R)	Cu	Pb	Zn	Au(R)	As	Distance	Line	Horizon
H1603	<0.01	<1	28	25	18	<0.01	-	20 metres	Diamond Hill 360N	A
H1477	<0.01	<1	21	29	58	-	<50	40 metres	Diamond Hill 360N	A
H1478	<0.01	4	15	21	27	-	<50	60 metres	Diamond Hill 360N	A
H1479	<0.01	12	99	94	33	-	<50	80 metres	Diamond Hill 360N	A
H1480	<0.01	1	40	29	33	-	<50	100 metres	Diamond Hill 360N	A
H1481	<0.01	6	21	78	42	-	<50	120 metres	Diamond Hill 360N	A
H1482	<0.01	6	31	54	33	-	<50	140 metres	Diamond Hill 360N	A
H1483	0.04	<1	38	16	37	0.03	<50	160 metres	Diamond Hill 360N	A
H1484	<0.01	4	83	31	63	-	<50	180 metres	Diamond Hill 360N	A
H1485	<0.01	10	92	53	47	-	<50	200 metres	Diamond Hill 360N	A
H1486	0.18	7	94	50	77	0.21	<50	220 metres	Diamond Hill 360N	A
H1487	<0.01	2	181	58	65	-	<50	240 metres	Diamond Hill 360N	A
H1488	<0.01	7	18	16	30	0.01	<50	260 metres	Diamond Hill 360N	A
H1490	<0.01	3	25	25	34	<0.01	-	280 metres	Diamond Hill 360N	A

Sample	Au		Cu	Pb	Zn	Au(R)	As	East	Line	Horizon
H1489	<0.01		12	6	22	<0.01	<1	280 metres	Diamond Hill 360N	B/C

577169

V-3

H1491	<0.01		13	10	17	-	<1		260 metres	Diamond Hill 360N	B/C
H1492	<0.01		6	<3	4	-	2		240 metres	Diamond Hill 360N	B/C
H1493	<0.01		7	3	6	-	<1		220 metres	Diamond Hill 360N	B/C
H1494	<0.01		30	14	28	-	25		200 metres	Diamond Hill 360N	B/C
H1495	<0.01		15	6	15	-	<1		180 metres	Diamond Hill 360N	B/C
H1496	<0.01		10	3	7	-	<1		160 metres	Diamond Hill 360N	B/C
H1497	<0.01		21	51	24	<0.01	<1		140 metres	Diamond Hill 360N	B/C
H1498	<0.01		9	188	15	-	14		120 metres	Diamond Hill 360N	B/C
H1499	<0.01		18	12	23	-	<1		100 metres	Diamond Hill 360N	B/C
H1500	<0.01		31	29	26	-	<1		80 metres	Diamond Hill 360N	B/C
H1601	<0.01		10	10	19	-	<1		60 metres	Diamond Hill 360N	B/C
H1602	<0.01		17	18	19	-	4		40 metres	Diamond Hill 360N	B/C
H1604	<0.01		14	14	9	-	<1		20 metres	Diamond Hill 360N	B/C

APPENDIX VI

Magnetic Survey Raw Data

Diamond Hill ground magnetics			Time 9:30					
Base line traverse								
Position	Position	Reading	Reading		Position	Position	Reading	Reading
East	North	(nT-62000)	nT		East	North	(nT-62000)	nT
0	0	205	62205		0	245	185	62185
0	5	210	62210		0	250	190	62190
0	10	200	62200		0	255	188	62188
0	15	193	62193		0	260	189	62189
0	20	190	62190		0	265	180	62180
0	25	203	62203		0	270	190	62190
0	30	195	62195		0	275	199	62199
0	35	183	62183		0	280	188	62188
0	40	192	62192		0	285	188	62188
0	45	195	62195		0	290	191	62191
0	50	200	62200		0	295	184	62184
0	55	191	62191		0	300	187	62187
0	60	226	62226		0	305	187	62187
0	65	205	62205		0	310	185	62185
0	70	205	62205		0	315	186	62186
0	75	185	62185		0	320	190	62190
0	80	195	62195		0	325	188	62188
0	85	196	62196		0	330	189	62189
0	90	200	62200		0	335	185	62185
0	95	195	62195		0	340	187	62187
0	100	196	62196		0	345	193	62193
0	105	187	62187		0	350	191	62191
0	110	187	62187		0	355	195	62195
0	115	189	62189		0	360	189	62189
0	120	205	62205		0	365	183	62183
0	125	200	62200		0	370	193	62193
0	130	190	62190		0	375	190	62190
0	135	190	62190		0	380	193	62193
0	140	195	62195		0	385	183	62183
0	145	190	62190		0	390	192	62192
0	150	179	62179		0	395	192	62192
0	155	189	62189		0	400	189	62189
0	160	196	62196		0	405	194	62194
0	165	200	62200		0	410	191	62191
0	170	186	62186		0	415	193	62193
0	175	189	62189		0	420	198	62198
0	180	185	62185		0	425	192	62192
0	185	200	62200		0	430	190	62190
0	190	190	62190		0	435	200	62200
0	195	188	62188		0	440	198	62198
0	200	190	62190		0	445	191	62191
0	205	198	62198		0	450	194	62194
0	210	185	62185		0	455	186	62186
0	215	190	62190		0	460	190	62190
0	220	195	62195		0	465	190	62190
0	225	185	62185		0	470	186	62186
0	230	195	62195		0	475	184	62184
0	235	182	62182		0	480	192	62192
0	240	262	62262		0	485	195	62195

Diamond Hill ground magnetics								
Base line traverse								
Position East	Position North	Reading (nT-62000)	Reading nT		Position East	Position North	Reading (nT-62000)	Reading nT
0	490	197	62197		0	735	190	62190
0	495	190	62190		0	740	197	62197
0	500	187	62187		0	745	187	62187
0	505	180	62180		0	750	181	62181
0	510	195	62195		0	755	192	62192
0	515	179	62179		0	760	184	62184
0	520	182	62182		0	765	190	62190
0	525	197	62197		0	770	180	62180
0	530	196	62196		0	775	185	62185
0	535	190	62190		0	780	188	62188
0	540	198	62198		0	785	185	62185
0	545	190	62190		0	790	180	62180
0	550	193	62193		0	795	182	62182
0	555	195	62195		0	800	181	62181
0	560	193	62193					
0	565	208	62208					
0	570	205	62205					
0	575	180	62180					
0	580	199	62199					
0	585	194	62194					
0	590	190	62190					
0	595	185	62185					
0	600	199	62199					
0	605	186	62186					
0	610	188	62188					
0	615	200	62200					
0	620	194	62194					
0	625	203	62203					
0	630	200	62200					
0	635	186	62186					
0	640	200	62200					
0	645	189	62189					
0	650	189	62189					
0	655	190	62190					
0	660	195	62195					
0	665	190	62190					
0	670	194	62194					
0	675	185	62185					
0	680	195	62195					
0	685	181	62181					
0	690	184	62184					
0	695	182	62182					
0	700	185	62185					
0	705	190	62190					
0	710	184	62184					
0	715	186	62186					
0	720	190	62190					
0	725	181	62181					
0	730	182	62182					

577174

Diamond Hill ground magnetics								
North 360 line traverse								
Position	Position	Reading	Reading		Position	Position	Reading	Reading
East	North	(nT-62000)	nT		East	North	(nT-62000)	nT
0	360	195	62195		245	360	204	62204
5	360	188	62188		250	360	173	62173
10	360	182	62182		255	360	180	62180
15	360	172	62172		260	360	179	62179
20	360	188	62188		265	360	175	62175
25	360	184	62184		270	360	178	62178
30	360	183	62183		275	360	169	62169
35	360	186	62186		280	360	176	62176
40	360	180	62180		285	360	173	62173
45	360	182	62182		290	360	164	62164
50	360	184	62184		295	360	169	62169
55	360	183	62183		300	360	179	62179
60	360	192	62192		305	360	184	62184
65	360	178	62178		310	360	195	62195
70	360	190	62190		315	360	183	62183
75	360	190	62190		320	360	175	62175
80	360	181	62181		325	360	191	62191
85	360	196	62196		330	360	177	62177
90	360	180	62180		335	360	190	62190
95	360	188	62188		340	360	195	62195
100	360	189	62189		345	360	182	62182
105	360	188	62188		348	360	189	62189
110	360	190	62190					
115	360	186	62186					
120	360	189	62189					
125	360	175	62175					
130	360	184	62184					
135	360	170	62170					
140	360	172	62172					
145	360	178	62178					
150	360	185	62185					
155	360	183	62183					
160	360	175	62175					
165	360	165	62165					
170	360	188	62188					
175	360	174	62174					
180	360	188	62188					
185	360	177	62177					
190	360	167	62167					
195	360	174	62174					
200	360	190	62190					
205	360	176	62176					
210	360	189	62189					
215	360	176	62176					
220	360	180	62180					
225	360	172	62172					
230	360	172	62172					
235	360	171	62171					
240	360	188	62188					

577175

Diamond Hill ground magnetics								
North 320 line traverse								
Position East	Position North	Reading (nT-62000)	Reading nT		Position East	Position North	Reading (nT-62000)	Reading nT
0	320	177	62177		245	320	166	62166
5	320	181	62181		250	320	174	62174
10	320	164	62164		255	320	181	62181
15	320	184	62184		260	320	188	62188
20	320	181	62181		265	320	182	62182
25	320	151	62151		270	320	181	62181
30	320	176	62176		275	320	185	62185
35	320	146	62146		280	320	185	62185
40	320	174	62174		285	320	192	62192
45	320	185	62185		290	320	194	62194
50	320	170	62170		295	320	208	62208
55	320	186	62186		300	320	206	62206
60	320	158	62158		305	320	205	62205
65	320	183	62183		310	320	210	62210
70	320	177	62177		315	320	206	62206
75	320	188	62188		320	320	209	62209
80	320	168	62168		325	320	210	62210
85	320	180	62180		329	320	190	62190
90	320	176	62176					
95	320	174	62174					
100	320	173	62173					
105	320	192	62192					
110	320	186	62186					
115	320	197	62197					
120	320	180	62180					
125	320	183	62183					
130	320	190	62190					
135	320	184	62184					
140	320	197	62197					
145	320	167	62167					
150	320	176	62176					
155	320	173	62173					
160	320	174	62174					
165	320	173	62173					
170	320	175	62175					
175	320	170	62170					
180	320	171	62171					
185	320	170	62170					
190	320	147	62147					
195	320	184	62184					
200	320	179	62179					
205	320	188	62188					
210	320	181	62181					
215	320	174	62174					
220	320	171	62171					
225	320	172	62172					
230	320	174	62174					
235	320	177	62177					
240	320	173	62173					

Diamond Hill ground magnetics								
North 260 line traverse								
Position East	Position North	Reading (nT-62000)	Reading nT		Position East	Position North	Reading (nT-62000)	Reading nT
0	260	180	62180		205	260	162	62162
5	260	179	62179		210	260	165	62165
10	260	168	62168		215	260	170	62170
15	260	173	62173		220	260	176	62176
20	260	190	62190		225	260	185	62185
25	260	195	62195		230	260	172	62172
30	260	190	62190		235	260	177	62177
35	260	187	62187		240	260	176	62176
40	260	187	62187		245	260	170	62170
45	260	190	62190		250	260	176	62176
50	260	184	62184		255	260	184	62184
55	260	199	62199		260	260	175	62175
60	260	192	62192		265	260	174	62174
65	260	185	62185		270	260	177	62177
70	260	197	62197		275	260	185	62185
75	260	215	62215		280	260	189	62189
80	260	199	62199		285	260	177	62177
85	260	198	62198		290	260	188	62188
90	260	195	62195		295	260	192	62192
95	260	185	62185		300	260	181	62181
100	260	193	62193		305	260	170	62170
105	260	189	62189		309	260	173	62173
110	260	195	62195					
115	260	179	62179					
120	260	202	62202					
125	260	215	62215					
130	260	186	62186					
135	260	201	62201					
140	260	210	62210					
145	260	210	62210					
150	260	199	62199					
155	260	196	62196					
160	260	188	62188					
165	260	195	62195					
170	260	195	62195					
175	260	210	62210					
180	260	183	62183					
185	260	196	62196					
190	260	183	62183					
195	260	174	62174					
200	260	160	62160					
Diamond Hill ground magnetics			Time 13:11					
Final reading								
Position East	Position North	Reading (nT-62000)	Reading nT					
0	0	201	62201					

577177

North Diamond Hill ground magnetics								
Position West	Position North	Reading (nT-62000)	Reading nT		Position West	Position North	Reading (nT-62000)	Reading nT
1000	0	175	62175		745	0	172	62172
995	0	172	62172		740	0	172	62172
990	0	171	62171		735	0	172	62172
985	0	167	62167		730	0	172	62172
980	0	171	62171		725	0	172	62172
975	0	170	62170		720	0	172	62172
970	0	171	62171		715	0	174	62174
965	0	170	62170		710	0	174	62174
960	0	169	62169		705	0	175	62175
955	0	170	62170		700	0	173	62173
950	0	172	62172		695	0	173	62173
945	0	173	62173		690	0	174	62174
940	0	171	62171		685	0	175	62175
935	0	174	62174		680	0	174	62174
930	0	172	62172		675	0	176	62176
925	0	173	62173		670	0	175	62175
920	0	173	62173		665	0	178	62178
915	0	174	62174		660	0	175	62175
910	0	172	62172		655	0	176	62176
905	0	174	62174		650	0	176	62176
900	0	169	62169		645	0	177	62177
895	0	168	62168		640	0	179	62179
890	0	170	62170		635	0	180	62180
885	0	170	62170		630	0	177	62177
880	0	170	62170		625	0	179	62179
875	0	171	62171		620	0	177	62177
870	0	172	62172		615	0	179	62179
865	0	171	62171		610	0	179	62179
860	0	169	62169		605	0	177	62177
855	0	171	62171		600	0	180	62180
850	0	169	62169		595	0	176	62176
845	0	171	62171		590	0	183	62183
840	0	170	62170		585	0	182	62182
835	0	171	62171		580	0	181	62181
830	0	174	62174		575	0	180	62180
825	0	172	62172		570	0	183	62183
820	0	174	62174		565	0	178	62178
815	0	176	62176		560	0	180	62180
810	0	177	62177		555	0	179	62179
805	0	176	62176		550	0	179	62179
800	0	174	62174		545	0	180	62180
795	0	172	62172		540	0	179	62179
790	0	171	62171		535	0	179	62179
785	0	170	62170		530	0	180	62180
780	0	174	62174		525	0	180	62180
775	0	173	62173		520	0	182	62182
770	0	170	62170		515	0	182	62182
765	0	173	62173		510	0	182	62182
760	0	170	62170		505	0	183	62183
755	0	172	62172		500	0	183	62183
750	0	172	62172		495	0	184	62184

North Diamond Hill ground magnetics							
Position West	Position North	Reading (nT-62000)	Reading nT	Position West	Position North	Reading (nT-62000)	Reading nT
490	0	181	62181	245	0	171	62171
485	0	182	62182	240	0	174	62174
480	0	180	62180	235	0	172	62172
475	0	179	62179	230	0	174	62174
470	0	182	62182	225	0	175	62175
465	0	182	62182	220	0	173	62173
460	0	182	62182	215	0	170	62170
455	0	182	62182	210	0	172	62172
450	0	184	62184	205	0	171	62171
445	0	183	62183	200	0	165	62165
440	0	183	62183	195	0	171	62171
435	0	185	62185	190	0	170	62170
430	0	184	62184	185	0	168	62168
425	0	185	62185	180	0	167	62167
420	0	186	62186	175	0	166	62166
415	0	186	62186	170	0	166	62166
410	0	186	62186	165	0	165	62165
405	0	187	62187	160	0	168	62168
400	0	184	62184	155	0	165	62165
395	0	185	62185	150	0	165	62165
390	0	182	62182	145	0	166	62166
385	0	185	62185	140	0	165	62165
380	0	187	62187	135	0	164	62164
375	0	192	62192	130	0	163	62163
370	0	192	62192	125	0	164	62164
365	0	185	62185	120	0	163	62163
360	0	188	62188	115	0	162	62162
355	0	191	62191	110	0	164	62164
350	0	190	62190	105	0	165	62165
345	0	186	62186	100	0	160	62160
340	0	185	62185	95	0	160	62160
335	0	184	62184	90	0	156	62156
330	0	184	62184	85	0	155	62155
325	0	188	62188	80	0	153	62153
320	0	189	62189	75	0	155	62155
315	0	186	62186	70	0	152	62152
310	0	189	62189	65	0	151	62151
305	0	195	62195	60	0	150	62150
300	0	190	62190	55	0	150	62150
295	0	189	62189	50	0	144	62144
290	0	186	62186	45	0	142	62142
285	0	183	62183	40	0	135	62135
280	0	172	62172	35	0	133	62133
275	0	174	62174	30	0	144	62144
270	0	174	62174	25	0	161	62161
265	0	174	62174	20	0	181	62181
260	0	173	62173	15	0	187	62187
255	0	175	62175	10	0	192	62192
250	0	172	62172	5	0	198	62198
				0	0	212	62212

577179

APPENDIX VII

Surface Rock Chip Assay Results

DataSet	samp_id	reg_north	reg_east	reg_rl	reg_grid_id	au_ppm	au_ppb
YR	adit no.1	5343092.11	377018.501	274.191	AMG55_66		
YR	h1350	5343105.979	377015.637	280.415	AMG55_66	-0.01	
YR	h1327	5343167.799	376996.707	284.118	AMG55_66	0.06	
YR	h1316	5343152.668	377013.555	287.969	AMG55_66	0.14	
YR	h1317	5343154.502	377019.398	290.342	AMG55_66	2.29	
YR	h1333	5343284.612	377135.423	290.528	AMG55_66	0.08	
YR	h1318	5343151.611	377028.5	293.588	AMG55_66	0.04	
YR	h1332	5343276.448	377134.598	293.684	AMG55_66	-0.01	
YR	h1326	5343169.51	377026.659	294.837	AMG55_66	0.12	
YR	h1319	5343145.909	377035.645	295.423	AMG55_66	0.01	
YR	h1320	5343145.804	377041.593	297.047	AMG55_66	0.01	
YR	h1325	5343168.188	377035.105	297.139	AMG55_66	0.1	
YR	h1269	5343165.677	377040.205	297.533	AMG55_66	0.15	
YR	h1321	5343144.08	377046.874	297.66	AMG55_66	0.02	
YR	H1300	5343167.916	377043.531	298.974	AMG55_66	1.78	
YR	H1270	5343167.916	377043.531	298.974	AMG55_66	0.05	
YR	h1324	5343167.916	377043.531	298.974	AMG55_66	3.65	
YR	h1331	5343275.548	377079.711	299.032	AMG55_66	-0.01	
YR	h1322	5343149.218	377055.058	299.333	AMG55_66	-0.01	
YR	h1323	5343170.548	377052.011	302.006	AMG55_66	0.26	
YR	h1330	5343266.882	377090.036	302.741	AMG55_66	0.02	
YR	h1329	5343263.452	377097.134	304.76	AMG55_66	-0.01	
YR	h1349	5343158.278	377067.041	305.438	AMG55_66	0.12	
YR	h1346	5343075.913	377173.352	305.77	AMG55_66	0.01	
YR	H1328	5343258.373	377101.045	306.043	AMG55_66	-0.01	
YR	h1348	5343163.758	377069.44	306.238	AMG55_66	0.82	
YR	h1345	5343091.119	377181.678	306.784	AMG55_66	1.22	
YR	h1271	5343157.883	377079.617	308.68	AMG55_66	0.24	
YR	adit no.4	5343162.193	377091.731	311.329	AMG55_66		
YR	h1334	5343241.707	377101.71	313.019	AMG55_66	0.04	
YR	adit no.3	5343154.317	377112.767	315.572	AMG55_66		
YR	h1335	5343223.067	377109.454	317.617	AMG55_66	0.01	
YR	H1339	5343170.05	377102.647	318.874	AMG55_66	0.23	
YR	H1340	5343170.05	377102.647	318.874	AMG55_66	4.15	
YR	H1341	5343170.05	377102.647	318.874	AMG55_66	0.09	
YR	H1298	5343170.05	377102.647	318.874	AMG55_66	0.24	
YR	H1299	5343170.05	377102.647	318.874	AMG55_66	1.02	
YR	H1273	5343176.458	377111.868	320.275	AMG55_66	0.02	
YR	H1274	5343176.458	377111.868	320.275	AMG55_66	0.01	
YR	H1275	5343176.458	377111.868	320.275	AMG55_66	0.09	
YR	H1276	5343176.458	377111.868	320.275	AMG55_66	-0.01	
YR	H1277	5343176.458	377111.868	320.275	AMG55_66	0.4	
YR	h1347	5343152.216	377143.119	320.637	AMG55_66	-0.01	
YR	adit no.2	5343180.017	377111.623	321.174	AMG55_66		
YR	h1338	5343182.432	377111.695	323.711	AMG55_66	5	
YR	h1343	5343178.617	377134.705	323.965	AMG55_66	0.38	
YR	h1344	5343174.237	377135.179	324.059	AMG55_66	0.03	
YR	H1336	5343191.469	377109.265	324.535	AMG55_66	0.52	
YR	H1297	5343191.469	377109.265	324.535	AMG55_66	18.3	
YR	H1342	5343184.285	377127.134	324.63	AMG55_66	0.41	
YR	H1294	5343184.285	377127.134	324.63	AMG55_66	1.4	

DataSet	samp_id	reg_north	reg_east	reg_rl	reg_grid_id	au_ppm	au_ppb
YR	h1272	5343185.3	377124.464	324.877	AMG55_66	0.24	
YR	H1337	5343188.607	377116.932	325.309	AMG55_66	1.51	
YR	H1295	5343188.607	377116.932	325.309	AMG55_66	0.38	
YR	H1296	5343188.607	377116.932	325.309	AMG55_66	0.4	

577182

APPENDIX VIII

Adit Channel Sampling Assay Results

577183

Rock Chip Geochemistry : Diamond Hill Adits

VIII-1

VIII-1

Sample	Assay values in ppm							Distance	sampled	Adit	Rock
Number	Au	Au(R)	Cu	Pb	Zn	As	As	From	To	No.	Type
H4520	<0.01	-	9	25	59	102	>100	82	80	1	Vcc Breccia
H4521	<0.01	-	10	17	69	N.A.	40	80	78	1	Vcc Breccia
H4522	<0.01	-	6	5	68	N.A.	2	78	76	1	Vcc Breccia
H4523	<0.01	-	9	74	31	N.A.	83	76	74	1	Vcc Breccia
H4524	<0.01	-	16	100	27	208	>100	74	72	1	Vcc Breccia
H4525	<0.01	-	9	74	21	N.A.	8	15	14	1	Vcc Breccia
H4526	<0.01	-	21	74	27	N.A.	47	14	12	1	Vcc Breccia
H4527	<0.01	-	20	111	26	403	>100	12	10	1	Vcc Breccia
H4528	<0.01	<0.01	8	50	21	N.A.	44	10	8	1	Vcc Breccia
H4529	<0.01	<0.01	4	41	20	N.A.	20	8	6	1	Vcc Breccia
H4530	0.02	-	2	214	17	N.A.	65	6	4	1	Vcc Breccia
H4531	0.07	0.06	3	64	16	393	>100	4	2	1	Vcc Breccia
H4532	0.05	-	10	59	23	561	>100	2	0	1	Vcc Breccia
H4533	0.13	0.15	10	52	21	134	>100	6	4	1	Vcc Breccia
H4534	0.03	-	8	30	20	332	>100	4	2	1	Vcc Breccia
H4535	<0.01	<0.01	6	30	20	209	>100	2	0	1	Vcc Breccia
H4536	0.02	0.02	13	40	21	513	>100	70	68	1	Vcc Breccia
H4537	<0.01	-	2	17	16	N.A.	23	68	66	1	Vcc Breccia
H4538	<0.01	-	12	91	23	N.A.	93	66	64	1	Vcc Breccia
H4539	<0.01	-	11	345	22	N.A.	21	64	62	1	Vcc Breccia
H4540	<0.01	-	13	175	42	N.A.	59	62	60	1	Vcc Breccia
H4541	<0.01	-	7	50	41	N.A.	44	60	58	1	Vcc Breccia
H4542	<0.01	-	4	15	25	N.A.	6	58	56	1	Vcc Breccia
H4543	<0.01	-	4	22	32	N.A.	7	56	54	1	Vcc Breccia
H4544	<0.01	-	4	31	40	N.A.	11	54	52	1	Vcc Breccia
H4545	<0.01	-	4	33	30	N.A.	18	52	50	1	Vcc Breccia
H4546	<0.01	-	6	52	47	N.A.	16	50	48	1	Vcc Breccia
H4547	<0.01	<0.01	6	54	47	N.A.	6	48	46	1	Vcc Breccia
H4548	<0.01	-	6	92	44	N.A.	8	46	44	1	Vcc Breccia
H4549	<0.01	<0.01	4	46	52	N.A.	5	44	42	1	Vcc Breccia
H4550	<0.01	-	5	63	54	N.A.	6	42	40	1	Vcc Breccia
H4551	<0.01	-	6	33	42	N.A.	5	40	38	1	Vcc Breccia
H4552	<0.01	-	5	56	33	N.A.	5	38	36	1	Vcc Breccia
H4553	<0.01	<0.01	4	32	23	N.A.	13	36	34	1	Vcc Breccia
H4554	<0.01	-	3	161	31	N.A.	4	34	32	1	Vcc Breccia
H4555	<0.01	-	5	28	41	N.A.	17	32	30	1	Vcc Sandstone
H4556	<0.01	-	5	22	31	N.A.	4	30	28	1	Vcc Sandstone
H4557	0.01	<0.01	4	29	30	N.A.	12	28	26	1	Vcc Sandstone
H4558	<0.01	<0.01	5	31	36	N.A.	4	26	24	1	Vcc Sandstone
H4559	<0.01	-	5	18	28	N.A.	12	24	22	1	Vcc Sandstone
H4560	<0.01	-	4	16	27	N.A.	<1	22	20	1	Vcc Sandstone
H4561	<0.01	-	4	25	53	N.A.	21	20	18	1	Vcc Sandstone
H4562	<0.01	-	5	23	24	N.A.	8	18	16	1	Vcc Sandstone
H4563	<0.01	-	10	13	21	N.A.	18	16	14	1	Vcc Sandstone
H4564	<0.01	-	5	<3	12	N.A.	9	14	12	1	Vcc Sandstone
H4565	<0.01	<0.01	3	15	15	N.A.	<1	12	10	1	Vcc Sandstone
H4566	<0.01	-	4	15	15	N.A.	<1	10	8	1	Vcc Sandstone
H4567	<0.01	-	3	10	10	N.A.	<1	8	6	1	Vcc Sandstone
H4568	<0.01	-	3	9	9	N.A.	<1	6	4	1	Vcc Sandstone
H4569	<0.01	-	2	7	7	N.A.	<1	4	2	1	Vcc Sandstone
H4570	<0.01	<0.01	3	<3	10	N.A.	<1	2	0	1	Vcc Sandstone
H4571	<0.01	-	3	<3	6	N.A.	<1	36	34	2	Quartz porphyry
H4572	0.03	0.03	2	31	2	N.A.	<1	34	32	2	Quartz porphyry
H4573	0.04	0.03	<2	8	<2	N.A.	<1	32	30	2	Quartz porphyry

H4574	0.03	-	<2	14	<2	N.A.	<1	30	28	2	Quartz porphyry
H4575	0.02	-	2	<3	3	N.A.	2	28	26	2	Quartz porphyry
H4576	0.05	-	<2	7	7	N.A.	3	26	24	2	Quartz porphyry
H4577	0.08	0.06	<2	22	8	N.A.	3	24	22	2	Quartz porphyry
H4578	<0.01	<0.01	3	7	3	N.A.	2	22	20	2	Quartz porphyry
H4579	0.03	0.02	<2	18	3	N.A.	<1	20	18	2	Quartz porphyry
H4580	0.04	-	<2	48	3	N.A.	<1	18	16	2	Quartz porphyry
H4581	0.05	-	<2	39	4	N.A.	49	16	14	2	Quartz porphyry
H4582	0.05	-	<2	72	8	N.A.	13	14	12	2	Quartz porphyry
H4583	0.03	-	<2	24	5	N.A.	2	12	10	2	Quartz porphyry
H4584	0.04	-	2	73	7	N.A.	3	10	8	2	Quartz porphyry
H4585	0.02	-	3	41	9	N.A.	8	8	6	2	Quartz porphyry
H4586	<0.01	-	4	31	9	N.A.	4	6	4	2	Vcc Breccia
H4587	<0.01	-	5	72	7	N.A.	2	4	2	2	Vcc Breccia
H4588	0.01	-	8	44	14	N.A.	12	2	0	2	Vcc Breccia
H4589	<0.01	<0.01	9	21	12	N.A.	23	35	34	3	Quartz porphyry
H4590	0.17	0.16	3	45	<3	N.A.	26	34	32	3	Quartz porphyry
H4591	0.2	0.2	3	34	7	N.A.	9	32	30	3	Quartz porphyry
H4592	0.12	0.11	<2	40	2	N.A.	9	30	26	3	Quartz porphyry
H4593	0.03	0.03	2	15	6	N.A.	6	28	26	3	Quartz porphyry
H4594	<0.01	-	2	13	9	N.A.	<1	26	24	3	Quartz porphyry
H4595	0.02	-	3	20	6	N.A.	7	24	22	3	Quartz porphyry
H4596	0.02	-	4	58	8	N.A.	<1	22	20	3	Quartz porphyry
H4597	0.02	-	2	20	3	N.A.	3	20	18	3	Quartz porphyry
H4598	0.02	-	2	13	3	N.A.	4	18	16	3	Quartz porphyry
H4599	0.01	0.01	2	24	3	N.A.	2	16	14	3	Quartz porphyry
H4600	0.05	-	2	32	2	N.A.	8	14	12	3	Quartz porphyry
H4601	0.12	-	3	23	7	N.A.	1	12	10	3	Quartz porphyry
H4602	0.03	-	3	33	4	N.A.	6	10	8	3	Quartz porphyry
H4603	0.03	0.03	<2	46	4	N.A.	1	8	6	3	Quartz porphyry
H4604	0.05	-	<2	23	4	N.A.	8	6	4	3	Quartz porphyry
H4605	0.04	0.05	3	62	7	N.A.	23	4	2	3	Quartz porphyry
H4606	0.11	0.12	3	231	8	137	>100	2	0	3	Quartz porphyry
H4607	0.03	0.02	<2	12	10	N.A.	4	6	4	4	Quartz porphyry
H4608	0.13	-	3	17	10	N.A.	2	4	2	4	Quartz porphyry
H4609	0.5	0.52	<2	35	15	N.A.	<1	2	0	4	Quartz porphyry
H4656	0.03	-	<2	8	3	N.A.	2			1	Quartz vein
H4657	0.01	-	<2	3	3	N.A.	1			1	Quartz vein
H4658	<0.01	0.01	<2	11	5	N.A.	<1			1	Quartz vein
H4659	0.03	0.02	<2	7	2	N.A.	<1			1	Quartz vein
H4660	0.02	-	<2	6	<2	N.A.	1			1	Quartz vein
H4661	0.26	0.23	<2	81	4	N.A.	3			1	Quartz vein
H4662	0.04	0.04	<2	28	5	N.A.	3			1	Quartz vein
H4663	0.03	-	2	6	4	N.A.	<1			1	Quartz vein
H4664	0.01	-	2	5	3	N.A.	6			1	Quartz vein
H4665	0.02	-	<2	7	3	N.A.	<1			1	Quartz vein
H4666	0.3	0.3	2	43	6	N.A.	<1			1	Quartz vein
H4667	0.09	0.1	2	56	2	N.A.	22			1	Quartz vein
H4668	0.04	0.05	20	81	20	569	>100			1	Quartz vein
H4669	0.07	-	<2	10	4	N.A.	10			1	Quartz vein
H4670	0.08	0.08	5	87	7	150	>100			1	Quartz vein
H4671	<0.01	-	16	436	44	N.A.	38			1	Quartz vein
Method	F650	F650	A102	A102	A102	A102	H102				
Units	ppm	ppm	ppm	ppm	ppm	ppm	ppm				
Detection											

Limit	0.01	0.01	2	3	2	50	1				
[redacted]	Au values 0.01+ ppm			[redacted]	Au values 0.10+ ppm						

APPENDIX IX

Magnetic Susceptibility Results

577187

Sample number	adit no.	Interval from	to	magnetic susceptibility
H4520	1	82	80	6
H4521	1	80	78	3
H4522	1	78	76	3
H4523	1	76	74	6
H4524	1	74	72	0
H4525	1	15	14	0
H4526	1	14	12	0
H4527	1	12	10	0
H4528	1	10	8	0
H4529	1	8	6	0
H4530	1	6	4	0
H4531	1	4	2	0
H4532	1	2	0	0
H4533	1	5	4	0
H4534	1	4	2	11
H4535	1	2	0	8
H4536	1	70	68	3
H4537	1	68	66	0
H4538	1	66	64	0
H4539	1	64	62	25
H4540	1	62	60	6
H4541	1	60	58	0
H4542	1	58	56	3
H4543	1	56	54	3
H4544	1	54	52	6
H4545	1	52	50	4
H4546	1	50	48	4
H4547	1	48	46	7
H4548	1	46	44	3
H4549	1	44	42	3
H4550	1	42	40	3
H4551	1	40	38	3
H4552	1	38	36	4
H4553	1	36	34	4
H4554	1	34	32	3
H4555	1	32	30	3
H4556	1	30	28	1
H4557	1	28	26	0
H4558	1	26	24	0
H4559	1	24	22	1
H4560	1	22	20	0
H4561	1	20	18	0
H4562	1	18	16	0
H4563	1	16	14	0
H4564	1	14	12	0
H4565	1	12	10	0
H4566	1	10	8	0
H4567	1	8	6	0
H4568	1	6	4	0
H4569	1	4	2	0
H4570	1	2	0	0
H4571	2	36	34	0
Sample number	adit no.	Interval from	to	magnetic susceptibility

H4572	2	34	32	39
H4573	2	32	30	49
H4574	2	30	28	51
H4575	2	28	26	111
H4576	2	26	24	88
H4577	2	24	22	23
H4578	2	22	20	155
H4579	2	20	18	57
H4580	2	18	16	36
H4581	2	16	14	76
H4582	2	14	12	62
H4583	2	12	10	45
H4584	2	10	8	54
H4585	2	8	6	49
H4586	2	6	4	29
H4587	2	4	2	43
H4588	2	2	0	20
H4589	3	35	34	7
H4590	3	34	32	20
H4591	3	32	30	59
H4592	3	30	28	69
H4593	3	28	26	27
H4594	3	26	24	35
H4595	3	24	22	23
H4596	3	22	20	36
H4597	3	20	18	104
H4598	3	18	16	11
H4599	3	16	14	6
H4600	3	14	12	52
H4601	3	12	10	11
H4602	3	10	8	43
H4603	3	8	6	97
H4604	3	6	4	40
H4605	3	4	2	7
H4606	3	2	0	59

577188

APPENDIX X

Specific Gravity Results

Tabulated specific gravity measurements of dominant rock types in Diamond Hill adits.

X-1

577190

Sample Number	Rock Type	Specific Gravity
		g/cm3
H4521	Sandstone	2.63
H4537	Sandstone	2.69
H4547	Sandstone	2.43
H4557	Siltstone	2.28
H4561	Siltstone	2.51
H4566	Siltstone	2.5
H4575	Qfb porphyry	2.55
H4584	Qfb porphyry	2.5
H4587	Sandstone	2.46
H4592	Qfb porphyry	2.48
H4597	Qfb porphyry	2.51
H4602	Qfb porphyry	2.55
Sandstone Range		2.43 - 2.69
Siltstone Range		2.28 - 2.51
Porphyry Range		2.48 - 2.55

Copper Mines of Tasmania

Map 1.

EL 27/95 Yolande River
Outcrop geology and Stream
sediment data.

Date: 16/4/1999
Author: AG
Office: Queenstown
Drawing: AS
Scale: 1:10000
Projection: AMG Zone 55 (AGD 66)

0 100 200 400 metres

5 cm

Queenstown

Murchison Highway

Pearl Creek Fault

Diamond Hill

North Diamond Hill Line

Diamond Creek

Yolande River

Pearl Creek

to Strahan

Legend

- Lithological Boundaries
- Interpreted Boundaries
- Main Roads
- 4WD Access Tracks
- Creeks & Rivers
- Major fault
- Minor fault
- Bedding strike & dip direction
- Cleavage direction
- Cut grid lines
- Stream sediment sample sites with Au assay values (ppb) — 5 H1442
- Quartz - Feldspar - Biotite Porphyry
- Quartz - Feldspar - Hornblende Porphyry
- Ash Tuff
- Volcaniclastic Siltstone
- Pumiceous Volcaniclastic Sandstone
- Bell Shale
- Basalt

376000 mE
377000 mE
378000 mE
379000 mE
380000 mE
5346000 mN
5345000 mN
5344000 mN
5343000 mN
5342000 mN
5341000 mN
5340000 mN

H1464 42
H1460 -0.05
H1465 -0.05
H1461 -0.05
H1462 -0.05
H1463 -0.05
H1475 -0.05
H1474 18
H1473 14
H1472 -0.05
H1424 175
H1427 -0.05
H1425 -0.05
H1426 21
H1469 4
H1466 3
H1467 -0.05
H1468 -0.05
H1448 29
H1449
H1447 -0.05
H1441 14
H1442 -0.05
H1423 -0.05
H1422 27
H1421 -0.05
H1420 10
H1419 1,090
H1414
H1451 -0.05
H1450 18
H1443 -0.05
H1418 6
H1411 108
H1410 8
H1415 -0.05
H1417 213
H1416 -0.05
H1432 32
H1445 -0.05
H1446 7
H1452 51
H1453 8
H1431 202
H1430 810
H1459 -0.05
H1456 -0.05
H1454 -0.05
H1458 14
H1429 -0.05
H1455 -0.05
H1457 -0.05
H1428 -0.05
H1437 -0.05
H1438 -0.05
H1439 113
H1444 53
H1440 -0.05
H1433 8
H1435 -0.05
H1434
H1436 -0.05
H1409 66
H1412 233
H1413 14
H1408 -0.05
H1400 66

Yolande River
North Diamond Hill Line
Diamond Hill
Diamond Creek
Pearl Creek
Pearl Creek Fault
Pearl Creek Fault
Murchison Highway
Queenstown
to Strahan

Legend

- Lithological Boundaries
- Interpreted Boundaries
- Main Roads
- 4WD Access Tracks
- Creeks & Rivers
- Major fault
- Minor fault
- Bedding strike & dip direction
- Cleavage direction
- Cut grid lines
- Stream sediment sample sites with Au assay values (ppb) — 5 H1442
- Quartz - Feldspar - Biotite Porphyry
- Quartz - Feldspar - Hornblende Porphyry
- Ash Tuff
- Volcaniclastic Siltstone
- Pumiceous Volcaniclastic Sandstone
- Bell Shale
- Basalt

Copper Mines of Tasmania

Map 2.	EL 27/95 Yolande River Interpreted geology and Stream sediment data.
Date:16/4/1999	
Author: AG	
Office: Queenstown	
Drawing: AS	
Scale: 1:10000	Projection: AMG Zone 55 (AGD 66)

0 100 200 400 metres

5 cm

577192

99-4317

YOLANDE EL 27/95 577193

MAP 3 : DIAMOND HILL ADITS

MAPPING OF QUARTZ VEINS AND LITHOLOGIES

Author: A Griffiths

99-4317

ANNUAL REPORT(YR 3) EL 27/95
COPPER MINES TAS. P HARBON
YOLANDE RIVER

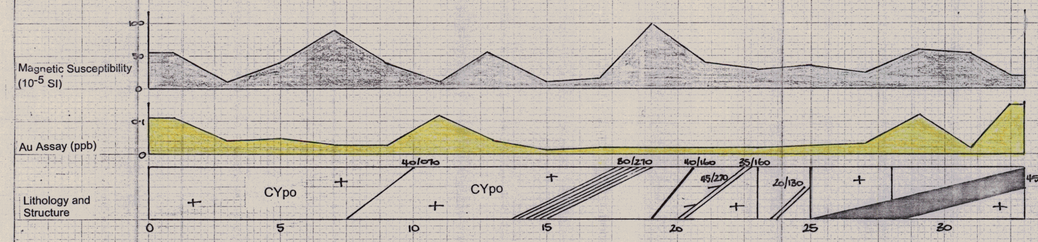

ADIT #3

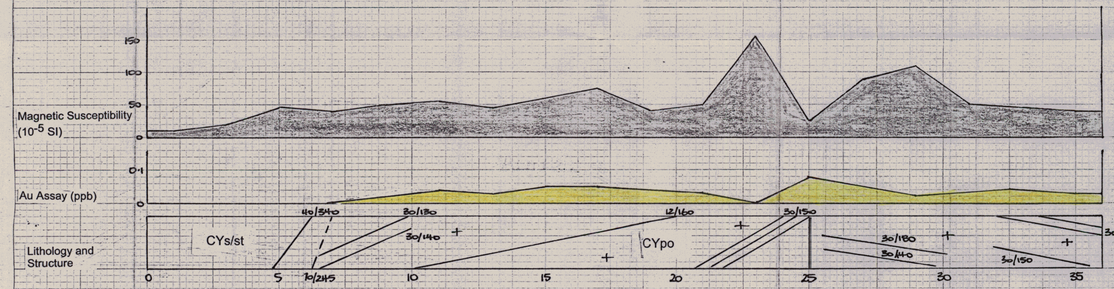

ADIT #2

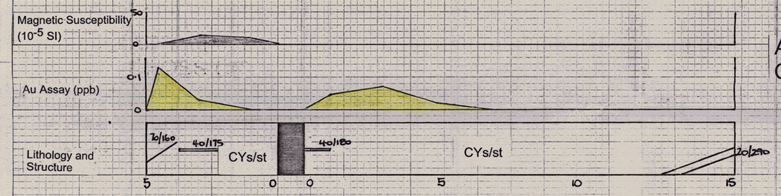

ADIT #1
CROSS-CUT

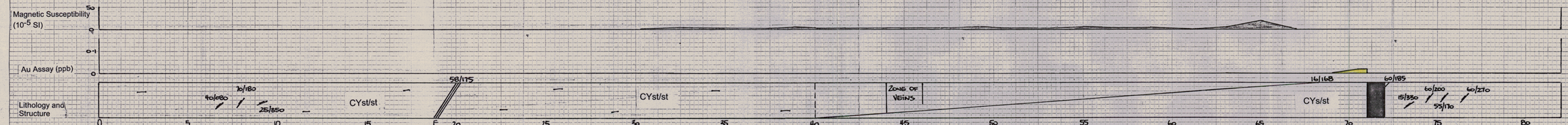

ADIT #1
MAIN DRIVE

0 1 2 5
SCALE IN METRES

5 cm

LEGEND

CYpo	Yolande River Sequence Quartz-feldspar-biotite porphyry		
CYs/st	Yolande River Sequene Volcaniclastic sandstone		
CYst/st	Yolande River Sequence siltstone		
	Quartz Veins + Dip/Dip direction	F	Fault
	Joints + joint direction		Lithological contact